

POSSIBLE ROLE OF ADENINE AND THYMINE RICH SEQUENCE IN THE
ENCAPSIDATION PATTERN OF PARVOVIRUS LUIII

By

Militza Rosas-Rodríguez

A thesis submitted in partial fulfillment of the requirements for the degree of

MASTER OF SCIENCE

in

BIOLOGY

UNIVERSITY OF PUERTO RICO

MAYAGUEZ CAMPUS

2007

Approved by:

Rafael Montalvo-Rodríguez, Ph.D.
Member, Graduate Committee

Date

Elsie I. Parés-Matos, Ph.D.
Member, Graduate Committee

Date

Nanette Difffoot-Carlo, Ph.D.
President, Graduate Committee

Date

María A. Aponte-Huertas, Ph.D.
Representative of Graduate Studies

Date

Lucy Bunkley-Williams, Ph.D.
Chairperson of the Department

Date

Abstract

LuIII is a small, non-enveloped, icosahedral autonomous parvovirus that contains a small linear (5 kb) single stranded DNA genome and infects human cell lines lytically with no evidence of integration into cellular DNA. This parvovirus has been considered as an appropriate vector where only transient expression of a transduced gene is desired. Comparison of the LuIII sequence with those of rodent parvoviruses, minute virus of mice (MVM) and H-1 revealed that these viruses are virtually identical with respect to their genomic organization and share 80% sequence homology. However there is a 47 bp AT-rich region starting at nucleotide position 4558 that is unique to LuIII. Previous studies postulated that this AT-rich region is responsible for the symmetric encapsidation of plus and minus strand genomes by LuIII since both MVM and H-1 encapsidate primarily minus strand. To address this hypothesis, two recombinant LuIII genomes lacking the AT-rich sequence, termed pGlu883ΔXbaA/T- and pGlu883ΔXbaA/T- *de novo*, were transfected into HeLa cells. Southern blot analysis and probe hybridization revealed that both pGlu883ΔXbaA/T- constructs are unable to replicate. Cotransfection assays with LuIII minigenomes and a helper construct containing the nonstructural protein NSI under the CMV promoter (pCMVNSI) resulted in similar findings as the transfections. Thus, it is possible that the AT-rich region is a *cis*-acting sequence required for LuIII DNA replication.

Resumen

LuIII es un parvovirus autónomo, icosaédrico y desnudo que contiene un genoma pequeño (5 kb) de DNA de cadena sencilla. Este virus infecta líticamente varias líneas celulares sin evidencia de integración en el DNA genómico. LuIII ha sido considerado como un vector adecuado cuando sólo se desea la expresión transitoria de los genes transfectados. La comparación entre las secuencias de los virus LuIII, los parvovirus de roedores, el “minute virus of mice” (MVM) y el virus H-1 revelan que estos virus son virtualmente idénticos con respecto a su organización genómica, y que comparten el 80% de homología en las secuencias de DNA. Sin embargo, LuIII tiene una región única de 47 pb la cual es rica en AT a partir del nucleótido 4558. Estudios anteriores han postulado que esta región es responsable de la encapsidación simétrica de los genomas con sentido positivo y negativo de LuIII; debido a que tanto el MVM y el H-1, que no tienen la región rica en ATs, encapsidan principalmente la cadena negativa. Para comprobar esta hipótesis, dos genomas recombinantes de LuIII sin la secuencia rica en ATs, llamados pGlu883ΔXbaA/T- y pGlu883ΔXbaA/T- *de novo*, fueron transfectados en células HeLa. Los análisis de Southern blot e hibridación de sondas revelaron que ambas construcciones LuIIIAT- son incapaces de replicarse. Ensayos de cotransfección con los minigenomas de LuIII y una construcción auxiliar que contiene la proteína no estructural NS1 bajo el promotor CMV (pCMVNSI) produjeron resultados similares a los de las transfecciones. Es posible que la secuencia rica en AT sea un elemento de acción cis necesario para que ocurra la replicación del genoma de LuIII.

Dedication

To my beloved family, for blessing me with their unconditional love and support throughout the years: my parents Marta and Jorge, my grandparents Santos and Calixto, my husband Iván and my biggest challenge yet, my beautiful daughter Paola Militza.

ACKNOWLEDGMENTS

First and foremost, I would like to thank the Lord Jesus for giving me the strength and courage to finalize this work and guiding me through this entire process.

Throughout the progress of my graduate studies in the Biology Department of the University of Puerto Rico at Mayagüez many people collaborated directly and indirectly with my project. I dedicate this section to acknowledging them.

My sincerest appreciation and outmost respect goes to Dr. Nannette Difffoot-Carlo, for her patience, advice and guidance. She gave me the opportunity to be part of the virology laboratory experience, for that I am forever grateful. The strong commitment she has for both her family and work, and the high standards that she strives for, has served as an empowerment for my personal and professional growth. She is both a mentor and a roll model. Thank you for showing me the way to excellence. I am also deeply grateful to Dr. Rafael Montalvo-Rodríguez and Dr. Elsie Parés-Matos for agreeing to serve on my committee and for their invaluable help.

A special thanks to Idaris De Jesús: my lab partner, my teacher, my friend, my big sister, my counselor and the president of my support group. I have no words to express how grateful I am. You gave me the will to finish. I know God sent you because without you, I wouldn't have done it.

A heartfelt thanks to my virology family, the parvo-virology sisterhood: Alina De La Mota-Peynado (fearless and in style), Omayra Rivera-Denizard (mathematical wizard), Lisandra Vélez-Pérez (the quiet Einstein), Idaris De Jesús-Maldonado (the problem solver), Sara Mari-González (Mrs. Too fast to clone). I will never forget the extensive laboratory meetings, the productive discussions on the square table and the fun with extracurricular activities; I learned so much from you, you are all beautiful, brilliant women! To the ones that went away, Erick

Román, Mildred Santana, Ixia Ortíz, Priscilla Hernández and a special thanks to Nancy Arroyo for believing and trusting me and for teaching me from molecular cloning to emotional and spiritual growth. To Aixa Sánchez, my deepest gratitude for her help, patience and faith in me, and for constructing the MgLuIII A/T's. To the new laboratory generation of the Parvovirus Family: Samir A. Bello-Melo, a brilliant and outstanding human being, and Alexa Báez-Crespo, her happiness and kindness make her a unique person. I wish the best to them. They have much to live up to, and they are definitely the ones for the job! To the great friends I made during my stay in graduate school from Puerto Rico, Argentina, Venezuela, Perú, Dominican Republic and Colombia. To my two good friends, Ana Argüeyo and María Fernanda Rojas, for their patience and understanding. Throughout the years, I experienced a rainbow of emotions, from happiness to frustration and draw-backs, thanks for being there and God bless you all!

The incredible people of the Biology Department: From the ones that inspire me with their love and devotion for their work, to name a few: Dr. Vivian Navas, Dr. Carlos Muñoz, Dr. Carlos Ríos, Dr. Rafel Montalvo, Dr. Carlos Acevedo, Dr. Martínez Cruzado, Dr. Carlos Betancourt and Dr. Lucy Williams. To the ones that make the graduate experience an easier one like, María Méndez (wonder woman), Mary Jiménez, Brenda Soto, Magaly Zapata, Don Luis Rodríguez (from the Celis building), Zayda Ortíz and to Don Domingo Justiniano and José (Pito) Soto for taking care of some of the restriction endonuclease digestions at night.

Finally, I want to thank my family: To my soul mate, my best friend, my love, my husband Iván for his infinite support, love, and cheerful encouragement. To my parents for their love, devotion, direction, and tireless sacrifices as well as for their constant support. To my mom Marta, the strongest woman I know. To my grandma Santos, her unparalleled faith makes me believe that nothing is impossible in this life. To my dad Jorge, he is so brave and driven, he

makes me think there is nothing you can't do. To grandpa Calixto, the wisest, smartest and most humble person I now. Someday, I would like to be half of what you are. And, to my personal discovery and inspiration, my daughter Paola, my love for you is immeasurable.

Table of Contents

	Page
List of Tables	x
List of Figures	xi
Chapter I: Introduction	1-2
Chapter II: Literature Review	3
a. <i>Parvoviridae</i> Classification	3
b. Virion Morphology	8
c. Genomic Structure	9
d. Viral Protein and Transcription	12
e. Parvovirus Replication	19
f. Viral Encapsidation	31
g. Gene Therapy	35
Chapter III: Objectives, Materials and Methods.	39
Objectives	39
Materials and Methods	40
a. Construction of the pGLu883 Δ XbaAT- clone	41
b. Construction of the pGLu883 Δ Reverse clone	44
c. Construction of the pGLu883 Δ XbaAT- <i>de novo</i> clone	47
d. Preparation and transformation of competent cells	50
e. Isolation of DNA Recombinants	51
f. Tissue Culture	52
g. Transfection assay	52
h. Southern blot analysis	55
Chapter IV: Results and Discussion.	57
Chapter V: Conclusion	90
Chapter VI: Recommendations	91
Literature Cited	92

List of Tables

Tables	Page
Table 1. Classification of the <i>Densovirinae</i> Sub-family of the <i>Parvovirinae</i> Family	5
Table 2. Classification of the <i>Parvovirinae</i> Sub-family of the <i>Parvoviridae</i> Family.	7
Table 3. Encapsidation Pattern of Selected Parvovirus	31
Table 4. Expected restriction enzyme patterns for the LuIII clone	51
Table 5. DNA samples used for transfection assays	54
Table 6. Transformations of <i>E. coli</i> SURE [®] 2 cells with pGLu883Δ <i>Xba</i> AT- clone.	59
Table 7. Transformations of <i>E. coli</i> SURE [®] 2 cells with pGLu883Δ <i>Xba Reverse</i> clone.	72
Table 8. Transformations of <i>E. coli</i> SURE [®] 2 cells with pGLu883Δ <i>Xba</i> AT- <i>de novo</i> clone.	80

List of Figures

Figures	Page
Figure 1. Flip and Flop Conformation of Parvovirus LuIII.	10
Figure 2. Terminal Hairpin and Genomic Structure of Parvovirus MVM.	14
Figure 3. Terminal Hairpin and Genomic Structure of Parvovirus LuIII.	16
Figure 4. Terminal Hairpin and Genomic Structure of Parvovirus AAV.	18
Figure 5. Rolling Hairpin Replication Model.	20
Figure 6. Terminal resolution at the MVM right terminus	23
Figure 7. Organization of MVM dimer bridge	25
Figure 8. Modified Rolling Hairpin Model for MVM DNA Replication.	27
Figure 9. Proposed Model for the Replication of Parvovirus LuIII.	30
Figure 10. Map of MgLuIII Δ Xba/T- and pGLu883 Δ Xba clones.	40
Figure 11. Strategy used to construct pGLu883 Δ XbaA/T-.	42
Figure 12. Digestion of pGLuIII883 Δ Xba and MgLuIII Δ Xba/T- with <i>NheI</i> and <i>KpnI</i> and isolation of desired fragments for cloning.	43
Figure 13. Strategy used to construct pGLu883 Δ Xba <i>Reverse</i>	45
Figure 14. Digestion of pGLuIII883 Δ Xba and pGLuIII883 Δ XbaA/T- with <i>NheI</i> and <i>KpnI</i> and isolation of desired fragments for cloning	46
Figure 15. Strategy used to construct pGLu883 Δ XbaAT- <i>de novo</i>	48
Figure 16. Digestion of pGLuIII883 Δ Xba and pGLuIII883 Δ XbaA/T- with <i>SspI</i> and isolation of desired fragments for cloning	49
Figure 17. <i>KpnI/NheI</i> and <i>KpnI/ClaI</i> digestions of the pGLuIII883 Δ XbaA/T- recombinants. ...	60
Figure 18. HeLa cells electroporated with pGLuIII883 Δ XbaAT-.	62

Figure 19. Gel electrophoresis and Southern blot analysis of transfected samples of pGlu883Δ <i>Xba</i> AT-64
Figure 20. HeLa cells electroporated with pGLuIII883Δ <i>Xba</i> A/T- recombinant clone.67
Figure 21. Gel electrophoresis and Southern blot analysis of transfected samples.70
Figure 22. Digestions of possible pGlu883Δ <i>Xba Reverse</i> with <i>Kpn</i> I / <i>Nhe</i> I74
Figure 23. HeLa cells electroporated with pGLuIII883Δ <i>Xba Reverse</i> recombinant clone.76
Figure 24. Gel electrophoresis and Southern blot analysis of transfected samples79
Figure 25. Digestions of the pGLu883Δ <i>Xba</i> A/T- <i>de novo</i> recombinant molecule82
Figure 26. HeLa cells electroporated with pGLuIII883Δ <i>Xba</i> A/T- <i>de novo</i> recombinant clone.84
Figure 27. Gel electrophoresis and Southern blot analysis of transfected pGLuIII883Δ <i>Xba</i> A/T- <i>de novo</i>86
Figure 28. Schematic diagram of the position of the LuIII AT-rich region with respect to the inboard <i>cis</i> -acting elements of MVMp89

CHAPTER I

Introduction

Molecular characterization of parvoviruses has been encouraged because of their broad host range and great dissemination (Maxwell and Maxwell, 1999). It has been established that parvoviruses could be a valuable tool for gene therapy. The possible use of vectors based on the autonomous parvovirus LuIII for use in cancer therapy and the general potential use for therapeutic purposes can only be accomplished by elucidating the basic biology of this parvovirus (Cornelis et al., 2004). Viruses of the family *Parvoviridae* have DNA genomes that are both single stranded and linear. The termini of their 5 kb genome contains palindromic sequences that fold into stable double stranded hairpin-like structures allowing self-primed DNA synthesis from the 3'-OH group (Berns, 1990). The palindromic sequences not only act as replication origins, they also have the signals required for encapsidation (Cotmore and Tattersall, 1996). Some rodent parvoviruses, including the minute virus of mice (MVM) and the H-1 virus, encapsidate predominantly the minus strand (complementary to the mRNA) of the genome and have non identical 5' and 3' terminal sequences (Bates et al., 1984). Parvoviruses like the adeno-associated virus (AAV) and B19, efficiently possess identical terminal sequences and encapsidate either strand of their genome with the same frequency (Berns, 1990). LuIII is an autonomous parvovirus which encapsidates either strand of its genome with similar efficiency and frequency. A sequence comparison of LuIII with MVMp and H-1 revealed that they not only have similar terminal sequences but, their genome organization is identical except for two regions (Diffoot et al., 1993). One of these regions has one copy of a sequence found as a direct repeat in MVMp and H-1, believed to function as an internal origin of replication. LuIII has an

AT-rich region of 47 bp long, unique to LuIII (5'TATGCTCTATGCTTCATATATATATATATATATTATTATAC TAACTAA-3'), located near the end of the right ORF at nucleotide position 4560 of the LuIII genome. Previous studies suggest that the AT-rich region may act as a replication origin in yeast (Román-Pérez, 2000; Arroyo, 2000; De Jesús-Maldonado, 2004).

Usual production of LuIII transducing virus has been accomplished by co-transfection of a plasmid based on a helper transducing genome construct (Corsini et al., 1995). During co-transfections to generate transducing virus, recombination between the helper and transducing genomes can regenerate infectious virus with variable frequencies. To eliminate this possibility and to determine the role of the AT-rich region, the full length genomic clone of the LuIII virus pGLuIII883 Δ Xba was modified in order to lack the AT-rich region. Two recombinant LuIII transducing genomes lacking the AT-rich sequence were constructed. Deletion of the AT-rich region results in a genome almost identical to MVM and thus, encapsidation of primary minus strands was expected. Both molecules were transfected into HeLa cells and no cytopathic effect was observed. Transfected DNA was analysed for replication using the *DpnI* and *MboI* restriction endonucleases but no replicated DNA was recovered. Subsequent co-transfections with the helper construct pCMVNSI and minigenomes containing both terminals of the LuIII virus resulted in no replication of the LuIII A/T- molecules. Thus, these data suggest that the AT-rich sequence might be a *cis*-acting element, part of a multipartite origin of replication, similar as described for MVM (Tam and Astell, 1993; Tam and Astell, 1994; Brustein and Astell, 1994).

CHAPTER II

Literature Review

The *Parvoviridae* is the only known virus family with linear single-stranded DNA genomes. Parvoviruses are some of the smallest viruses found in nature, hence their name from Latin *parvus* meaning *small*. Their chromosomes range from 4 to 6 kb in length and consist of a single-stranded coding region of less than 5.8 kb, flanked by short imperfect terminal palindromes that fold back on themselves to form duplex hairpin telomeres. The telomeres together with some adjacent nucleotides provide all the *cis*-acting information required for viral replication and progeny genome encapsidation, serving both as origins of replication and as critical hinges that allow quasi-circular amplification of the linear chromosome through a series of duplex intermediates (Cotmore and Tattersall, 2006). In general, members of the *Parvoviridae* family show a high degree of host species specificity and infect a broad range of invertebrate and vertebrate hosts, from arthropods to man, reason for the current classification be based primarily on virus host range and helper virus dependence (Lukashov and Goudsmit, 2001).

Classification

The *Parvoviridae* family is characterized by morphological and physicochemical properties as well as individual characteristics of genome organization, replication and encapsidation. Members of this family are non-enveloped, icosahedral animal viruses that encapsidate a linear single stranded DNA genome (Berns, 1990; Berns, 1996; Luckashov and Goudsmit, 2001). Taxonomical classification of this family has divided in two subfamilies *Densovirinae* and *Parvovirinae*, which infect invertebrates and vertebrates respectively.

Densonucleosis viruses or densoviruses (DNVs) are invertebrate viruses belonging to the subfamily *Densovirinae*. The *Densovirinae* subfamily is sub-divided in four genera: *Brevivirus*, *Densovirus*, *Iteravirus* and a new genus *Pefudensovirus*. DNVs are characterized by their autonomous replication and the separate encapsidation of either complementary single stranded DNA sequence (Van Munster et al., 2003). Among arthropods hosts, representatives of at least five orders from the class Insecta (Lepidoptera, Diptera, Orthoptera, Odonata and Hemiptera) and one order from the class Crustacea are known to be infected by DNVs (Bando et al., 1990; Giraud et al., 1992). Common symptoms resulting from a densovirus infection include hypertrophy of infected nuclei caused by denso-nucleosis (accumulation of viral particles in the nuclear compartment), progressive paralysis and death of the insect host (Dumas et al., 1992). Because of their pathogenicity on economically and medically important insects, they are being studied for their potential use as a tool in biological control of pests as well as for their possible use as gene transfer vehicles (Bossin et al., 2003).

Members of the *Parvovirinae* subfamily have been also studied for their applications as vectors, particularly in gene therapy, ranging from long-term gene replacement to short-term expression. The *Parvovirinae* subfamily is further subdivided into five genera: *Abdovirus*, *Bocavirus*, *Dependovirus*, *Erythrovirus* and *Parvovirus* (Table 1). Taxonomically all parvoviruses except the members of the genus *Dependovirus* are autonomous parvoviruses. Of the five genera that are included in the *Parvovirinae* subfamily, *Dependoviruses*, *Erythroviruses* and *Parvoviruses* contain important members that infect humans (Cotmore and Tattersall, 2006). The RA-1 virus of *Parvovirus*, the B19 virus of *Erythrovirus*, and the adeno-associated viruses of *Dependovirus*, all infect humans.

Table 1. Classification of the *Densovirinae* Sub-family of the *Parvoviridae* Family as established by the ICTV*

<i>Genus</i>	<i>Type species</i>	<i>Natural Host</i>
<i>Densovirus</i>	<i>Junonia coenia densovirus</i>	Buckeye butterfly
<i>Iteravirus</i>	<i>Bombyx mori densovirus</i>	Silkworms
<i>Brevivirus</i>	<i>Aedes aegypti densovirus</i>	Mosquito
<i>Pefudensovirus</i>	<i>Periplaneta fuliginosa densovirus</i>	Cockroaches

*ICTV = International Committee on Taxonomy of Viruses. <http://www.ncbi.nlm.nih.gov/ICTVdb/ICTVdB/index.htm>

Dependovirus genus consists of adeno-associated viruses that have a single stranded DNA genome flanked by identical and inverted terminal repeats (ITRs) at both ends. The ITRs contain all *cis*-acting elements required for the replication, integration, packaging, and in some cases, the transcriptional activation of the viral genome (Spears et al., 1977; Lusby et al., 1980; Lusby et al., 1981; Qui et al., 2006). In 1965, Atchinson, et al., identified a contaminating virus (original isolates 1, 2, 3, 4 and 6) in human and simian adenoviral preparations. Due to its inability to replicate in the absence of adenovirus, this defective parvovirus was named adeno-associated, AAV (Timpe et al., 2006). AAVs have also been isolated from animal adenovirus stocks (Table 2) but the best characterized of all AAVs is the AAV2. In the absence of a coinfection by a helper virus, AAV2 enters in a latent state by integration of its genome into a specific region of the human chromosome 19q13-qter, designated the AAVS1 locus. If the latently infected cell is subsequently infected by a helper virus or is exposed to genotoxic chemicals or radiation, a copy of the latent AAV genome is released from the chromosomal

content and proceeds to replicate (Linden et al., 1996; Tullis and Shenk, 2000; Ward et al., 2003). All AAVs are able to infect both dividing and nondividing cells, achieve stable chromosomal integration, transduce a broad range of tissues *in vivo* such as brain, liver, muscle, lung, retina, and cardiac muscle, and to initiate long-term gene expression in these tissues. Lack of known human pathogenicity or cell mediated immune response has been observed (Ding et al., 1997; Li et al., 2005).

Erythroviruses are named for their tropism for red blood progenitor cells. Parvovirus B19 of the *Erythrovirus* genus is the only member of the *Parvoviridae* family known to be pathogenic towards humans (Faisst and Rommelaere, 2000). B19 is a global and common infectious human pathogen, hence prevalence of IgG antibodies directed against B19 are common in the general population. However, viremia or presence of viral DNA is rare (Heegaard and Brown, 2002). B19 is known to cause several diseases such as aplastic crisis in patients with chronic hemolytic anemia, erythema infectiosum, persistent infections manifesting as chronic anemia in immunocompromised patients, fetal myocarditis, non-immune hydrops fetalis leading to intrauterine fetal death, arthralgias and arthritis (Heegaard and Hornsleth, 1995; Respondek et al., 1997; Pallier et al., 1997). The mechanistic basis for these B19 virus-associated diseases is poorly understood. Nonetheless, most symptoms appear to be related to the unique tissue tropism of B19 virus. Cells permissive for B19 virus replication are proliferating erythroid precursors in human bone marrow and fetal liver tissues (García-Tapia et al., 2005). Although the target cell specificity for B19 infection has been suggested to be mediated by the erythrocyte P-antigen receptor (globoside), a number of non erythroid cells that express this receptor are nonpermissive for B19 replication (Wang et al., 1995; Gareus et al., 1998; Zhi et al., 2006). Recently, a B19 isolate termed V9 was identified as the causing agent for transient aplastic anemia, but its sequence was markedly

different from B19 sequences (Heegaard and Brown, 2002). Cell death is directly induced by infection with B19 and related viruses like B19-V9 as well as most autonomous parvoviruses (Morita et al., 2003).

Table 2. Classification of the *Parvovirinae* Sub-family of the *Parvoviridae* Family as established by the ICTV*

<i>Genus</i>	<i>Type species</i>	<i>Natural Host</i>
<i>Amdovirus</i>	Aleutian mink disease virus (AMDV)	Mink, skunk, raccoon
<i>Bocavirus</i>	Bovine parvovirus (BPV)	Cow
<i>Dependovirus</i>	Adeno-associated virus-2 (AVV)	Human
<i>Erytrovirus</i>	Human Parvovirus B19	Human
<i>Parvovirus</i>	H-I parvovirus (H-1PV) LuIII parvovirus (LuIII) Minute virus of mice (MVM)	Rat Unknown Mouse, Rat

*ICTV = International Committee on Taxonomy of Viruses. <http://www.ncbi.nlm.nih.gov/ICTVdb/ICTVdB/index.htm>

Members of the *Parvovirus* genus are lytic viruses best known for being autonomous parvovirus, APVs. Because of their low genomic complexity and the flexibility of their single strands, parvoviruses condense a considerable amount of DNA into their capsids. However, this simple structure limits their parasitic potential, as incoming virions lack accessory proteins, chromatin, or even a duplex transcription template and are forced to remain silent in the cell until cellular factors are expressed as a function of proliferation and cell division. Thus, APV's infect and replicate in the nucleus of mammalian cells in S phase or early G2 phase without integration into the host genome (Lukashov and Goudsmit, 2001). APVs are widespread in nature but are

host-specific viruses (López-Guerrero et al., 1997). However, the autonomous parvovirus LuIII has a high sequence homology to MVM and H-1, two of the most studied rodent parvoviruses. LuIII was originally isolated from human lung carcinoma cells (Soike et al., 1976; Diffoot et al., 1989). Meanwhile, MVM was isolated from a stock of mouse adenovirus and H-1 was originally isolated as a contaminant of a human tumor cell line passaged in a rodent research laboratory (Berns, 1996; Lukashov and Goudsmit, 2001). RA-1 virus, named rheumatoid associated parvovirus-like agent, was recovered from the synovial tissue of a patient with severe rheumatoid arthritis (Simpson et al., 1984). RA-1 resembles parvoviruses in physicochemical and morphological properties and sequence analysis shows homology to bovine parvovirus, although it is lethal for mice. Polyclonal antibodies detect the presence of RA-1 in patients with rheumatoid arthritis but not in people with osteoarthritis, which supports the possible link between RA-1 and chronic rheumatoid arthritis in humans, making RA-1 the only known human pathogen from the *Parvovirus* genus. However, no further work has been published on this virus (Kerr, 2000).

Virion Morphology

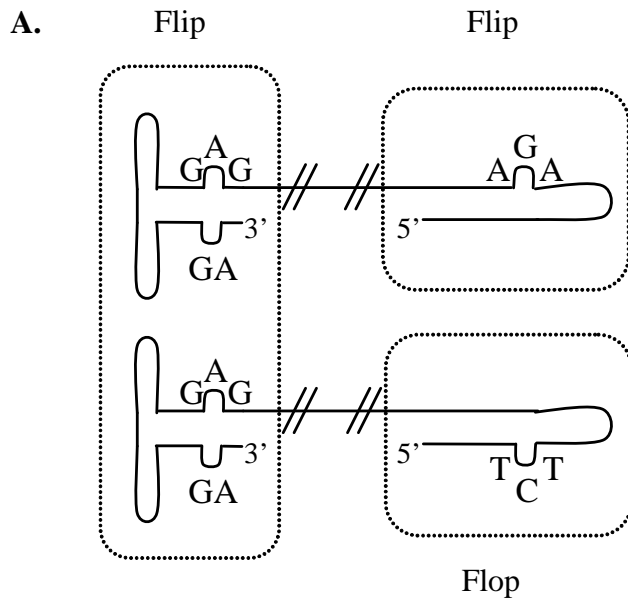
Parvoviruses are among the smallest and structurally simplest of eukaryotic viruses. Viral particles consist of a non-enveloped icosahedral protein capsid, of about 18-26 nm in diameter containing one linear single stranded DNA molecule. The capsid consists of 60 molecules of several capsid proteins (VP); (Llamas-Saiz et al., 1997) of which around 95% is the major viral protein VP2 (Bärbel et al., 2004). The number of capsid VP species per virion differs among parvoviruses. For example, MVM has three capsid proteins, VP1 to VP3, and members of the subfamily *Densovirinae* have four, VP1 to VP4 (Kontou et al., 2005). Virions have a molecular weight of $5.5-6.2 \times 10^6$ kDa (Berns, 1996). About 50% of the virion mass content is protein, the

remaining being DNA. Because of the relatively high DNA to protein ratio, the buoyant density of the intact virion is 1.39-1.42 g/cm³ (Siegl, 1976). The available structural information indicates that differences in the capsid surface determine tissue tropism, pathogenicity and antigenicity, among different parvoviruses and among the strains of a particular virus (McKenna et al., 1999). Widespread in nature is explained by the resistance of the virions, surviving alcohol or ether treatment, temperatures of up to 56°C (for longer than 30 min) and pH changes between 3 and 9. The virus can be inactivated by formalin, β -propiolactone, hydroxylamine, and oxidizing agents (Faisst and Rommeleare, 2000).

Genomic Structure

Sequence comparison of several members of the Parvovirus genus has established similarities in their genomic organization (Banerjee et al., 1983; Diffoot et al., 1993; Lukashov and Goudsmit, 2001). The parvoviral chromosome comprises a single stranded DNA molecule of either plus or minus polarity, flanked by a small palindromic telomere capable of adopting a self priming hairpin configuration that is stabilized by self-hydrogen bonding (Figure 1). The linear strands vary from 4 to 6 kb in length with most of its DNA sequence devoted to the coding region. The genome contains two sets of genes: one that encodes proteins involved in transcription (NS or REP proteins) and another that encodes the coat proteins (VP proteins). However, the expression of these genes is complex, with multiple splicing patterns for each gene (Besselsen et al., 1996). The termini consist of less than 10% of the total genome and range in size from 120 to 420 bases, and can be dissimilar in sequence and secondary structure within individual genomes and species.

The terminal palindromes are essential for the initiation of genome replication and the encapsidation of progeny DNA (McLaughlin et al., 1988). All known DNA directed, DNA



B. Flip Conformation

GGTTGACCATGACCAACCAACG^ACGAG^GTTGGTTGGTCTGGCCGA^G
 CCAACTGGTACTGGTTGGTTGC - -GCTC-AACCAACCAGACCGGCA^G

Flop Conformation

GGTTGACCATGACCAACCAACG - -CGAG-TTGGTTGGTCTGGCCGT^C
 CCAACTGGTACTGGTTGGTTGC_T_CGCTC_CAACCAACCAGACCGGCT_C

Figure 1. Flip and Flop Conformations of Parvovirus LuIII. **A.** Schematic illustration of the flip and flop conformations at both LuIII termini. **B.** DNA sequence of the right end terminus (5' end) of the plus strand of LuIII with the flip and flop conformation. (Adapted from Diffoot et al., 1989).

polymerases require a primer in addition to a template for replication initiation. Because of this requirement and to maintain their integrity, all linear, viral DNA genomes have evolved as specialized DNA sequences at their termini. All parvovirus termini, so far characterized, contain palindromic sequences. AAV, the human B19 virus and all Dependoviruses have the same DNA sequences at both termini. However, the rest of the parvoviruses characterized have different 3' and 5' terminal sequences (Berns, 1990).

The AAV contains identical, yet, inverted terminal repeats (ITR) sequences with a length of 145 nucleotides. The terminal nucleotide repeat sequences of AAV have the potential of assuming a complex T-shaped secondary structure by folding the terminal 125 self complementary nucleotides (Lefebvre et al., 1984; Berns, 1996). Each 3'- and 5'- hairpin structure contains two sets of DNA sequences that are the inverted complement of each other (Ward et al., 2003). Since equivalent palindromes are present at each end of the genome, the replication and resolution processes of both termini are similar.

The autonomous parvoviruses also have hairpin duplexes at both the 3' and 5' ends of their genomes. However, they do not contain inverted terminal repetitions. In addition, the 3'- and 5'-hairpin structures differ both in size and DNA sequence. MVM has two physically and functionally divergent terminal palindromes that utilize different resolution strategies (Astell et al., 1983; Astell et al., 1985). The 5' end of the minus strand, conventionally termed the right hand terminus, can assume a T or U shaped structure and is 200-211 nucleotides long. Meanwhile, the 3' end or left hand palindrome, is 115-122 nucleotides long and has only been observed in the T or Y shaped conformation conventionally known as rabbit ear conformation (Difffoot et al., 1993; Cotmore and Tattersall, 1995). In contrast to AAV's ITRs, the 3'-hairpin structures of several autonomous parvoviruses have essentially identical DNA sequences and

contain 115 or 116 nucleotides that are unique, because of which base mismatches occur (Astell et al., 1985).

The terminal palindromes also exhibit two alternative sequence orientations known as flip and flop, due to a few nucleotide mismatches that form a “bubble”-like structure. While in the hairpin configuration a GAA triplet on one strand is paired to a GA doublet, in the complementary strand. The bubble-like structure is a result of both, the nature of the palindromes and their inversions during the process of hairpin transfer and replication. In LuIII, the right hairpin shows either a flip conformation (GAA paired to GA) or a flop conformation (TTC paired to TC) while the left exhibits exclusively the flip conformation (Difffoot et al., 1993). Both conformations have been linked to the parvoviral DNA replication (Chen et al., 1988; Cotmore and Tattersall, 1988; Berns, 1996).

Viral Proteins and Transcription

The template for transcription in parvoviruses is double-stranded viral DNA in the nucleus of the infected cell. This DNA is not associated to histones and does not form nucleosomes, but it is bound to unidentified cellular proteins (Doerig, 1986). Transcription goes from 5' to 3' and starts at two promoters, although autonomous parvovirus B19 has only one active promoter (Berns, 1996; Raab et al., 2001). Parvoviral genomes contain two large open reading frames (ORFs), one coding for replication (REP) or non-structural (NS) proteins and the other coding for structural or capsid proteins (VP) (Figure 2).

Most autonomous parvovirus genomes, like MVM and LuIII, are organized (Figure 3) in two large open reading frames on the viral coding strand and transcription starts at promoters P4 located at m.u. 4 and P38 at m.u. 38 from left to right, respectively (Figures 2 and 3); (Difffoot et al., 1993). The P4 promoter codes for the non-structural (NS) proteins. There are two NS

products, NS1 and NS2, even though the role of the NS1 protein has been well studied, the role of the NS2 protein is more elusive.

The NS2 is a 25 kDa phosphoprotein that is mainly cytoplasmic and consists of two or three isoforms that differ at their carboxy termini as a result of alternative splicing of a small intron located at m.u. 44 to m.u. 46. Although their mode of action is not known, NS2 proteins are somehow involved in efficient translation of viral mRNAs and in accumulation of viral DNA replication intermediates in mature virions (Brockhaus et al., 1996). All NS2 isoforms share their first 85 N-terminal amino acid residues with NS1.

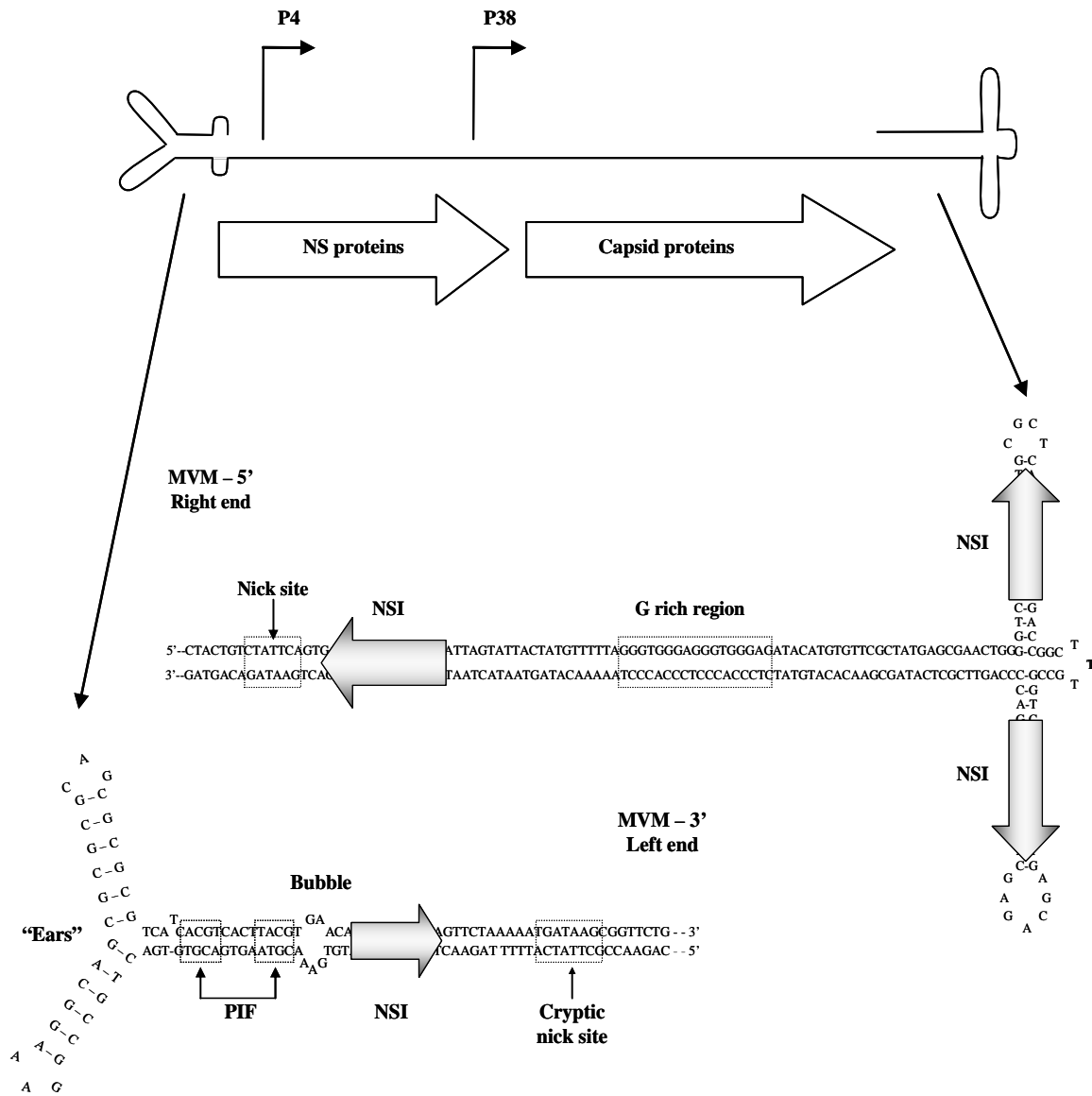


Figure 2. Terminal Hairpin and Genomic Structure of Parvovirus MVM. DNA sequence of MVM termini of the plus strand forming the Y and T-shape secondary structure are shown. The positions of the promoters (P4, P38) are indicated by bent arrows, and the major genes indicated by open arrows represent the direction of the amino- to carboxy-terminal. NSI binding sites are denoted by shaded arrow boxes, nick sites are indicated by vertical arrows. Since the left end is not a nicking substrate in the hairpin configuration, it was termed cryptic nick site. (Adapted from Cotmore and Tattersall, 2006)

The NS1 protein is an 83 kDa cytotoxic, multifunctional nuclear phosphoprotein with nickase, helicase and ATPase activities that participates in driving viral replication transcription and gene expression (Pujol et al., 1997; Maxwell and Maxwell, 1999; James et al., 2004; Hickman et al., 2004). NS1 function, as a DNA replication initiator and is dependent on protein kinase C phosphorylation. The initiation protein up-regulates the late promoter P38 as well as its own promoter P4 to a small extent, and likely acts in concert with NS2 to direct the packaging of progeny single strand DNA (Hanson and Rhode, 1991). NS1 binds to DNA in a sequence-specific manner through a (ACCA)₂₋₃ motif that is highly represented in the parvoviral genome but not restricted to other sequences in the strand. Multiple *cis*-acting elements including a *trans*-activation GC motif and TATA boxes, and a downstream element were reported to be important for the activity and NS1 induction of the P38 promoter (Pujol et al., 1997).

The P38 transcript encodes two capsid proteins, the larger VP1 (83 kDa) and the major VP2 (64 kDa) whose mRNAs are also generated by alternative splicing (Lombardo et al., 2002). Empty capsids can be assembled only from VP2 (Xie and Chapman, 1996). Proteolytic enzymes can shorten some of the amino-terminal regions of the VP2 molecules in the virion to produce a third polypeptide, VP3 (62 kDa) after capsid assembly and packaging of the viral genome (Cotmore and Tattersall, 1986). Although dependoviruses and autonomous parvovirus have different life cycles, both their structural and non structural proteins have similar functions.

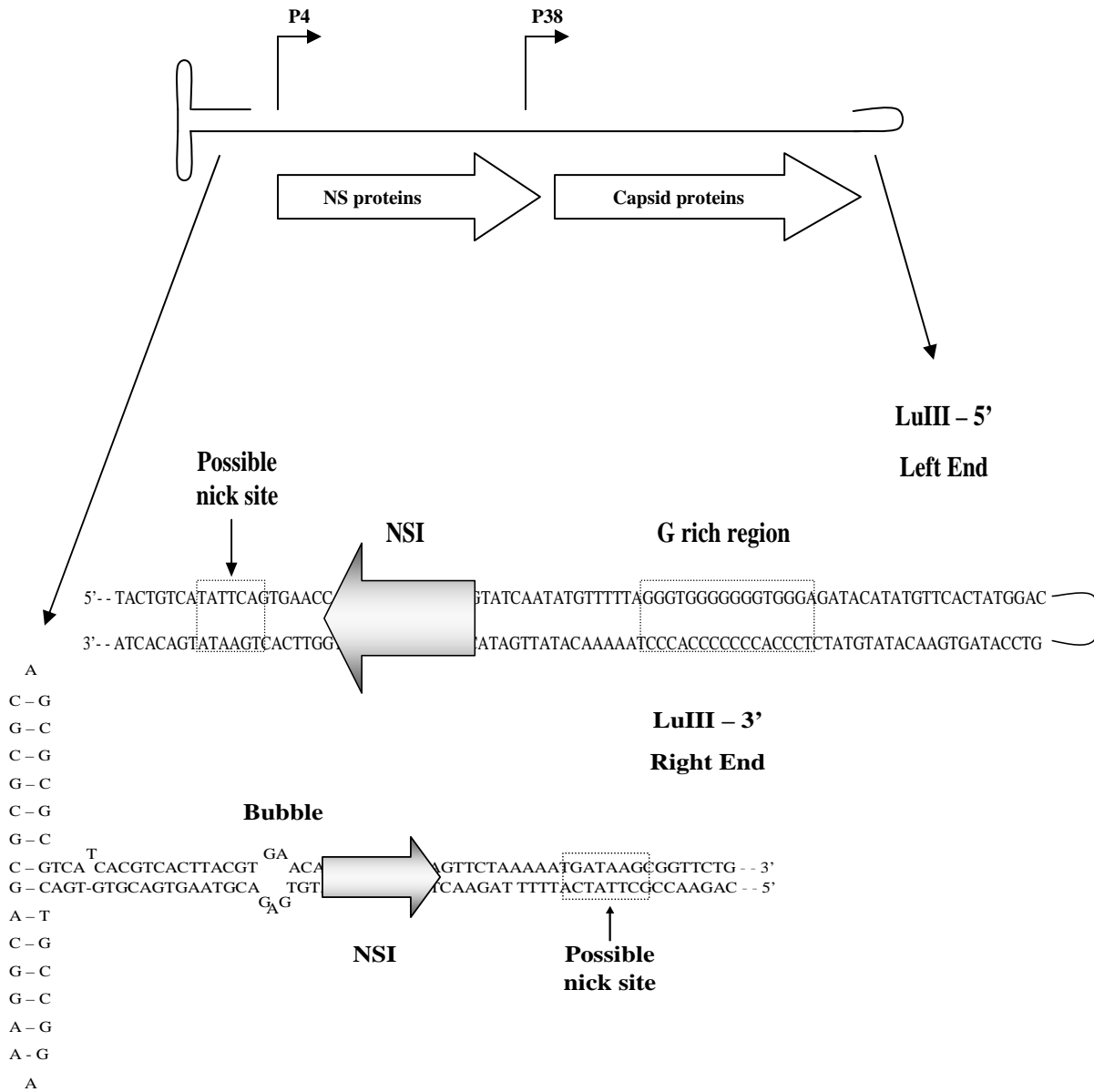


Figure 3. Terminal Hairpin and Genomic Structure of Parvovirus LuIII. DNA sequence of the left and right termini of the plus strand of LuIII forming the T and U-shape secondary structure. The positions of the promoters (P4, P38) are indicated by bent arrows, and the major genes are indicated by open arrows represent the direction of the amino- to carboxy-terminal. NSI binding sites are denoted by shaded arrow boxes, nick sites are indicated by vertical arrows. (Adapted from Diffoot et al., 1989)

The dependovirus AAV contains only two major open reading frames, *rep* and *cap*, named from their roles in DNA replication and encapsidation. The Rep78 and Rep68 proteins are generated from transcripts that derive from the P5 promoter, and they differ in their C-termini due to alternative splicing of the P5 transcripts. Rep78 and Rep68 are DNA helicases that also have a single-stranded DNA endonuclease activity, and both proteins are sufficient to support AAV DNA replication. These proteins are also required for site-specific integration of AAV DNA into the host cell genome and for DNA excision. Rep52 and Rep40 are translated from transcripts generated from promoter P19, located within the *rep* gene and translated from the same open reading frame as Rep78 and Rep68, and vary in their C-termini due to the same alternative splicing. Rep52 and Rep40 lack DNA binding and endonuclease domains of the larger Rep proteins but retain a functional helicase domain. Rep 52 and Rep 40 are not required for the replication of double stranded DNA, but both are required for the efficient production of single-stranded AAV DNA. The *cap* gene encodes the three structural proteins VP1, VP2 and VP3, generated from transcripts initiated from the P40 promoter.

The genome of the B19 virus contains two promoter-like elements, in which only one is functional. The active promoter, termed P6, is located at the 5' end and regulates all the viral transcripts (Raab et al., 2001). B19 extreme tropism for replication in erythroid progenitor cells is attributed to the activity of the P6 promoter of the viral genome in combination with both cell and cell cycle-specific factors and the *trans*-activator protein NS1 (Eiji et al., 2003). NS1-mediated transactivation is dependent on the presence of two GC-rich elements arranged in tandem, upstream of the TATA box (Gareus et al., 1998).

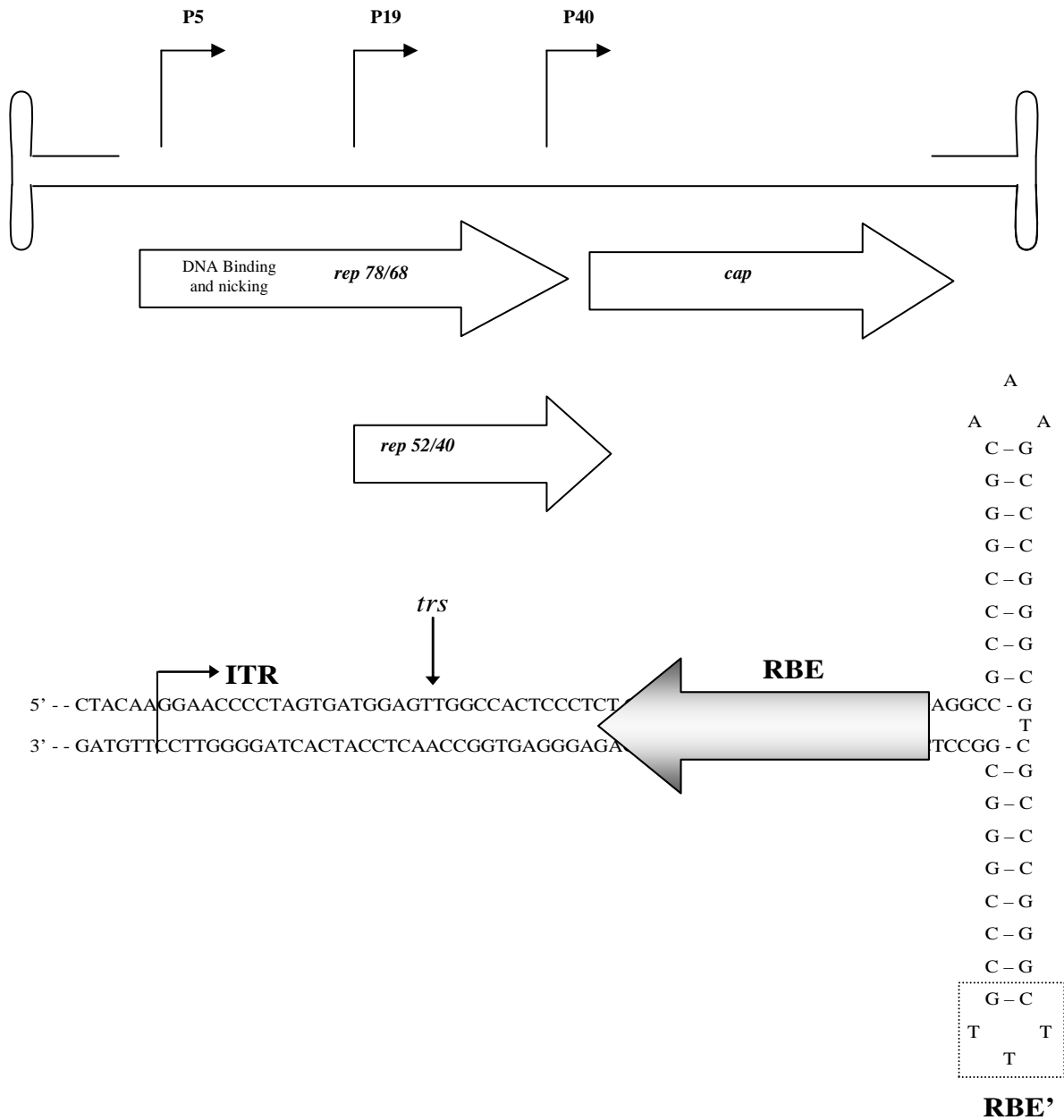


Figure 4. Terminal Hairpin and Genomic Structure of Parvovirus AAV. DNA sequence of the ITR for the right termini of the plus strand of AAV forming the T-shape secondary structure. The positions of the promoters are indicated by bent arrows (P5, P19, P40) and the ORFs are indicated by open arrows representing the direction of amino- to carboxy-terminal. Rep Binding Element (RBE) is depicted by the shaded arrow box, the RBE' position is depicted by the cross-hatched box, the inboard end of the ITR is marked by a rightward arrow, and nick sites are indicated by arrows. (Adapted from Cotmore and Tattersall, 2006)

The B19 genome contains two main ORFs and two polyadenylation sites, located in the middle and at the end of the genome in combination with alternative splicing events. These are responsible for the production of a total of nine viral transcripts, seven of which are used as mRNAs (Gareus et al., 1998). The left hand ORF encodes the nonstructural cytotoxic protein NS1 (77 kDa), which is involved in viral DNA replication, transcription and cell death, and the right hand ORF encodes both the major VP2 (83 kDa) and the minor VP1 (58 kDa) structural capsid proteins (Moffatt et al., 1998). VP1 and VP2 are similar except for a unique sequence of 227 amino acids (aa) at the N-terminal end of the VP1 protein (the VP1 unique region). The VP1 DNA coding sequence is followed by the entire coding sequence of VP2. VP1 has proven to have a particular role in the viral life cycle since neutralizing antibodies interact preferentially with the VP1 unique region (Dorsch et al., 2002). Overlapping the main right hand ORF, there are two additional ORFs encoding two small proteins of 7.5 kDa and 11 kDa. The functions of both proteins are still unknown (Servant et al., 2002).

Parvovirus Replication

The Rolling-Hairpin Replication (RHR) is the unidirectional single strand-specific displacement mechanism used by Parvoviruses to amplify their genomes through a series of concatemeric duplex intermediates, shown on Figure 5 (Astell et al., 1985). In general, viral replication precedes in two distinct phases, an initial amplification phase that generates a high molecular-weight duplex replicative form (RF) DNA, followed by a progeny genome displacement phase, in which individual single strand genomes are excised and displaced for encapsidation (Cotmore and Tattersall, 1995). In RHR, the hairpin joins the 3' terminal nucleotide of the incoming virion DNA with an internal base, creating a DNA primer that allows the host DNA polymerase to initiate DNA synthesis of a complementary DNA strand.

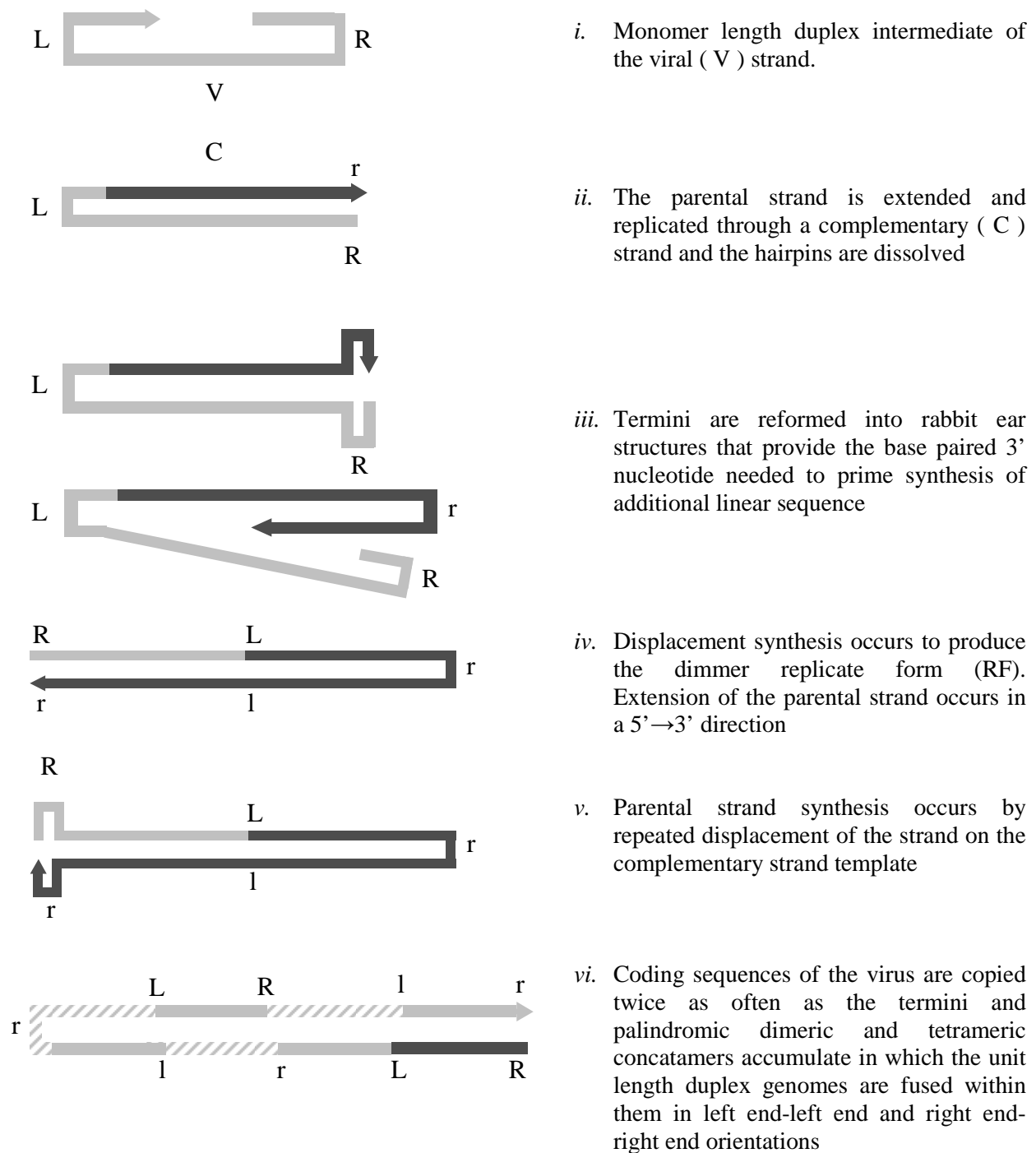


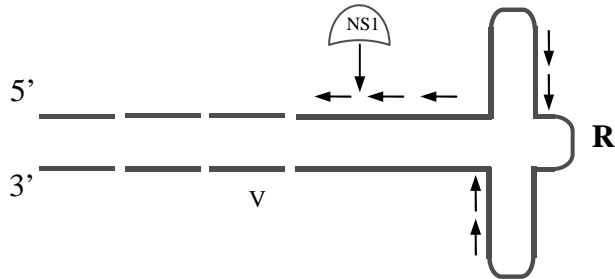
Figure 5. Rolling hairpin replication. In steps (i) through (v) newly synthesized DNA is shown as a black bar. L and R correspond to the left and right palindromic sequences of the termini, respectively. The l and r, are their complements. Step (vi) produces a tetramer in which 3' progeny genomes are shown in crosshatched and white bars and the parental sequence in black. (Adapted from Cotmore and Tattersall, 1995)

This generates a monomer length, duplex intermediate in which the two strands are covalently cross linked at one end via a single copy of the viral 3' telomere (Liu et al., 1994). Amplification proceeds by unidirectional strand displacement with all functions provided by the host cell during S phase (Siegl and Gautschi, 1976; Gautschi et al., 1976; Berns, 1996; Delau et al., 1999). In order for amplification to take place, the hairpins must first be unwound by the NSI or Rep protein, working as a 3' to 5' replicative helicase. As a result of the replication process, a series of palindromic duplex dimeric and tetrameric concatemers are created. In these concatemers the unit-length genomes are fused in left-end:left-end and right-end:right-end combinations (Cotmore and Tattersall, 1996). Sequential rounds of replication are initiated from the concatemers and individual genomes are then excised and displaced by a site specific single strand nick at the telomeric origins performed by the viral initiator nuclease NSI or Rep protein. The initiator protein remains covalently attached to the 5' end of the progeny genomes (Cotmore and Tattersall, 1988). Subsequent to the accumulation of the displaced progeny, single strands appears to be dependent on the availability of preformed capsids and packaging itself is driven by an ongoing viral DNA synthesis. Active sites of viral genome replication and viral capsid assembly have been identified after infection, termed APAR or autonomous parvovirus-associated replication bodies (Bashir et al., 2001; Young et al., 2002).

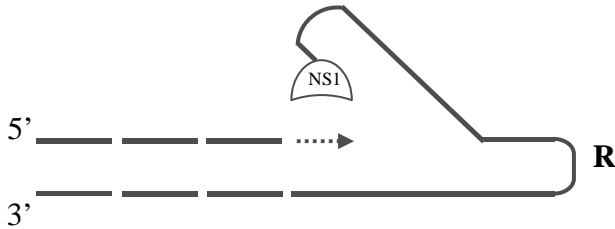
To date, replication strategies have been best explored for the apathogenic defective *Dependovirus* AAV and for the autonomous replicating *Parvovirus* MVM (Faist and Rommelaere, 2000). In viruses with ITRs, like AAV, the monomer length duplex intermediate creates a replication origin that can be activated by Rep 68/78 (homologous to NS1) in a process called terminal resolution, whereas in viruses such as MVM, where the left-end telomere is not like its right telomere, the (left-end) terminus has to be in an extended dimer configuration to

serve as a replication origin (Cotmore and Tattersall, 1996). In either case, replication proceeds according to the RHR mechanism as depicted in Figures 5 and 6, but because of the differences in the telomeres and genome structure each replication mechanism has its particularities (Cotmore and Tattersall, 1992).

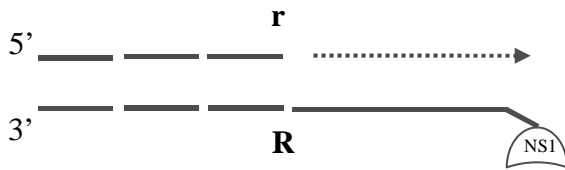
Terminal resolution is the process by which the duplex form of the AAV genome, that are covalently continuous at one end by a single copy of the terminal palindrome, can be resolved to an extended form configuration by containing two copies of the palindrome (Im and Muzyczka, 1990; Snyder et al., 1990a; 1990b). Within AAV ITRs, just two sequence elements are required for the origin of replication to function, the RBE and the *trs*. The RBE is a 22 bp Rep-Binding Element composed of two tetranucleotide repeats (5'-GAGC-3') which positions Rep 68/78 in the correct orientation and cleavage position on the viral DNA. The *trs* is a 7 nucleotide sequence located at 16 nucleotides inboard of the RBE and flanked by short palindromic sequences that stabilize the exposure of the critical phosphodiester bond by folding into a stem-loop structure (Snyder et al., 1993; Brister and Muzyczka, 1999). This structure moves the nick site toward the active site of the RBE-bound Rep complex. The initiation efficiency at this origin can be enhanced by the cellular DNA bending protein, HMG1 (Costello et al., 1997). A third element depicted the RBE', has the DNA sequence 5'-GTTTC-3', but is not required for origin function because it has the capacity to enhance origin efficiency. The RBE' is located at the tip of the hairpin arm, opposite the nick site in the same position in either of two inverted complementary forms of the termini.



i. NS1 recognizes the viral sense strand (V) and binds to the ACCA sequence (depicted by small black arrows). NS1 cuts inside the nick consensus sequence CTWWTCA.



ii. Cleavage results in the formation of a phosphodiester bond between the 5' terminal and the NS1. The nick invert the original complex palindrome onto the progeny strand, while providing a new base-paired 3' hydroxyl to prime synthesis of its complement.



iii. Terminal resolution replaces the original sequence of the hairpin "R" with its inverted complement "r". Since the inversion is repeated with every round of resolution progeny genomes contain equal number of termini in both flip and flop orientations.

Figure 6. Terminal resolution at the MVM right terminus. Diagram illustrates the NS1 (depicted by the open wedge) interaction with the 5' terminus of the viral DNA strand (portrayed by line segments) of parvovirus MVM during terminal resolution. "R" depicts the parental strand and "r" its inverted complement. (Adapted from Cotmore and Tattersall, 1995)

The MVM termini differ from each other in size, sequence and structure (Astell et al., 1983). However, the right end telomere is resolved in its hairpin configuration, by a terminal resolution reaction similar to that of AAV (Figure 6). This reaction generates both flip and flop sequence orientations whereas the left end telomere utilizes a junction resolution mechanism generating termini in a single orientation (Astell et al., 1985). The minimal sequence requirement for nicking the right end origin is 125 bp long, and constitutes the entire right end hairpin (Cotmore et al., 2000). There are three NSI recognition elements, two are located in the hairpin and one is located 120 bp from the nick site in the stem, next to the hairpin axis. The right end terminal forms a duplex with three unpaired bases at the axis and a single mismatch region on the stem in which a three nucleotide insertion (AGA or TCT) on one strand separates opposing pairs of NSI binding sites, creating a 36 bp palindrome. NSI binds specifically to double stranded DNA at the tetranucleotide motif 5'-ACCA-3' repeated at multiple sites throughout the genome and viral replication origins (Cotmore et al., 1995). Recent studies by Cotmore et al. suggest that the NSI interaction with DNA is similar to what has been described for Rep 68/78 (Hickman et al., 2004). Thus, interactions with NSI molecules bound to the recognition elements is strengthened by the DNA bending protein HMG1/2. In MVM, this interaction is required for the formation of the cleavage complex (Cotmore et al., 2000). HMG1 induces a slight shift on the DNA sequences protected by NSI, making them to fold into double helical loops that extend for 30 bp through the G-rich element in the hairpin stem. The loop allows the terminus to adopt a three dimensional structure needed to activate the nickase.

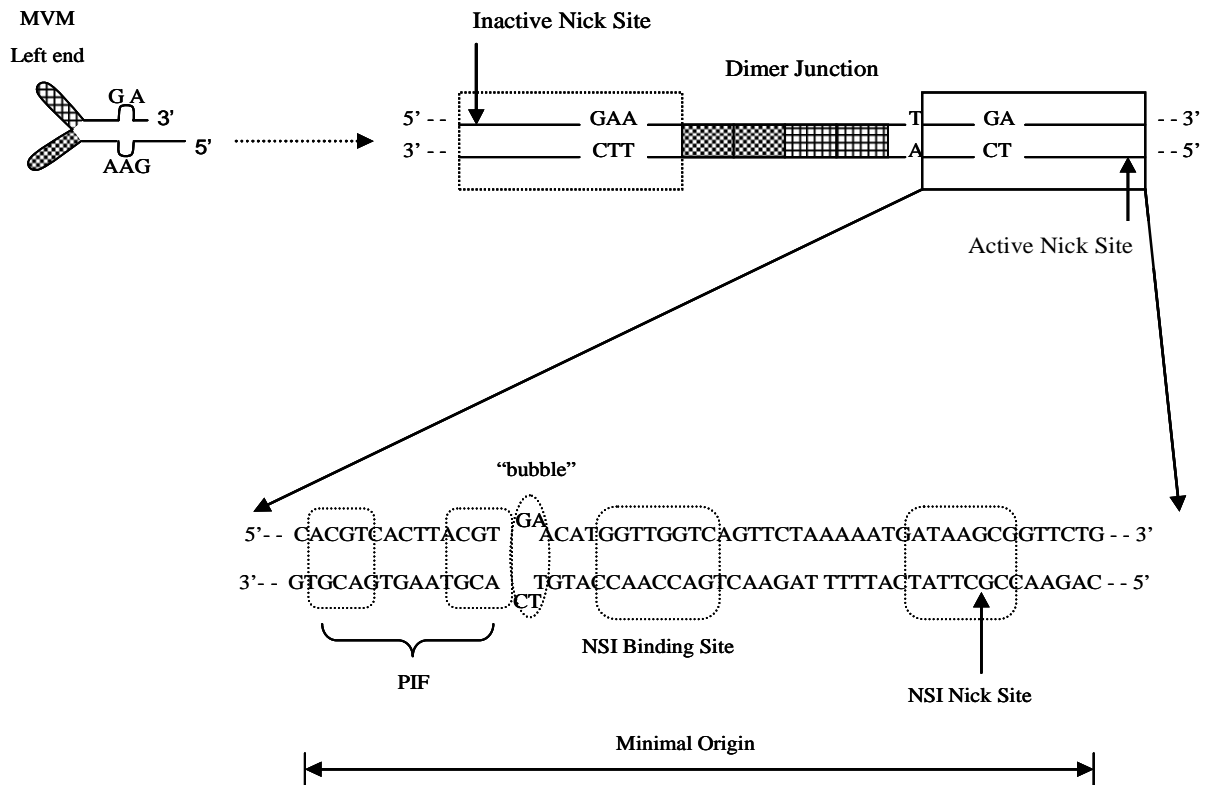


Figure 7. Organization of MVM dimer bridge. The left-end hairpin showing the 3'-OH used for priming replication and the mismatched bubble sequence is depicted above (top left). The dimer junction diagram condenses the in-vivo steps *i* through *iv* of the RHR figure. Cross-hatched boxes represent the palindromic sequences which fold to give the internal "ears" in the hairpin form of the 3' end of the MVM genome. The clear box at the right end depicts the minimal active replication origin of the 3' terminus. This box is expanded below with sequences corresponding to the PIF, "bubble", NSI Binding Site and NSI Nick Site shown in detail. (Adapted from Christensen et al., 2001)

The left end telomere of MVM exists as a single flip sense sequence containing internal palindromes designated the “ears” and an asymmetric mismatch “bubble” in the stem where the triplet GAA on the inboard arm is opposed to the doublet GA on the outboard strand (Cotmore and Tattersall, 1994; Kuntz-Simon et al., 1999). This telomere cannot function as a replication origin in its hairpin configuration, hence while the hairpin while is in the extended form, a single competent origin is generated. During replication, the hairpin is extended and copied to form a completely base paired palindromic junction (left end:left end) sequence that spans adjacent genomes in dimer RF (Baldauf et al., 1997). The resolution process resolved by this junction is called junction resolution. Throughout the junction resolution process, an asymmetric template with a nonfunctional nick site on one of the hairpin arms serves as the origin, instead of the terminal hairpin, while the same sequential extension and refolding reactions of the RHR amplification take place.

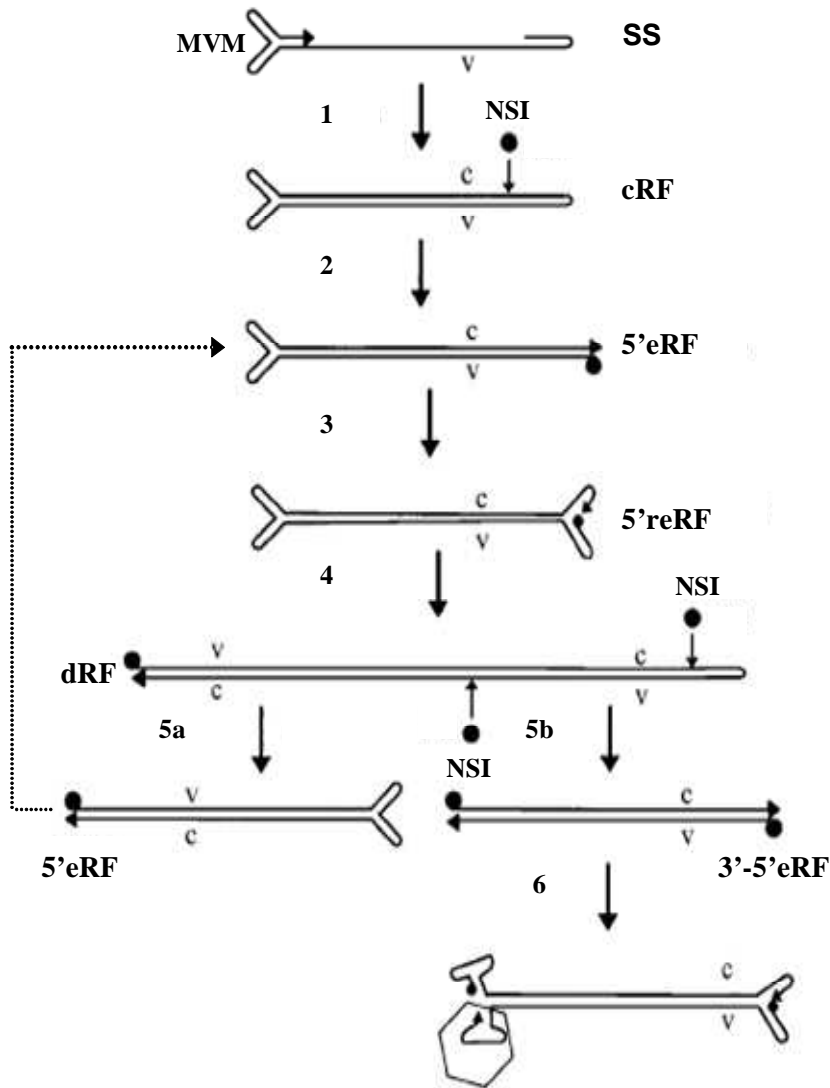


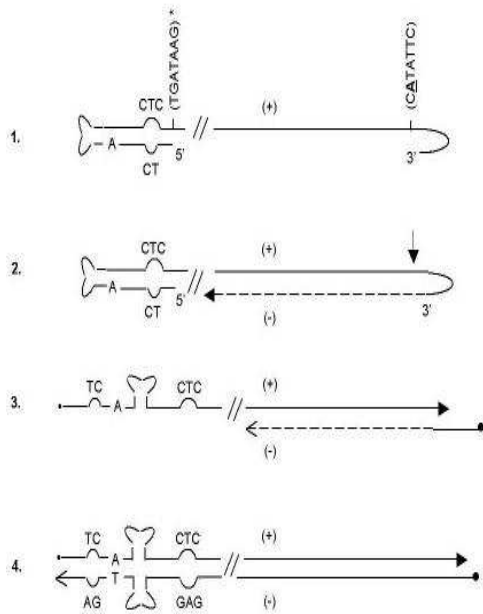
Figure 8. Proposed Modified Rolling Hairpin Model for MVM DNA Replication. Small black filled circles represent NSI. Small horizontal arrowheads indicate DNA 3' ends. The open polygon in step 6 depicts the parvovirus capsid structure. (Reprinted from Kuntz-Simon et al., 1999). Steps in the modified RHR are as follows: **1.** To serve as a primer for the initiation of the DNA synthesis the 3' end of the parental or viral (V) single strand (SS) genome folds into a hairpin structure. Elongation from the 3' OH of the hairpin allows it to synthesize a complementary (C) copy of the parental strand. **2.** The growing complementary strand reaches the fold back 5' terminus at the right end and the covalently closed DNA replicative form (cRF) is created. NSI becomes covalently attached to the viral DNA and nicks the right terminus of the viral genome. **3.** The right termini is displaced and copied giving rise to an extended molecule (5' eRF). **4.** Rearrangement of the copied right hand palindrome into the hairpin structures termed "rabbit-ears" creates the rabbit-eared replicative form (5'reRF) which serves as a primer for strand displacement synthesis. **5.** The synthesis leads to the formation of the dimer duplex intermediate (dRF) in which two unit length copies of the genome are joined by a single duplex copy of the original 3' palindrome. **6.** Each full length strand monomer is encapsidated into preformed capsids.

The minimal active left end origin proposed for MVM is a multi-domain structure of approximately 50 bp derived from the stem region of the hairpin (Cotmore and Tattersall, 1995; Cotmore et al., 1993). The origin is comprised of two 5'-ACGT-3' motifs spaced by 5 nucleotides, a “bubble” mismatch (a GAA triplet that opposes a GA doublet) that serves as a critical spacer element (Cotmore and Tattersall, 1994), the NSI binding (ACCA)₂ site, the NSI nick (5'-CTWW \downarrow TCA-3') site and 7 bp beyond the nick site. Only the sequence from the arm containing the GA dinucleotide serves as an origin, termed OriL_{TC}. Within the origin, the three essential recognition sequences are the NSI Binding Site, the NSI site and the two ACGT motifs (Cotmore et al., 1993; Liu et al., 1994). Although NSI binds to the origin through an ATP dependent manner, it is unable to initiate replication on its own (Christensen et al., 1997a). Thus, a cellular factor called the Parvovirus Initiation Factor (PIF) acts as a cofactor in the replication initiation process (Cotmore and Tattersal, 2006). PIF is a heterodimeric site, specific DNA binding factor, essential for the replication initiation process by allowing efficient and specific nicking of the 3'-end and leaving NSI covalently attached to the 5'-end of the origin. This factor binds specifically to two ACGT motifs, spaced from 1 to 9 nucleotides apart with an optimal spacing of 6 nucleotides (Christensen et al., 1997b), and then contacts NSI over the “bubble” sequence to stabilize the binding of NSI on the active form of the left-end origin OriL_{TC} (Christensen et al., 2001; Burnett et al., 2001). The region containing the PIF binding site is highly conserved in the 3' hairpin of parvoviruses related to MVM, as well as HI, MPV and LuIII (Christensen et al., 1997a).

Recent studies of the left end terminus of parvovirus LuIII suggest that contains all the *cis*-acting sequences required for DNA excision and replication. Thus, in its double stranded form the hairpin appears to have an active NSI driven origin of replication that lacks the

arrangement of the specific domains present in the dimer duplex intermediate proposed for MVM (Diffoot-Carlo et al., 2005). These studies have suggested that the left end terminus of the minus strand exists only on the flip conformation while the right terminus of the plus strand exists in both flip and flop conformations (Diffoot et al., 1989). Based on the functionality of the left hairpin of LuIII as an origin of replication, a replication model was proposed by Diffoot et al. (Figure 9). This model results in equivalent amounts of plus and minus DNA viral strands, therefore both strands independently commence replication (step 1). The plus strand starts replication from the right hairpin and the minus strand from the left hairpin. Both hairpins can serve as a primer, which allows a host polymerase to synthesize a complementary copy of the internal sequence of the viral genome until the growing strand reaches the folded back terminus, resulting in a cRF. NSI opens the cRF by nicking the viral strand (step 2). There are active NSI nick sites present at both termini of parvovirus LuIII. These nick sites differ from each other and from the NSI nick sites at MVM in an adenine residue insertion in the 5' terminus nick site (Diffoot et al., 1993). Following the NSI nick, there is strand displacement and copying of the initiating (step 3) that promotes the development of an extended molecule containing covalently joint viral and complementary DNA strands (step 4). The model suggests that each strand gives rise to a copy of self and complement sequences in both flip and flop conformations (step 5) contrary to what was previously proposed (Diffoot et al., 1989).

A. Replication of LuIII using plus strand



B. Replication of LuIII using minus

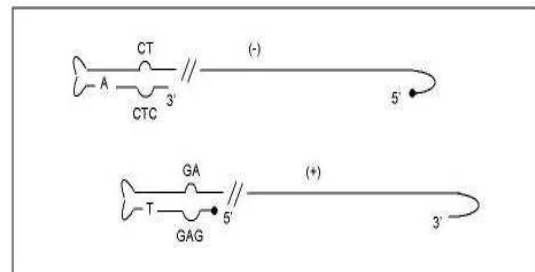
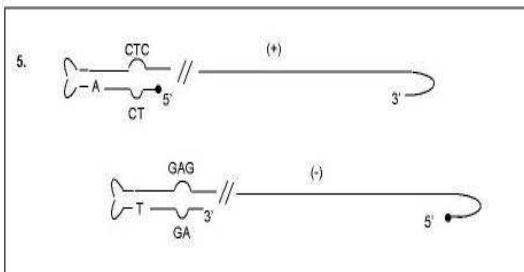
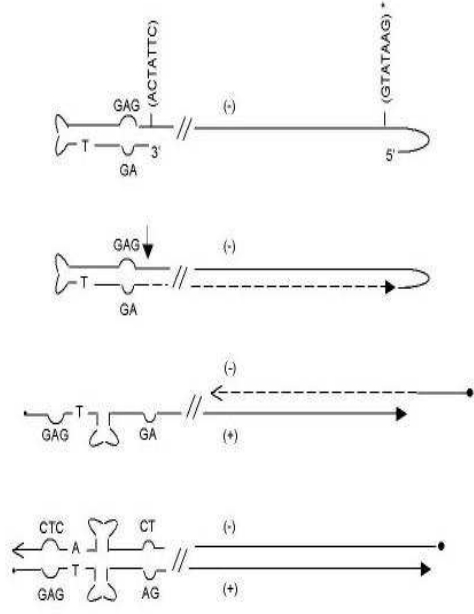


Figure 9. Proposed Model for the Replication of Parvovirus LuIII. The model depicts the replication mechanism for both the plus (+) and minus (-) strands of LuIII. The NS1 nick site and its complementary DNA sequence are indicated with an asterisk, (*). Replication of the (+) strand and (-) strand shown in section A and B, respectively. Unpaired sequences present at the left hairpin are shown. Vertical arrows point to the NS1 nick sites. A corresponds to the insertion in the NS1 nick site present at the right terminus of LuIII. (Diffoot-Carlo et al., 2005)

Viral Encapsidation

Viruses from the *Parvoviridae* family display two particular encapsidation patterns. They can either package equal amounts of plus and minus strands or mostly minus strand DNA. It has been established that the *cis*-elements required for packaging DNA reside in the parvoviral genomic termini. Details for this packaging have not been elucidated, but available data suggest that emerging genomes are inserted into preformed capsids (Muller and Siegl, 1983). The rodent autonomous parvoviruses MVM and H-1 have non-identical genomic termini and encapsidate 99% minus strand. *Dependovirus* AAV and autonomous parvovirus B19 have identical genomic termini and encapsidate plus and minus strand with equal frequency. Originally, it was understood that the presence of identical termini in the viral genome was necessary for encapsidation of equal amounts of plus and minus viral DNA strand. Conversely, Diffoot and colleagues proved that identical terminal ends are not required for the encapsidation of both strands since the autonomous parvovirus LuIII has non-identical termini (Diffoot et al., 1989) and encapsidates both strands with equal frequency (Bates et al., 1984).

Table 3. Encapsidation Pattern of Selected Parvovirus (Berns, 1996)

Sub-family	<i>Parvovirus</i>	<i>Terminal Hairpin</i>	<i>Encapsidation Pattern</i>
<i>Dependovirus</i>	AAV	Identical	50 % (+), 50 % (-)
<i>Erythrovirus</i>	B19	Identical	50 % (+), 50 % (-)
<i>Parvovirus</i>	H1	Non-identical	99 % (-)
	MVM	Non-identical	99 % (-)
	LuIII	Non-identical	50 % (+), 50 % (-)

LuIII was sequenced and has shown to have greater than 80% identity with rodent parvoviruses MVMp and H-1 (Diffoot et al., 1993). Two regions of the LuIII genome, both downstream from the capsid coding region, differ significantly from those of MVMp and H-1. One of the sequences is in tandem at the end of the right ORF of MVMp and H-1, while only one copy of a similar sequence is present in MVMi and LuIII at m.u. 92. The presence of a single copy of this sequence is not expected to influence LuIII encapsidation pattern, because it may function as an internal origin of replication. The other region is a possible sequence determinant of the packaging bias. This region is an AT-rich stretch of 47 nucleotides (TATGCTCTATGCTTCATATATATTATATATATTATTATACTAACTAA) at m.u. 89, located at 6 bases downstream from the end of the right ORF. Sequence alignment of LuIII with the MVMp genome shows that in LuIII, the AT-rich region exists as an insertion that interrupts a sequence near the right palindrome of MVM, previously identified as a *cis*-acting replication signal (Tam and Astell, 1993). This region has been shown to bind four cellular proteins which are thought to be involved with replication of the MVM genome (Tam and Astell, 1994). Since replication and encapsidation seem to be linked, Corsini and colleagues (1995) hypothesize that it is possible that binding of cellular proteins to this region of MVM and H-1 virus hinders binding of the MVM capsid to the right end, preventing encapsidation of the plus strand. Thus, disruption of this protein-binding region by the AT-site might eliminate strand-selective encapsidation and confers LuIII the ability to encapsidate either strand. As a consequence, deletion of this sequence from LuIII could result in a genome virtually identical to that of MVMi and encapsidation of primarily minus strands would be expected.

Although the LuIII AT-rich sequence is not present in the closely related parvoviruses MVM or H-1, there are AT-like sequences in other parvoviruses such as the feline

panleukopenia virus (FPV) and the canine parvovirus (CPV) which encapsidate predominantly the minus strand of their genome (Parrish et al., 1988; Martyn et al., 1990). As in LuIII, these AT-like regions occur near the coat protein termination codons of FPV and CPV. For FPV and CPV both the presence and occurrence of the AT-like sequences might suggest that the presence of the AT-rich sequence is not sufficient for encapsidation of the plus strand.

If the virion or the nonstructural proteins could determine the packaging bias, a recombinant LuIII genome with the nonstructural and structural proteins of H-1 or MVM parvoviruses would be expected to produce virus particles containing only minus strand. Corsini and colleagues materialized this experiment and the results suggested that the ability of LuIII to package either strand is a property of the LuIII genome and not of the proteins, since its encapsidation pattern was maintained (Corsini et al., 1995). Thus, both the mechanism underlying strand-packaging bias and the role of the AT-rich sequence unique to the LuIII genome have not been determined.

Recent studies using genomic chimeras of the MVM and LuIII genomes established a possible connection between the mechanistic differences in the processing of Ori_{LC} and Ori_R, and the strand packaging bias of these parvoviruses (Cotmore and Tattersall, 2005b). Accordingly, the relative efficiency with which the two genomic termini are resolved and replicated eventually determines the polarity with which single strands are excised from replicating RF, and that these are then packaged with equal efficiency. Their data analyses indicated that the packaging substrate is the newly released single strand and not the duplex RF forms of the genome. They also proposed a single-strand displacement model in which the functional asymmetries between the right and left hairpins restrict the release of positive-sense strands from the RF during the packaging phase of infection. Hence, the plus strands are only

released if the right end nick site is suboptimal, making the displaced minus strands cycle through an obligatory dimer duplex intermediate.

Viruses package their genomes into protein capsids either via association of structural proteins with the viral genomes or via insertion of viral genomes into preassembled capsids (King et al., 2001). The parvovirus initiator protein is left covalently attached to the 5'-end of the nicked DNA after replication (Im and Muzyczka, 1990; Prasad and Trempe, 1995). Therefore, the genomes are marked for packaging by their association with the non structural proteins, which in turn, bind efficiently to intact empty capsids. The underline mechanism of how the empty capsids are recruited to newly displaced single strands remains unknown.

Single strand DNA accumulates in cells that are assembling competent viral particles and the displacement of the single strand progeny occurs during active DNA replication. In AAV2, the genomes are translocated into preformed capsid particles via a reaction that has been shown to require the helicase activity of the Rep 40/52 proteins (King et al., 2001). DNase protection data suggest that insertion of progeny strands into viral particles proceeds from the 3'-end (Cotmore and Tattersall, 2005a) and the helicase has a processivity of 3' to 5' (King et al., 2001). King and colleagues also propose a model in which the Rep 40/52 proteins function as a molecular motor, associating with a single capsid opening and effectively pumping the DNA into the virion. These studies also suggest that Rep 40 may have the ability to form a hexameric ring (James et al., 2004) in which peptide loops project into a central pore, through which the single strand could pass during unwinding or strand translocation (Yoon-Robarts et al., 2004). The peptide loops carry the residues K404 and K406, known to be essential for the single strand binding and packaging (Yoon-Robarts et al., 2004). The structure and precise mechanism of interaction of this molecular motor remains unknown.

Gene Therapy

Gene therapy is a technique used for correcting defective genes responsible for disease development (Faisst et al., 2000). The most common approach used by researchers for correcting faulty genes is to replace the nonfunctional gene by a normal gene. Thus, a vector must be used in order to deliver the therapeutic gene (transgene) to the patient's target cells. Currently, the most studied vectors are viruses, among which the most promising are the small non-pathogenic viruses from the *Parvoviridae* family, AAV, MVM, H-1 and LuIII (Corsini et al., 1996). Several parvoviruses, including H-1 and MVM, have been shown to exert an oncosuppressive effect. They are able to inhibit the formation of spontaneous as well as chemically or virally induced tumors in laboratory animals (Avalosse et al., 1996). Implants of tumor cells, including human neoplastic cells, can also be targets for the parvoviral oncosuppressive activity in recipient animals (Spegelaere et al., 1991). Despite their oncolytic properties in cell cultures, parvoviruses injected in tumor-bearing mice are often not potent enough to irreversibly arrest the tumor growth (Kimsey et al., 1986). In order to take advantage of the oncotropism of parvoviruses, recombinant derivatives containing a therapeutic transgene are being engineered (Russell et al., 1992; Maxwell and Maxwell, 1993; Maxwell et al., 1995; Maxwell et al., 1996; Maxwell et al., 2002).

Recombinant parvoviruses are infectious DNA clones that contain the full-length viral genome inserted in a bacterial plasmid (Faisst et al., 2000). Their strategy consists on the replacement of part of the parvoviral capsid genes with a therapeutic gene whose product can kill the tumor cells or stimulate the patient's immune system (Russell et al., 1992; Maxwell et al., 1995). Recombinant Parvoviruses retain the NS1/2 coding sequences under the control of the parvoviral P4 promoter. Usually, the transgene is placed under the control of the P38 promoter

which, as mentioned before, is *trans*-activated by NS1. Thus, a strong DNA expression of the transgene is achieved. These vectors also retain the parvoviral genome telomers (5'- and 3'-end palindromic sequences), that fulfill all *cis*-acting requirements for the viral DNA amplification and packaging in the presence of the replication protein NS-1 (Tullis and Shenk, 2000; Musatov et al., 2002). Other alternatives for gene therapy are provided by the use of the recombinant parvovirus vector with a helper plasmid that provides all the necessary viral products (structural and nonstructural proteins) in the *trans* arrangement.

AAV vectors are among the smallest and most chemically defined particulate gene delivery system (Maxwell et al., 1993). Some of the more relevant advantages of the recombinant AAV vectors (rAAV) are that they can mediate stable and high levels of transgene expression in both dividing and non-dividing terminally differentiated cells without inducing significant inflammatory toxicity. The rAAV vectors have become increasingly recognized as having some superiority to other viral and non viral gene delivery systems with regard to their safety because viral administration is less frequent and without known pathology (Goudy et al., 2001). The primary limitation of rAAV has been the small size of the virion (20 nm), that only permits the packaging of 4.7 kb of exogenous DNA including the promoter, the polyadenylation signal and any other enhancer elements required. Recent reports have exploited a unique feature of rAAV genomes such as their ability to link together in doublets or strings in order to bypass the size limitation. The development of this technology may improve the chances for successful gene therapy of diseases like cystic fibrosis or Duchenne Muscular Dystrophy (Flotte et al., 2000).

The autonomous parvoviruses are also promising therapeutic agents, particularly for transient expression because their infectious cycle does not involve integration into cellular DNA

(Cotmore and Tattersall, 1987). Experimental studies indicate that both transformed and tumor-derived cell lines of animal and human origin are far more favorable to the parvoviral life cycle, than the normal cells from which they derive (Cornelis et al., 1990; Maxwell et al., 1993; Maxwell and Maxwell, 1999). Moreover the parvoviruses, MVM, H-1 and LuIII efficiently infect human cell lines (Maxwell et al., 2002).

Recent experiments performed in animals to assess whether MVM or H-1-based vectors carrying the interleukin 2 (IL-2) cytokine gene have reinforced anti-cancer capacity showed that these recombinant viruses suppressed tumor formation more efficiently than viruses devoid of a transgene (Cornelis et al., 2004). Strong anti-cancer effects of recombinant parvoviruses expressing interferon gamma-inducible protein-10 (IP-10) and monocyte chemotactic protein-3 (MCP-3) were also observed against established hemangiosarcomas and melanomas in immunocompetent mice, respectively (Maxwell et al., 2002; Cornelis et al., 2004).

Extensive work with LuIII recombinants has been done because of the successful infection of human cells and the highly infectious genomic clone of LuIII, pGLu883 (Diffoot et al., 1993). Viral coding sequences of this clone were replaced by reporter genes like luciferase while terminal regions and P4 promoter were left untouched (Maxwell et al., 1993). This recombinant vector was used to prove that transducing viruses could be produced by transient co-transfection of these plasmids with helper constructs supplying the viral NS and VP proteins, but lacking terminal sequences. Assays were developed for titrating the LuIII recombinants in terms of total number of DNA-containing particles and of infectious units (Maxwell and Maxwell, 1994). Other experimental research also conducted by Maxwell and colleagues aimed at replacing the P4 promoter by non-viral, regulated promoters in which resulted in maintained trans-activation responses to tissue specific factors (Maxwell and Maxwell, 1994). It was also

demonstrated that LuIII recombinant genomes can also be packaged in other parvoviruses capsids like those of MVM and H-2 (Maxwell et al., 1996; Maxwell et al., 2004). Substitution of the P4 promoter by prokaryotic tetracycline operator sequences lead to a constitutive expression in transient transfected cells. Their previous experiment lead to believe that potential use for systemic LuIII recombinants in targeting metastases might be enhanced if NS1 expression and viral replication could be controlled by a safe drug such as tetracycline (Maxwell and Maxwell, 1999).

CHAPTER III

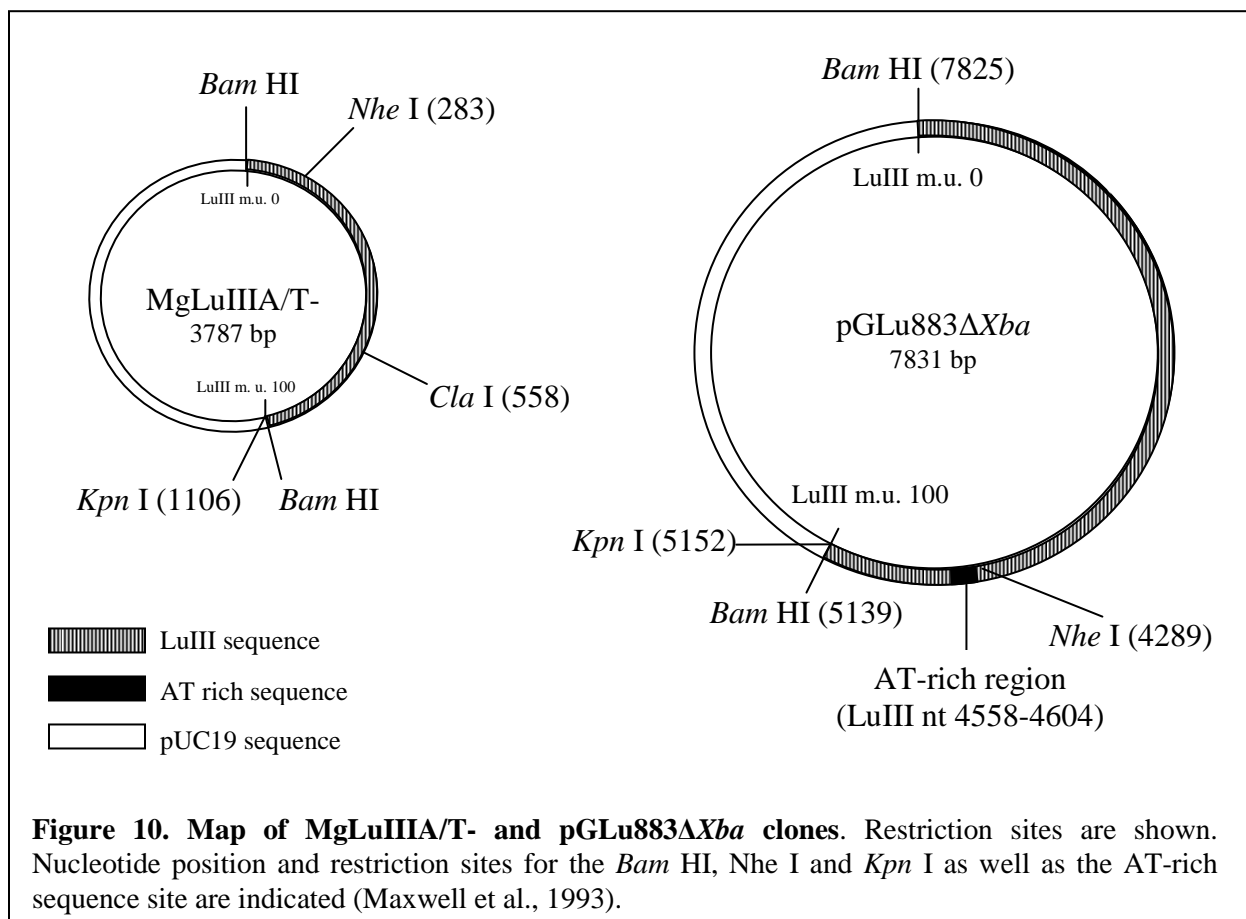
Objectives

The objective of this research was to determine the effect of deleting the 47 nucleotide AT- rich region, unique to the LuIII genome, in the encapsidation pattern of the viral DNA. In order to accomplish this objective it was necessary to:

1. Construct a genomic clone of the parvovirus LuIII lacking the 47 bp AT-rich region.
2. Transfect the modified genomic clone into HeLa cells.
3. Study the encapsidation pattern of viral progeny generated from the replication of this clone.

Materials and Methods

A helper minigenome construct named LuIII A/T minus (MgLuIII A/T-) was used for the construction of pGLu883 Δ Xba A/T-. MgLuIII A/T- contains LuIII nucleotide sequences 1 to 277 and 4924 to 5135, the left and right end palindromes respectively. These were isolated from the original genomic clone of LuIII, pGLu883 (Difffoot et al., 1989). A *Cla* I (AT/CGAT) (Roche Molecular Biochemical, Indianapolis) site was introduced at nt 4562 and the AT-rich sequence of LuIII (nt 4558 to 4604) was deleted. The *Cla* I site is immediately followed by nt 4605-7801 of pGLu883 Δ Xba, containing the right end terminal palindrome. These sequences were cloned into pUC 19 plasmid vector (Figure 10).



Construction of the pGLu883 Δ XbaAT- clone:

For the construction of pGLu883 Δ XbaA/T- (Figure 11), the full length genomic clone of the LuIII parvovirus, pGLu883 Δ Xba and the MgLuIII A/T- were digested with the restriction enzymes *Kpn* I (GTAC/CATG) and *Nhe* I (G/CTAG) obtained from Roche Molecular Biochemicals, Indianapolis. The digested pGLu883 Δ Xba and MgLuIII A/T- plasmid DNA were electrophoresed (Figure 12 A) on a 1.2% agarose gel (Fisher, Molecular Biology Grade, BP1356-100) in 1X TAE buffer (40 mM Tris-acetate, 2 mM EDTA, pH 8.5) at 70 V. Gel slices containing a pGLu883 Δ Xba fragment of 6968 bp spanned by the restriction enzyme sites for *Kpn* I and *Nhe* I (nt 5152 and 4288, respectively) and a MgLuIII A/T- fragment of 823 bp spanned by *Kpn* I and *Nhe* I restriction sites (1107 and 283, respectively) were extracted and purified (Figure 12, B) by the Gene Clean Spin Kit[®] (QBio-gene, No. 1101-200, Montréal, Canada). The extracted 6968 bp and 823 bp DNA fragments were ligated for one hour by using the Rapid DNA Ligation Kit (Roche Molecular Biochemicals, No. 11635379001, Indianapolis) at 20°C for one hour. All possible recombinant molecules were used for transformation with *E.coli* SURE[®]2 competent cells (Stratagene, 200152, U.S.A.).

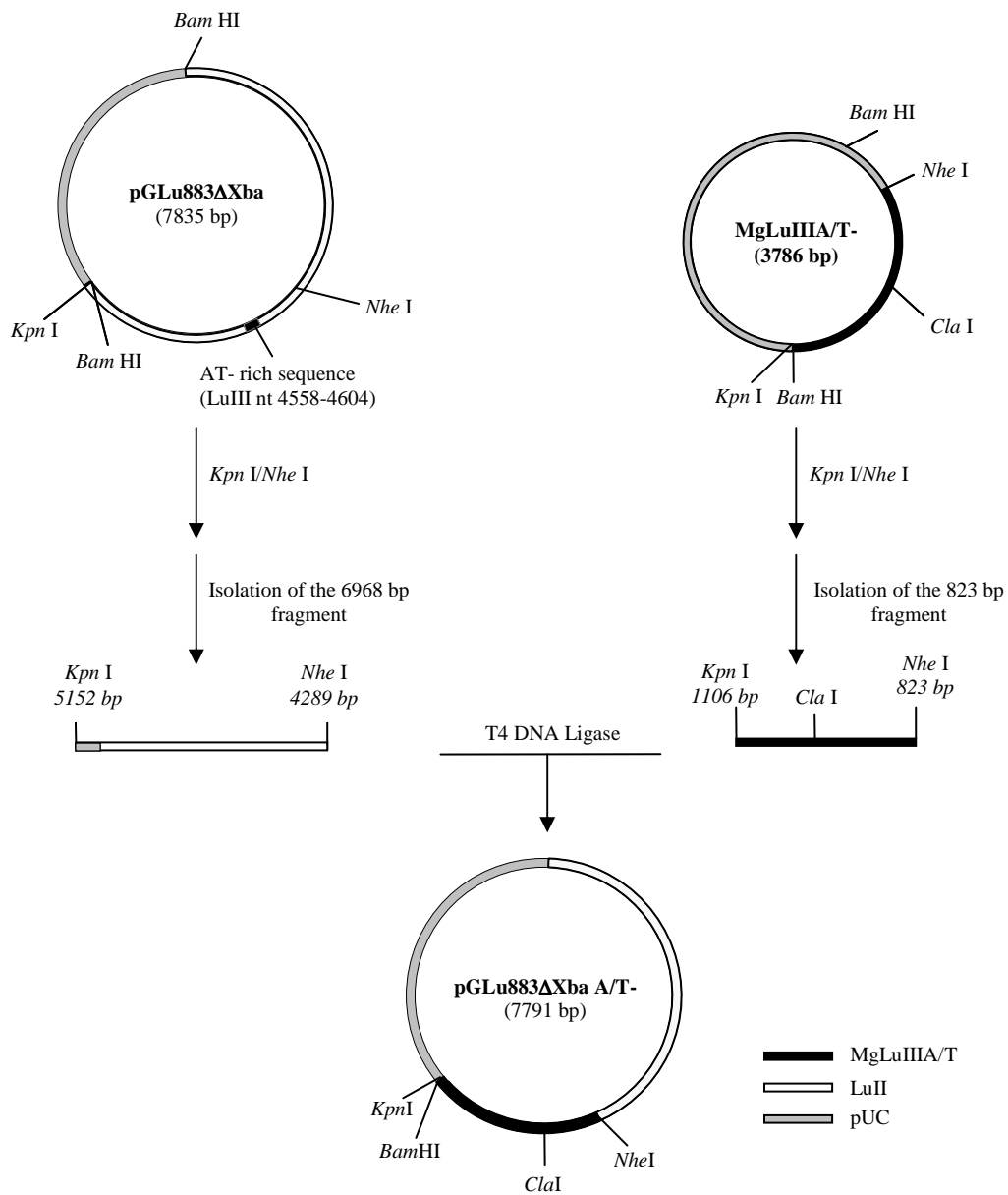


Figure 11. Strategy used to construct pGLu883ΔXba A/T-. The nucleotide positions as well as the restriction sites are indicated.

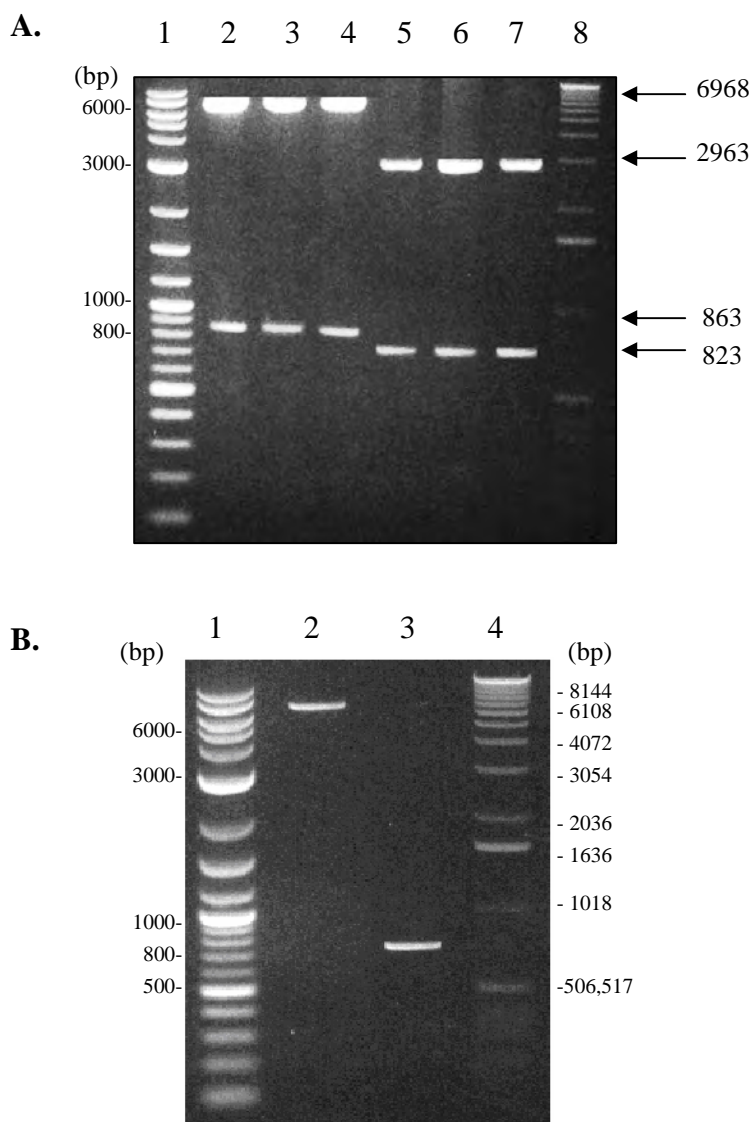


Figure 12. Digestion of pGLuIII883Δ*Xba* and MgLuIII A/T- and isolation of desired fragments for cloning. **A.** Digestion of pGLu883Δ*Xba* and MgLuIII A/T- with restriction enzymes *Kpn* I and *Nhe* I. Lane 1: 2-log Ladder, lanes 2-4: pGLu883Δ*Xba*, Lanes 5-7: MgLuIII A/T-, lane 8: 1 kb Ladder. Desired fragments are shown in bold. **B.** Isolation of the 6968 and 823 bp fragments. Lane 1: 2-log Ladder, lane 2: a purified fragment of 6968 bp obtained from the digestion of pGLu883Δ*Xba*, lane 3: purified fragment of 823 bp obtained from the digestion of the MgLu A/T-. Lane 4: 1 kb Ladder. Samples were electrophoresed on a 1.2% agarose gel in 1X TAE buffer at 76 V.

Construction of pGLu883 Δ Xba Reverse:

The strategy performed for this new construct is shown on Figure 13. The pGLu883 Δ XbaA/T- and the original genomic clone of parvovirus LuIII pGLu883 Δ Xba were digested with restriction enzymes *Kpn* I and *Nhe* I. The digested pGLu883 Δ Xba and pGLu883 Δ XbaA/T- DNA were electrophoresed (Figure 14, A) on a 1.2% agarose gel (Fisher, Molecular Biology Grade, BP1356-100) in 1X TAE buffer (40 mM Tris-acetate, 2 mM EDTA, pH 8.5) at 70 V. Gel slices containing the pGLu883 Δ XbaA/T- DNA fragment of 6968 bp and corresponding to the restriction enzymes sites for *Kpn* I and *Nhe* I (nt 5152 and nt 4288, respectively) and the pGLu883 Δ Xba DNA fragment of 863 bp corresponding to the restriction enzyme sites for *Kpn* I and *Nhe* I (nt 5151 and nt 4289, respectively) were isolated and purified (Figure 14, B) by using the GeneClean Spin Kit[®] (QBio-gene, 1101-200, Montréal, Canada). Isolated fragments were ligated by using the Rapid DNA Ligation Kit (Roche Molecular Biochemicals, No. 11635379001, Indianapolis) at 20°C for one hour. A sample containing all possible recombinant molecules were used for transformation with *E.coli* SURE[®]2 competent cells.

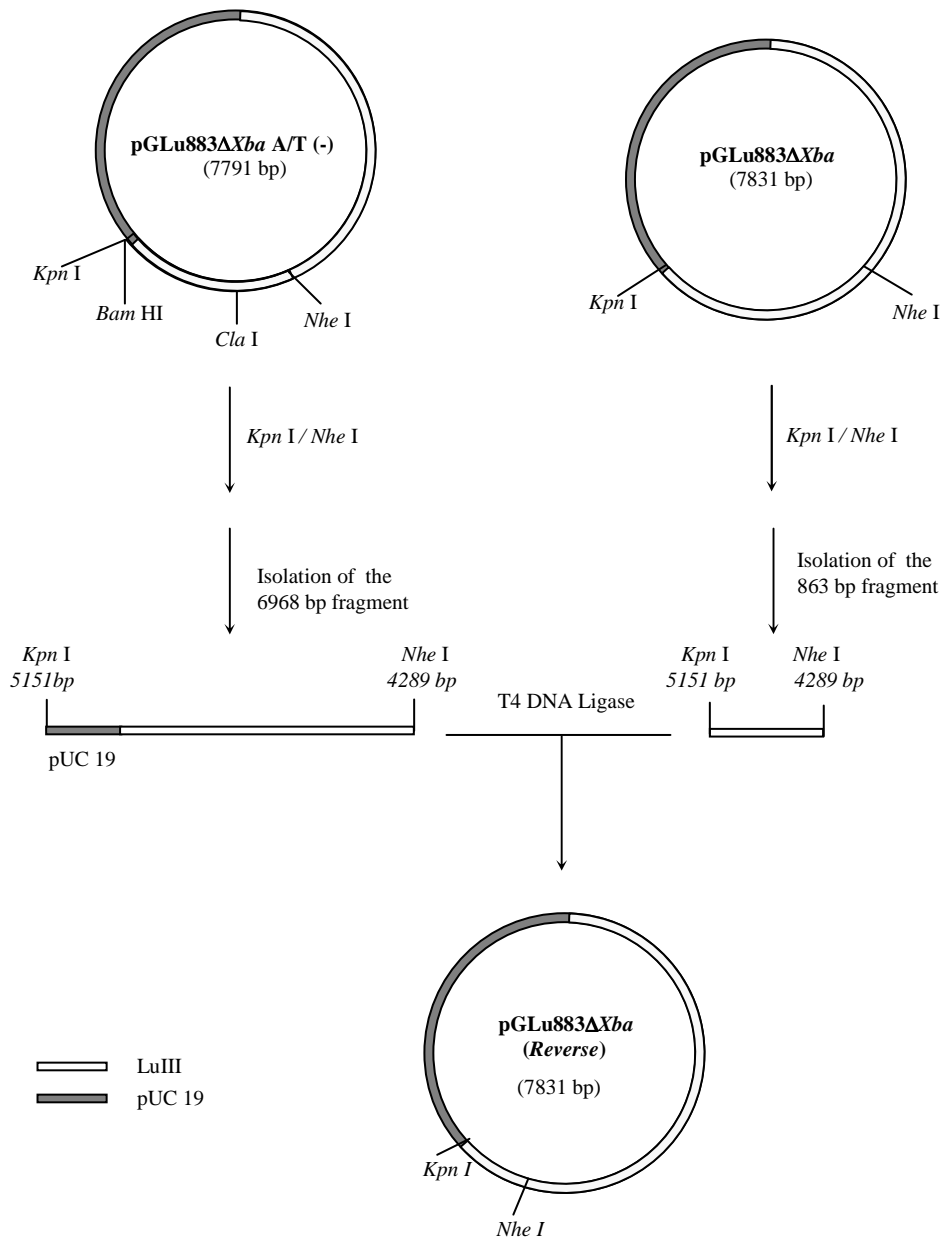


Figure 13. Strategy used to construct pGLu883ΔXba Reverse. The nucleotide positions as well as the restriction sites are indicated.

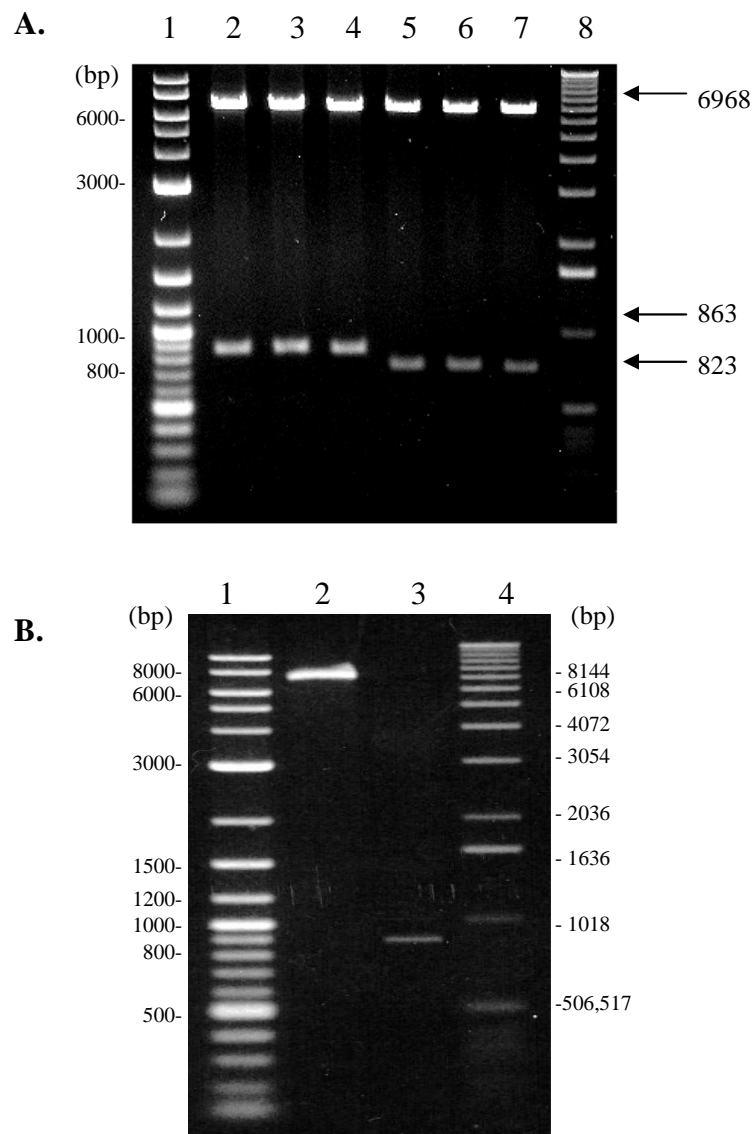


Figure 14. Digestion of pGLu883Δ*Xba* and pGLu883Δ*Xba*A/T- and isolation of the desired fragments for cloning. **A.** Digestion of pGLu883Δ*Xba* and pGLu883Δ*Xba*A/T- with restriction enzymes *Kpn* I and *Nhe* I. Lane 1: 2-log Ladder, lanes 2-4: pGLu883Δ*Xba*, lanes 5-7: pGLu883Δ*Xba*A/T, lane 8: 1 kb Ladder. **B.** Isolation of the 6968 and 863 bp fragments. Lane 1: 2-log Ladder, Lane 2: the 6968 bp purified fragment obtained from the digestion of pGLu883Δ*Xba*A/T-, Lane 3: the 863 bp purified fragment obtained from the digestion of the pGLu883Δ*Xba*, Lane 4: 1 kb Ladder. Samples were electrophoresed on a 1.2 % agarose gel in 1X TAE buffer at 72 V.

Construction of pGLu883 Δ XbaA/T- *de novo*:

The parent molecules used for the construction of pGLu883 Δ XbaA/T- *de novo* were pGLu883 Δ Xba and pGLu883 Δ XbaA/T- (Figure 15). Both plasmids were digested with the endonuclease *Ssp* I for two hours at 37°C and electrophoresed on a 1.2% agarose gel in 1X TBE buffer (100 mM Tris-borate, 2 mM EDTA, pH 8.3) at 75 V. The *Ssp* I digestion with pGLu883 Δ Xba generated three DNA fragments of approximately 6727 bp, 1068 bp and 36 bp. The 1068 bp DNA fragment contains nts 4067-5135 of the LuIII sequence, enclosing the complete right-end terminal (nts 4924-5135) of the virus. In turn the digestion of pGLu883 Δ XbaA/T- with *Ssp* I also generated three DNA fragments, of approximately 6687 bp, 1068 bp and 36 bp, as shown on Figure 16, A. The 6687 bp DNA fragment corresponded to nt 1 to nt 4638 of LuIII and is included in a sequence from the pUC 19 vector that spans from *Ssp* I 2501 bp to the *Bam* HI 417 bp sites located at the multiple cloning site. The DNA sequence that corresponds to LuIII includes the *Cla* I site from the MgLuIII A/T- with lacking the AT-rich sequence.

The 6687 bp DNA fragment obtained from the *Cla* I and the left end hairpin in addition to the 1068 bp DNA fragment with the right end hairpin were isolated and purified as described above and characterized on a 1.2% agarose gel electrophoresis in 1X TBE buffer at 70 V (Figure 16, B). The 6687 bp DNA fragment and the 1068 bp DNA fragment were ligated in an overnight reaction at 4 °C by using 1U of T4 DNA ligase (Roche, 481220). A sample containing all the possible recombinant molecules was used for transformation with *E.coli* SURE[®]2 competent cells.

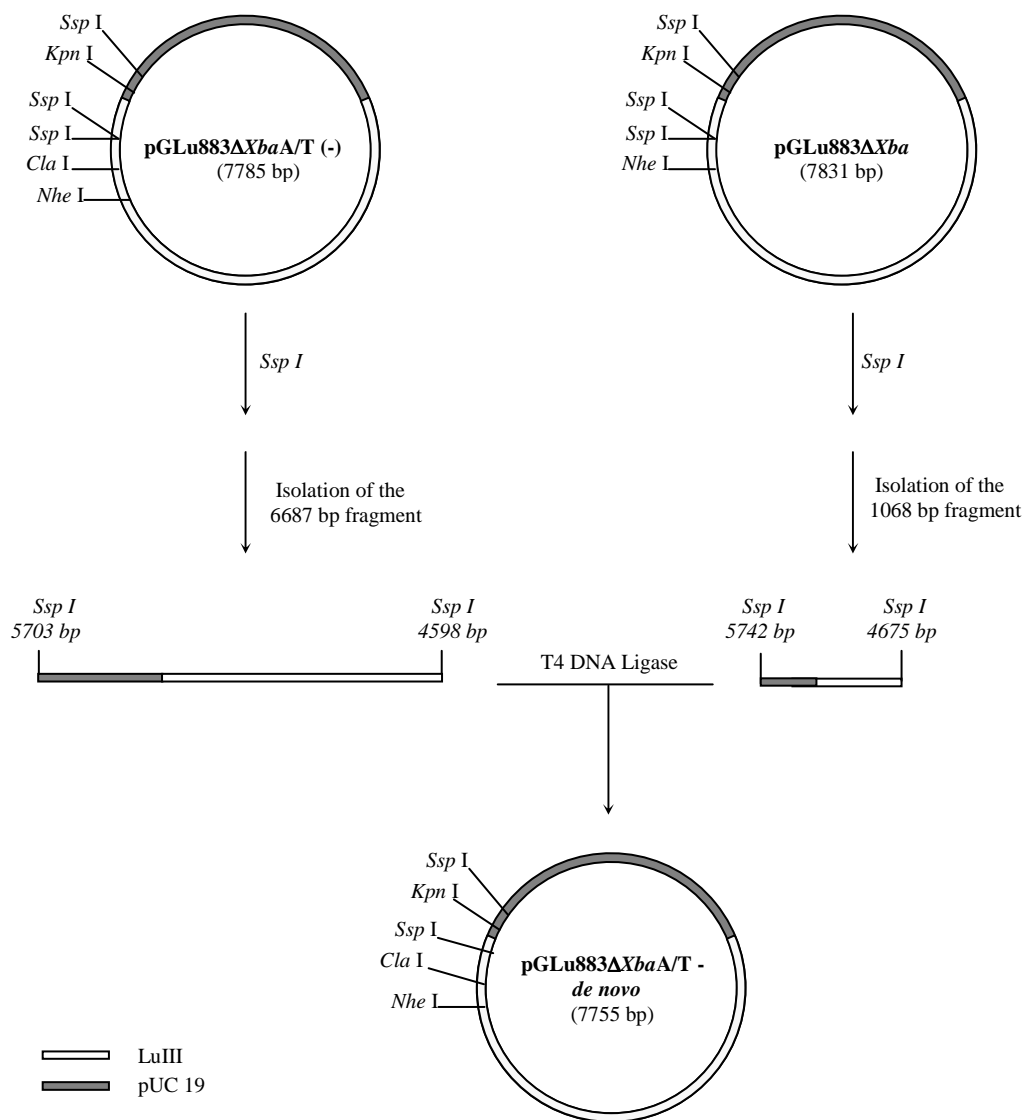


Figure 15. Strategy used to construct pGLu883ΔXbaA/T-de novo. The nucleotide positions as well as the restriction sites are indicated.

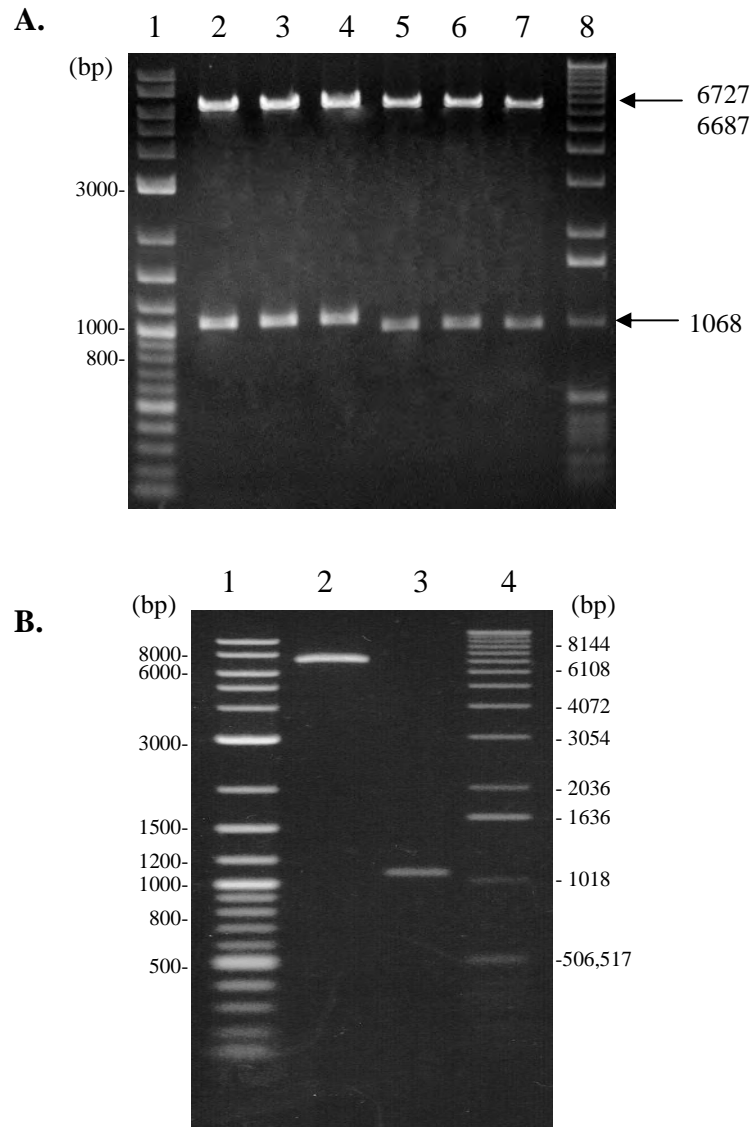


Figure 16. Digestion of pGLu883ΔXba and pGLu883ΔXbaA/T- and isolation of cloning fragments. **A.** Digestion of pGLu883ΔXba and pGLu883ΔXbaA/T- with restriction enzyme *Ssp* I. Lane 1: 2-log Ladder, lanes 2-4: *Ssp* I digests of pGLu883ΔXba, lanes 5-7: *Ssp* I digests of pGLu883ΔXbaA/T-, Lane 8: 1 kb Ladder. **B.** Isolation of the 6687 and 1068 bp fragments. Lane 1: 2-log Ladder, Lane 2: the 6687 bp purified fragment obtained from the digestion of pGLu883ΔXbaA/T- with *Ssp* I, Lane 3: the 1068 bp purified fragment obtained from the digestion of the pGLu883ΔXba also with *Ssp* I. Lane 4: 1 kb Ladder. Samples were electrophoresed on a 1.2% agarose gel in 1X TBE buffer at 76 V.

Preparation and Transformation of *E. coli* SURE[®]2 Competent Cells by the Calcium Chloride Method:

Competent cells were prepared by inoculating a single colony of *Escherichia coli* SURE[®]2 strain [(e14- (*McrA*-) Δ (*mcrCB-hsd SMR-mrr*) 171 *endA1supE44 thi-1 gyrA96 relA1 lac recB recJ sbcC umuC::Tn5* (Kan_r) *uvrC* [F' *proABlacI_qZ Δ M15 Tn10* (Tet_r) Amy Cam_r]] (Stratagene, La Jolla, California) into 1 mL of LB medium (1% Bacto[®]tryptone, 0.5% Bacto[®]yeast extract, 86 mM NaCl and 1 M NaOH). The SURE[®]2 cells were grown overnight at 37°C with constant shaking at 250 rpm. One milliliter from the culture was then transferred to 100 mL LB broth and grown until an OD₆₀₀ of 0.3-0.4 was reached. Cells were harvested by centrifugation at 2,500 rpm for 10 minutes at 4°C, and the pellet was gently resuspended in 25 mL of ice-cold 50 mM CaCl₂ and placed on ice for 30 minutes. Cells were centrifuged and gently resuspended in 5 mL of ice cold 50 mM CaCl₂ in 20% glycerol. Aliquots of 100 μ L were stored at -80°C or transferred into pre-chilled, sterile polypropylene 1.5 mL microtubes.

Between 25 ng and 40 ng of recombinant DNA from the ligation mixture were added to the SURE[®]2 competent cells. Competent cells with no plasmid DNA were used as a negative control and 10 ng of pUC 19 were added to the SURE[®]2 competent cells as a standard control. Transformants were incubated on ice for 30 minutes, heat-shocked for 30 seconds in a 42°C water bath and incubated on ice for 2 minutes. Subsequently, 100 μ L of pre-heated (42°C) LB broth were added to activate cells, and then, incubated at 37°C for one hour with constant shaking at 225 rpm. SURE[®]2 transformed cells were spread on plate of LB plates. The negative control was grown on LB plates without ampicillin. The standard control and all experimental samples were spread on LB plates containing 100 mg/mL ampicillin and 100 μ L of 10 mM IPTG. Plates were incubated overnight at 37°C.

Isolation of DNA Recombinants:

Colonies from target transformants were inoculated in 5 mL of LB broth with 100 µg/ml ampicillin, and incubated overnight at 37°C in an orbital shaker with constant shaking at 225 rpm. Plasmid DNA from transformant cells was isolated and purified by using the alkaline lysis miniprep protocol (Ausbel et al., 2005). Restriction enzyme digestion analysis was performed for all the possible recombinant molecules obtained. The restriction patterns for each of the recombinant molecules are shown in Table 4. Restriction patterns were analyzed either on a 1.2% agarose-TBE or 1.2% agarose-TAE. Large scale DNA preparations were made only for the recombinant molecules with the desired restriction patterns.

Table 4. Restriction Enzyme Patterns for three LuIII clones (bp)

Restriction Enzyme	pGLu883Δ<i>Xba</i>A/T-	pGLu883Δ<i>Xba</i> <i>Reverse</i>	pGLu883Δ<i>Xba</i>A/T- <i>de novo</i>
<i>Bam</i> HI	~5101, ~2686	~5145, ~2686	~5069, ~2686
<i>Cla</i> I	~7791	*	~7755
<i>Ssp</i> I	*	*	~6687, ~1068
<i>Bam</i> HI/ <i>Cla</i> I	~4570, ~2686, ~535	*	~4570, ~2686, ~499
<i>Bam</i> HI/ <i>Nhe</i> I	~4295, ~2686, ~810	~4295, ~2686, ~850	~4295, ~2686, ~774
<i>Nhe</i> I / <i>Kpn</i> I	~6968, ~823	~6968, ~863	~6968, ~787

*The reaction was not performed.

Tissue Culture:

HeLa (ATCC[®], No. CCL-2; Rockville, Maryland) cells were grown as monolayers until confluency at 37°C in a Minimal Essential Medium (MEM Eagle; MP Biomedicals, No. 10101; Aurora, Ohio) and supplemented with 10% fetal bovine serum (FBS; HyClone No. SH 30386.03; Logan, Utah) and PSG (8 mM Penicillin G, 3 mM Streptomycin Sulfate and 200 mM L-Glutamine).

HeLa cells were subcultured after 100% confluency (on day 4 to 5 after the passage) by rinsing the cultures twice with 1X Phosphate-Buffered Saline (1X PBS; 4.3 mM Na₂HPO₄, 1.4 mM KH₂PO₄, 137 mM NaCl, and 2.7 mM KCl, pH 7.4) to remove all traces of serum. Cells were detached from culture flasks by incubating with 1X Trypsin (Difco, No. 215240; Detroit, Michigan) for 5 minutes at 37°C, and subsequently harvested by centrifugation at 3,500 rpm for 5 minutes at 4°C. After centrifugation, the supernatant was discarded and the entire pellet was resuspended in fresh MEM media with serum and seeded into culture flasks at a dilution ratio of 1:3.

Transfection Assay:

New constructs were transfected into HeLa cells (Table 5) by the electroporation method with a capacitance discharge machine Gene Pulse II Electroporation System (Bio-Rad Laboratories, Hercules, California) at 230 V and 960 μF. Transfected HeLa cells were grown to 100% confluency, rinsed three times with 1X PBS at 37°C and incubated in 1X Trypsin for 5 minutes at 37°C. Cells were centrifuged twice at 3800 rpm for 5 minutes at 4°C. The pellets were rinsed again in 10 mL of 1X PBS and centrifuged as described before. Pelleted cells were then resuspended in 7.2 mL of fresh MEM media and collected into 1.5 mL microtubes (800 μL per microtube). Approximately 5 μg of every clone (Table 5) were added to the corresponding

microtubes and incubated at 37°C for 10 minutes. Cells were transferred into sterile cuvettes (4 mm gap width) and electroporated separately. Following each pulse, 700 µL of fresh MEM media containing 10% FBS were added to the cuvette and the cells were resuspended carefully. Transfected cells were incubated at 37°C for 45 minutes, and then, transferred to 25 cm² flasks with 3 mL of fresh MEM media containing 10% FBS. Flasks were incubated at 37°C overnight. The medium was changed and the cells returned to the incubator for 6-7 days post-transfection before isolating the incorporated DNA, (Tam and Astell, 1993). The DNA was treated with proteinase K for several hours at 37°C and extracted with phenol/chloroform, and precipitated with 2 volumes of isopropanol. DNA was resuspended in 30 µL TE buffer (10 mM Tris-HCl, 1 mM EDTA, pH 8.0) and treated with RNase for 1 hour at 37°C.

Table 5. DNA samples used for transfection assays with HeLa cells

Sample	Transfection Assay I	
	Plasmid DNA	Flask
1	Cells w/o plasmid DNA	Negative Control
2	pGLu883Δ <i>Xba</i>	Positive Control
3	pCMVNS1	Negative Control
4	pGLu883Δ <i>Xba</i> A/T-	Experimental
5	pGLu883Δ <i>Xba</i> A/T- + pCMVNS1	Co-transfection
6	pGLu883Δ <i>Xba</i> A/T- + MgLuIII A/T (+)	Co-transfection
7	pGLu883Δ <i>Xba</i> A/T- + Mg LuIII A/T (-)	Co-transfection

Sample	Transfection Assay II	
	Plasmid DNA	Flask
1	Cells w/o plasmid DNA	Negative Control
2	pGLu883Δ <i>Xba</i>	Positive Control
3	pGLu883Δ <i>Xba Reverse</i>	Experimental

Sample	Transfection Assay III	
	Plasmid DNA	Flask
1	Cells w/o plasmid DNA	Negative Control
2	pGLu883Δ <i>Xba</i>	Positive Control
3	pCMVNS1	Negative Control
4	pGLu883Δ <i>Xba</i> AT(-) <i>de novo</i>	Experimental
5	pGLu883Δ <i>Xba</i> AT(-) <i>de novo</i> + pCMVNS1	Co-transfection
6	pGLu883Δ <i>Xba</i> AT(-) <i>de novo</i> + MgLuIII A/T (+)	Co-transfection
7	pGLu883Δ <i>Xba</i> AT(-) <i>de novo</i> + MgLuIII A/T (-)	Co-transfection

Southern blot analysis:

Samples of the extracted DNA were treated with restriction enzymes and their buffers recommended by the manufacturer. Band patterns were analyzed on 1.2% agarose gel electrophoresis in 1X TBE or TAE buffer at 70 V. The restriction enzymes *Dpn* I and *Mbo* I were used to distinguish replicated DNA. These enzymes recognize methylated and unmethylated DNA, respectively. The replication of a transfected DNA plasmid in eukaryotic cells can be assayed by the resistance to *Dpn* I and sensitivity to *Mbo* I endonucleases. *Dpn* I gains activity when both adenosines from the enzyme recognition sequence (GATC) are methylated. A kind of methylation not performed by eukaryotic methylases. Resistance to *Dpn* I suggests that DNA has been hemimethylated or lacked methylation, a scenario that results from one or two rounds of DNA replication respectively, in an eukaryotic host. *Mbo* I will cleave DNA only when adenosines from the enzyme recognition sequence (GATC) are unmethylated, reflecting replication by the eukaryotic machinery (Cotmore and Tattersall, 1992). This feature allows differentiation between input (un-replicated) and output (replicated) DNA (Rhode, 1989).

Plasmid DNA was passively transferred to a Zeta-Probe[®] GT Nylon Membrane (Bio-Rad, No. 162-0196XTU; Hercules, California) using 0.4 M NaOH (Ausubel et al., 2005). An isolated fragment of 5,135 bp, corresponding to the LuIII viral genome, was labeled by a random primed DNA labeling method with Digoxigenin-11-dUTP and used as probe (Roche Applied Science No. 11004760001; Indianapolis, Indiana). The blot was hybridized overnight at 42°C with slow constant shaking. Washes were performed twice with 50 ml of 2X SSC (Saline-Sodium Citrate) / 0.1% SDS (Sodium Dodecyl Sulfate) for 20 minutes at 65°C and once with 0.1X SSC/ 0.1% SDS for 1 hour at 65°C. Detection of the Dig-labeled DNA was accomplished with the

Chemiluminescent Detection Protocol provided by the DIG System User's Guide for Filter Hybridization (Roche Diagnostics, No. 11585614910; Indianapolis, Indiana).

CHAPTER IV

Results and Discussion

Autonomous parvoviruses are single-stranded DNA viruses with palindromic termini that encapsidate strands of either plus or minus polarity (Faisst et al; 2000). Research data suggest that the termini together with few adjacent nucleotides provide all the *cis*-acting information required for both viral DNA replication and progeny genome encapsidation (Cotmore and Tattersall, 1996). To date, replication strategies for the autonomous replicating parvoviruses have been best explored for Minute Virus of Mice (MVM) species of the genus *Parvovirus* (Cotmore and Tattersall, 2006). Sequence comparison of MVM and LuIII demonstrate a 90% DNA sequence identity between their termini and a 80% DNA sequence identity between genomes. This phenomenon contrasts with the fact that 99% of the assembled MVM particles have a negative polarity genome, while LuIII encapsidates both strands with equal frequency. Sequence analysis of the full genome of parvovirus LuIII exposed an AT-rich stretch of 47 nucleotides long, starting at nucleotide position 4560, unique to the LuIII genome. The absence of a similar region in parvovirus MVM hinted other researchers with the possibility that this region might be related to the characteristic virion DNA distribution (Diffoot et al., 1993). Because LuIII is considered a promising vector for gene therapy, for proper protocols in future applications, its mechanisms of replication, strand encapsidation and translocation must be elucidated. The aim of this project was to determine the role of the AT-rich region of parvovirus LuIII in the packaging of its viral DNA. A highly infectious genomic clone of LuIII, the pGLu883 Δ Xba, was modified to lack the AT-rich sequence (47 bp) in order to address this hypothesis.

pGLu883Δ*Xba*A/T- plasmid:

A plasmid containing parvovirus LuIII without the AT-rich sequence was constructed as described in the Materials and Methods chapter. The construct pGLu883Δ*Xba*A/T- contains the complete genome of LuIII (from nucleotide (nt) 1 to 5135) but lacks the AT-rich sequence (nt 4558 to 4604). Results from bacterial transformation, restriction endonuclease analysis, transfection assay and Southern blot analysis of pGLu883Δ*Xba*A/T- were as follows.

Bacterial Transformation:

Transformation results are shown on Table 6. Transformation of *E. coli* SURE[®]2 cells with the pGLu883Δ*Xba*A/T- recombinant molecules resulted in a transformation efficiency of 5.7×10^5 cfu/μg. The cell control plate resulted in normal growth of bacterial lawn. No cell growth was observed in the ampicillin control plates, demonstrating that the cells exhibit sensitivity to this antibiotic. Blue colonies grew on the transformation control plates, while the white colonies grew on a selective media of the experimental samples. Since LuIII was cloned in the *Bam* HI site of the multiple cloning site (MCS) of the pUC 19 vector and the MCS is inserted after the fourth codon of the *lacZα* gene, LuIII interrupts the expression of the gene.

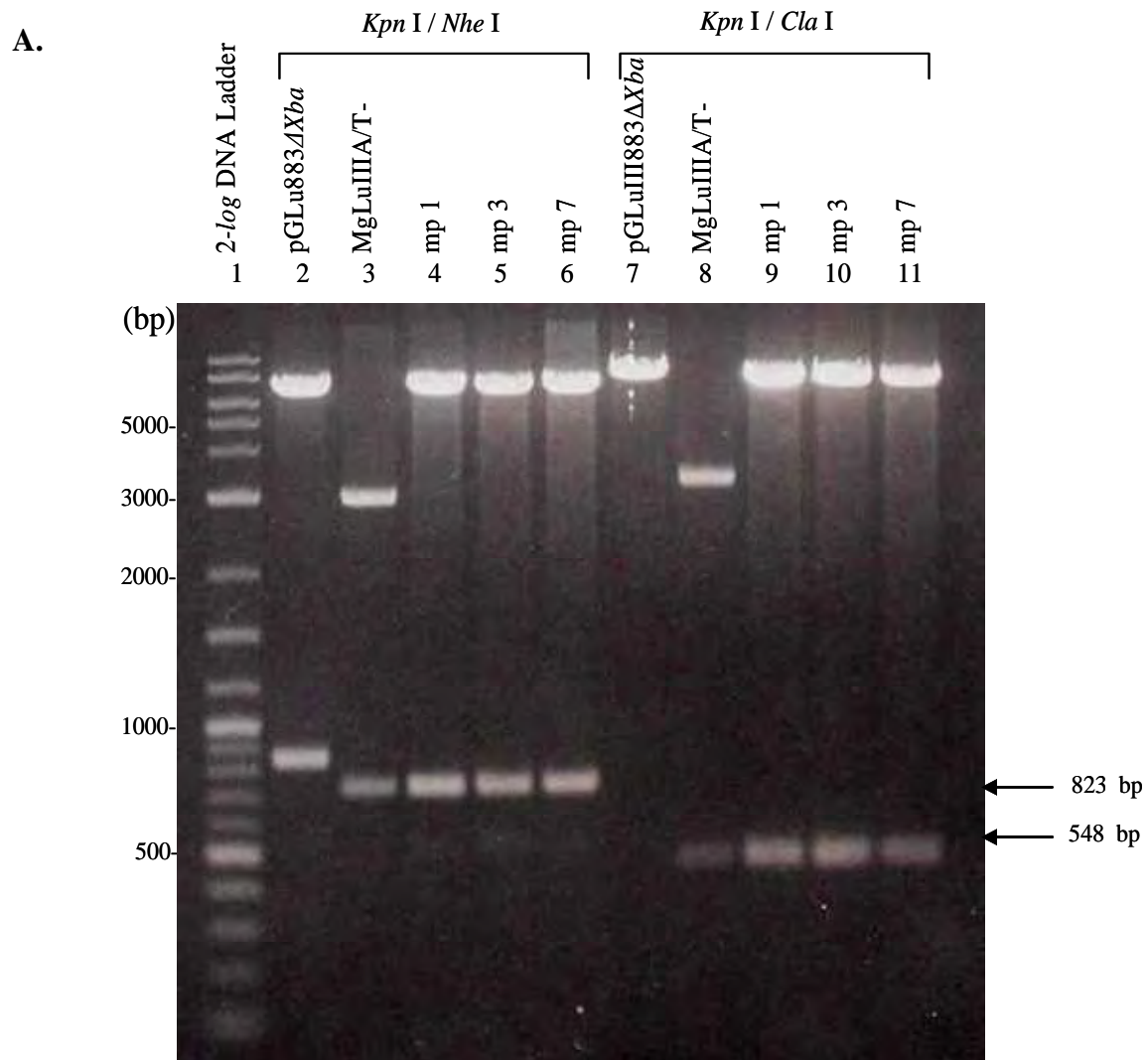
Table 6. Transformation of SURE[®] 2 competent cells with pGLu883Δ*Xba*A/T-

Transformation Sample	Plate	DNA added	DNA Concentration ^a (ng)	Results
1	Control for cell growth	none	0	bacterial lawn
2	Control for antibiotic	none	0	no colonies
3	Control of Transformation efficiency	pUC 19	~10	5,700 blue colonies
4	Experimental	pGLuΔ <i>Xba</i> A/T-	~36	93 white colonies

^a Estimated concentration is based on the amount of vector in the ligation reaction per 100 μl of competent cells.

Restriction enzyme analysis:

The isolated DNA plasmid was subjected to restriction enzyme digestion analysis and subsequently electrophoresed (Figure 17). Preparations of pGLu883Δ*Xba*A/T- recombinant DNA constructs were first characterized by digestion with *Kpn* I and *Nhe* I. Constructs with expected DNA fragments generated two bands of ~823 bp and ~6968 bp, indicating the presence of the MgLuIII A/T- insert and the pGLu883Δ*Xba* vector sequence, respectively (Figure 17; lanes 4-6). The *Cla* I site in the MgLuIII A/T- corresponds to the region that lacks the AT-rich sequence. To verify the presence of this *Cla* I site, recombinants these were also digested with *Cla* I and *Kpn* I. Expected DNA fragments of ~548 bp and ~7243 bp were observed (Figure 17; lanes 9-11). Three different mini-preparations, arbitrarily termed as mp 1, mp 3 and mp 7, exhibited restriction patterns as described. These results suggest that our target clone was constructed recovered from the bacterial transformation successfully.



B.

Plasmid	Restriction Enzyme	Cut sites	Approximate Length (bp)
pGLu883Δ <i>Xba</i>	<i>Kpn</i> I/ <i>Nhe</i> I	5152-4289	6968, 863
	<i>Kpn</i> I/ <i>Cla</i> I	5152	7831
MgLuA/T(-)	<i>Kpn</i> I/ <i>Nhe</i> I	1111-288	2963, 823
	<i>Kpn</i> I/ <i>Cla</i> I	1111-563	3242, 548
pGLu883Δ <i>Xba</i> A/T-	<i>Kpn</i> I/ <i>Nhe</i> I	5152-4289	6968, 823
	<i>Kpn</i> I/ <i>Cla</i> I	5152-4564	7243, 548

Figure 17. *Kpn* I/*Nhe* I and *Kpn* I/*Cla* I digestions of the recombinants pGLu883Δ*Xba*A/T-. A. Samples were electrophoresed on a 1.2% agarose gel in 1X TAE buffer at 76 V. Digestions of the plasmid minipreparations were compared to the *Kpn* I/*Nhe* I and *Kpn* I/*Cla* I digestions of pGLu883Δ*Xba* and MgLuIII A/T-. Sizes of the 2-log DNA Ladder (lane 1) are indicated. **B.** Expected length of the fragments generated for each plasmid when digested with the selected restriction enzymes.

Transfection of HeLa cells with pGLu Δ XbaA/T-:

HeLa cells were cultured at 37°C after eight days of incubation. No significant changes in the HeLa monolayer were observed during the first five days post-transfection since all samples grew until confluency was achieved. Control cells behaved confluent until day 8 post-transfection (Figure 18, A). On the day 6, the first sign of cytopathic effects (CPE) was evident for the cells transfected with pGLu883 Δ Xba (positive control), indicating a successful transfection. At the beginning, the CPE appeared to be localized but progressed to a 100% CPE after day 7 (Figure 18, B) demonstrating that the viral genome has excised and replicated for establishing an infection. The experimental sample, pGLu883 Δ XbaA/T-, was similar to the cell control. Thus, CPE was not observed, as shown in Figure 19, C.

The LuIII genome without the AT-rich sequence resembles the MVM genome and is expected to encapsidate a 99% of the negative (-) strand. Data from studies of the infectious capabilities of the plus and minus strands of parvovirus LuIII (De La Mota-Peynado, 2004) suggest that the single strand viral DNA alone is more effective than the mixture of single strand and double strand DNA. De La Mota-Peynado observed no difference between cells transfected with pGLu883 Δ Xba and cells transfected with the LuIII (-) strand, both infections progress similarly. Therefore, if the virus encapsidates mostly the (-) strand, CPE should be observed. If difficulties exist with the virus replication the viral strands will not be encapsidated and no CPE will be observed.

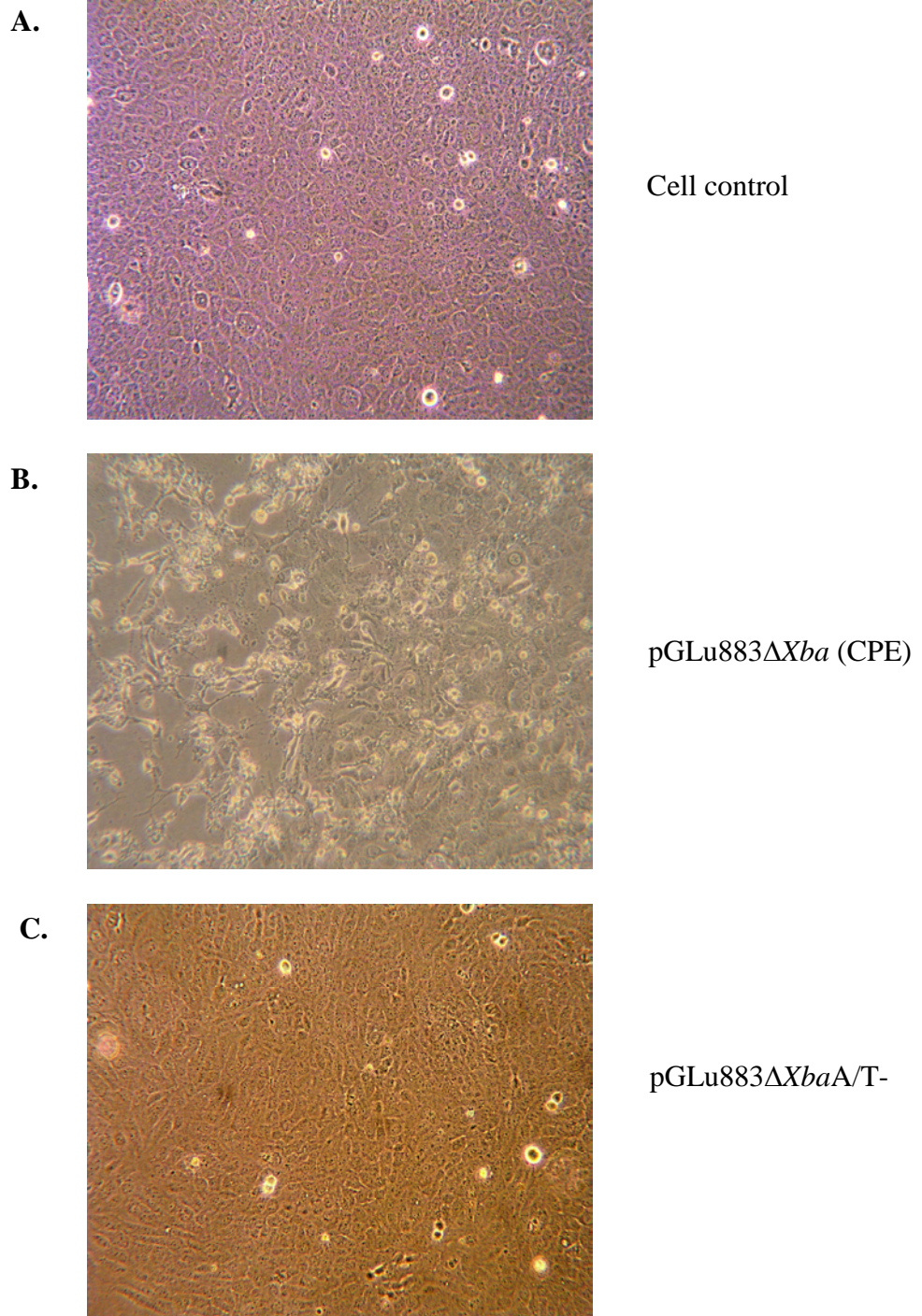


Figure 18. HeLa cells electroporated with pGLu883Δ*XbaA/T-*. Cells were photographed at day 8 post-transfection. **A.** Cell control with confluent HeLa cells, **B.** HeLa cells transfected with pGLu883Δ*Xba* with visible CPE, **C.** Confluent HeLa cells transfected with pGLu883Δ*XbaA/T-*.

Southern blot analysis of samples of transfection with pGLu883Δ*Xba*A/T-:

To determine if pGLu883Δ*Xba*A/T- had the ability to replicate in the eukaryotic cells, DNA isolated from these HeLa cells was digested with the restriction enzyme *Mbo* I and fragments were electrophoresed on a 1.2% agarose gel (Figure 19, A). *Dpn* I/ *Mbo* I sensitivity allows differentiation between input (unreplicated) and output (replicated) DNA. The results from the Southern blot analysis of the transfected DNAs digested with *Mbo* I are shown in Figure 19, B. Lane 1 shows the 2-*log* DNA Ladder, and lane 2 represents the negative control, in which no foreign DNA was added to the HeLa cells. No bands were observed in this lane indicating the absence of non-specific binding between the HeLa genomic DNA and the LuIII probe. A 5,135 bp band that corresponds to the full genome of parvovirus LuIII is shown in lane 3. In lane 4 it shown the banding pattern of pGLu883Δ*Xba* digested with *Dpn* I, used to compare plasmid DNA to the transfected DNA digested with *Mbo* I in lane 5. Similar banding patterns between the samples in lanes 4 and 5 are a positive indicator of replication. The transfected DNA of pGLu883Δ*Xba* digested with *Mbo* I is shown in lane 5. A positive signal of this sample suggests that, as expected, DNA was recovered from the transfected cells. Thus, pGLu883Δ*Xba* was replicated successfully in the eukaryotic cells. Lane 6 shows the restriction endonuclease pattern of pGLu883Δ*Xba*A/T- digested with *Dpn* I. Lane 7 shows the transfection DNA of pGLu883Δ*Xba*A/T-. If the DNA was able to replicate, the restriction endonuclease cleavage of *Mbo* I should give a similar banding pattern to that of the sample in lane 6. These results suggest that pGLu883Δ*Xba*A/T- was not capable of replicating. Four assays identical to the one described above were performed with a similar outcome each time.

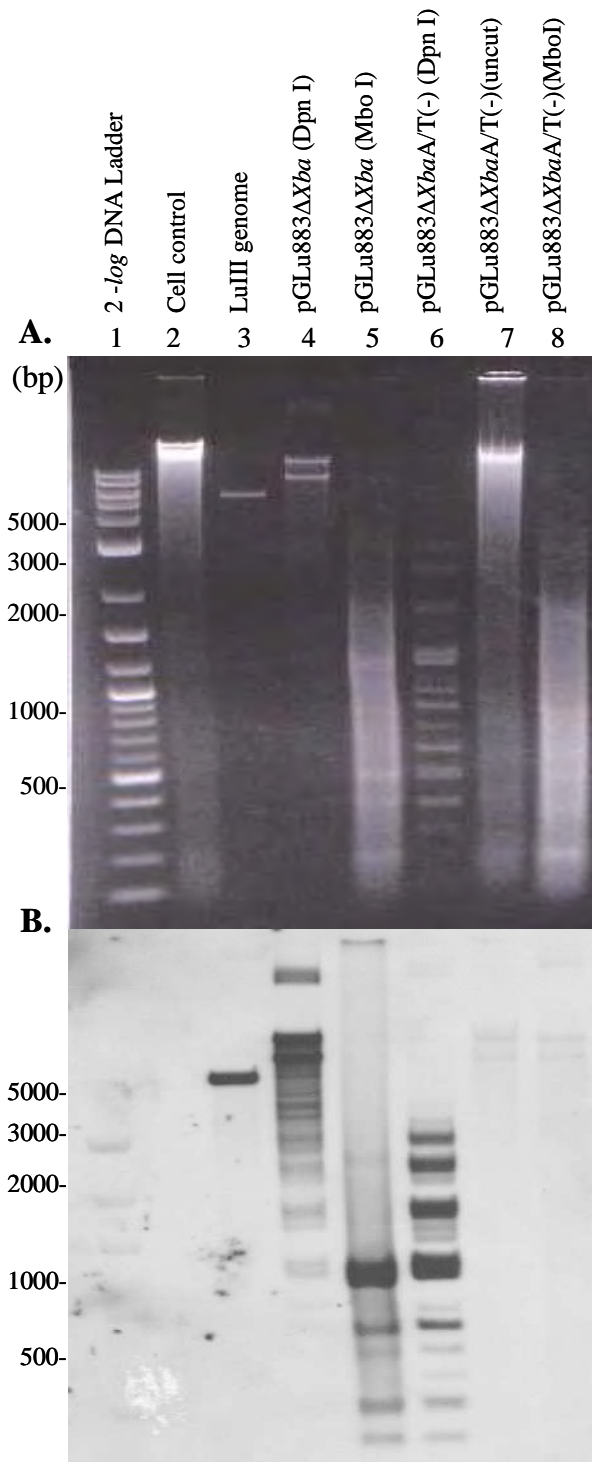


Figure 19. A. Agarose gel electrophoresis and B. Southern blot of DNA samples purified from transfected HeLa cells. Samples electrophoresed are indicated above. The blot was hybridized with the LuIII full-length genome, labeled by random primed Digoxigenin-11-dUTP. The radiograph was exposed for 4 hours.

Requirements for parvovirus replication are the non-structural protein NS1 and the *cis*-acting elements located in the terminal regions (Cotmore and Tattersall, 2006). The parental molecule used to construct pGLu883 Δ *Xba*A/T-, the genomic clone pGLu883 Δ *Xba*, is capable to replicate, encapsidate and infect HeLa cells as observed by the transfection assay. As a result, the integrity of both the NS1 coding sequence as well as the sequence of both termini should be conserved. In order to construct the pGLu883 Δ *Xba*A/T-, pGLu883 Δ *Xba* was digested with *Nhe* I and *Kpn* I. The *Nhe* I cut at a site located 2015 bp downstream from the end of the NS1 coding sequence and *Kpn* I cut at a site located 823 bp downstream of *Nhe* I. Accordingly, the digestion of pGLu883 Δ *Xba* with *Nhe* I and *Kpn* I should not interfere with the NS1 coding sequence of LuIII. Clones of plasmid DNA obtained from various parvovirus genomes have been found to require an intact NS1 gene sequence in either *cis* or *trans* orientation for the subsequent excision from the plasmid and replication of the viral sequences. When NS1 is provided in *trans*, minigenomes containing the right and left (RL), two right (RR) or two left (LL) termini become replication competent genomes (Tam and Astell, 1993). To address the possibility that the NS1 gene in pGLu883 Δ *Xba*A/T- is not functional, pGLu883 Δ *Xba*A/T- was cotransfected with pCMVNSI, a plasmid that contains the complete NS1 coding sequence of the MVMp (Minute Virus of Mice prototype strain) parvovirus under the CMV promoter (the human cytomegalovirus immediate-early gene promoter) cloned into the pCDNA3 vector. The pCMVNSI plasmid should provide the pGLu883 Δ *Xba*A/T- plasmid with NS1 in *trans*.

All *cis*-acting sequences required for both MVM and LuIII DNA replication reside in the terminal nucleotides of the left and right termini (Cotmore and Tattersall, 1996; Clément et al., 2001). Thus, in order to replicate, MVM and LuIII termini need to be intact. In cotransfections with defective viral molecules of MVM with a helper DNA the wild type virus is generated

through homologous recombination between vector and helper DNA (Clément et al., 2001). The pGLu883Δ*Xba*A/T⁻ was also cotransfected with LuIIIMgA/T⁻ or LuIIIMgA/T⁺ in order to promote recombinant events between their termini. If the pGLu883Δ*Xba*A/T⁻ molecule has a mutated termini, recombination with the helper molecule might restore function to the affected terminal palindrome. The construct LuIIIMgA/T⁺ is identical to LuIIIMgA/T⁻ but it has the 47 bp AT-rich sequence. The minigenomes have both the right and left end termini of LuIII and these have been shown to replicate in the presence of pGLu883Δ*Xba* (unpublished data). They can replicate when NS1 is provided by pGLu883Δ*Xba*, since both have all the *cis* elements in the viral termini needed for its replication.

Cotransfection of HeLa cells with pGLu883Δ*Xba*A/T⁻ and pCMVNS1, MgLuIIIA/T⁻ and MgLuIIIA/T⁺:

Cotransfected HeLa cells were incubated for 8 days at 37°C and the results are shown in Figure 20. In the cell control flask (no DNA added), the cells achieved confluency at day 8 post-transfection. In the flask transfected with pGLu883Δ*Xba* (a positive control), cells looked confluent until day 6 post-transfection, and started to show a localized infection (Figure 20). No CPE was observed from cells transfected with pCMVNS1. As described before, no CPE observed on cells transfected with pGLu883Δ*Xba*A/T⁻ or on cells cotransfected with pGLu883Δ*Xba*A/T⁻ and pCMVNS1, MgLuIIIA/T⁻ and MgLuIIIA/T⁺.

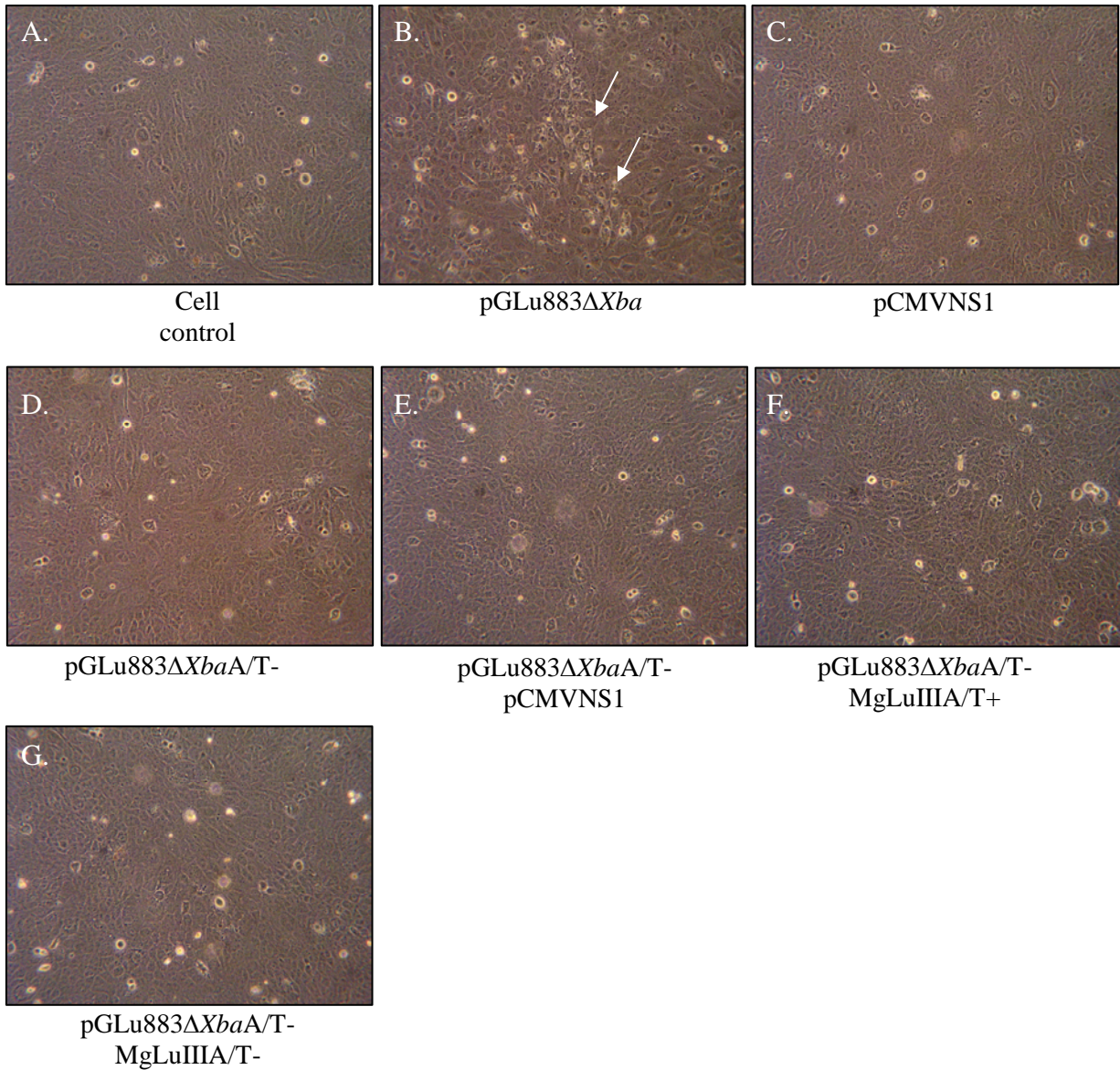


Figure 20. HeLa cells electroporated with pGLu883ΔXbaA/T- recombinant clone. White arrows on figure B. shows cells with CPE effects due to viral infection. Cells were photographed at day 8 post-transfection.

Southern blot analysis of samples from cotransfections with pGLu883Δ*Xba*A/T-:

After the cotransfection assay, total DNA was extracted and replication was assessed by digestion with *Dpn* I or *Mbo* I (Figure 21, A) followed by a Southern blot analysis (Figure 21, B). Lane 1 shows the 2-*log* DNA Ladder, lane 2 shows the 5,135 bp band that corresponds to the LuIII genome and can be used to compare the migration of the double stranded viral DNA, lanes 3 to 5 show the transfected pGLu883Δ*Xba* sample uncut, digested with *Dpn* I and with *Mbo* I, respectively. As observed on the blot, uncut samples of replicated pGLu883Δ*Xba* results in two bands. These bands migrate as a ~5 kb and ~2.5 kb double and single stranded linear DNA molecule, respectively. The ~5 kb band is comparable to the LuIII genome in lane 2. The pGLu883Δ*Xba* sample digested with *Dpn* I shows a band pattern similar to the uncut sample while the sample digested with *Mbo* I shows a restriction pattern as expected from the replicated plasmid. Plasmids capable to replicate in eukaryotic cells, when digested with *Dpn* I, should result in a restriction pattern similar to the uncut samples, because these samples are expected to lack methylation, and therefore, are not sensitive to the restriction endonuclease activity with *Dpn* I. Given that *Mbo* I recognizes the same nucleotide sequences as *Dpn* I in the non-methylated state, *Mbo* I digestion of replicated plasmids that lack methylation is expected to generate 24 DNA fragments with the largest fragment of ~1.2 kb and the smallest of ~8 bp. Lanes 6 to 8 correspond to pCMVNS1 samples of uncut, digested with *Dpn* I and *Mbo* I, respectively. The NSI sequence inserted in the pCDNA3 vector comes from parvovirus MVMp. The LuIII probe used here has a high sequence specificity and although LuIII and MVM share sequence homology, their DNA sequences are not identical. Hence, there is no visible probe signal on these lanes. Lanes 9 to 20 show the experimental results from pGLu883Δ*Xba*A/T-transfected DNA to pGLu883Δ*Xba*A/T- cotransfections with the pCMVNS1 plasmid and the

minigenomes. These samples share similar results because both the uncut and the *Mbo* I digested samples are analogous and the *Dpn* I digested samples have a restriction pattern similar to non replicated plasmid DNA. Accordingly, the pGLu883 Δ *XbaA*/T- transfection and cotransfections resulted in a non evident replication.

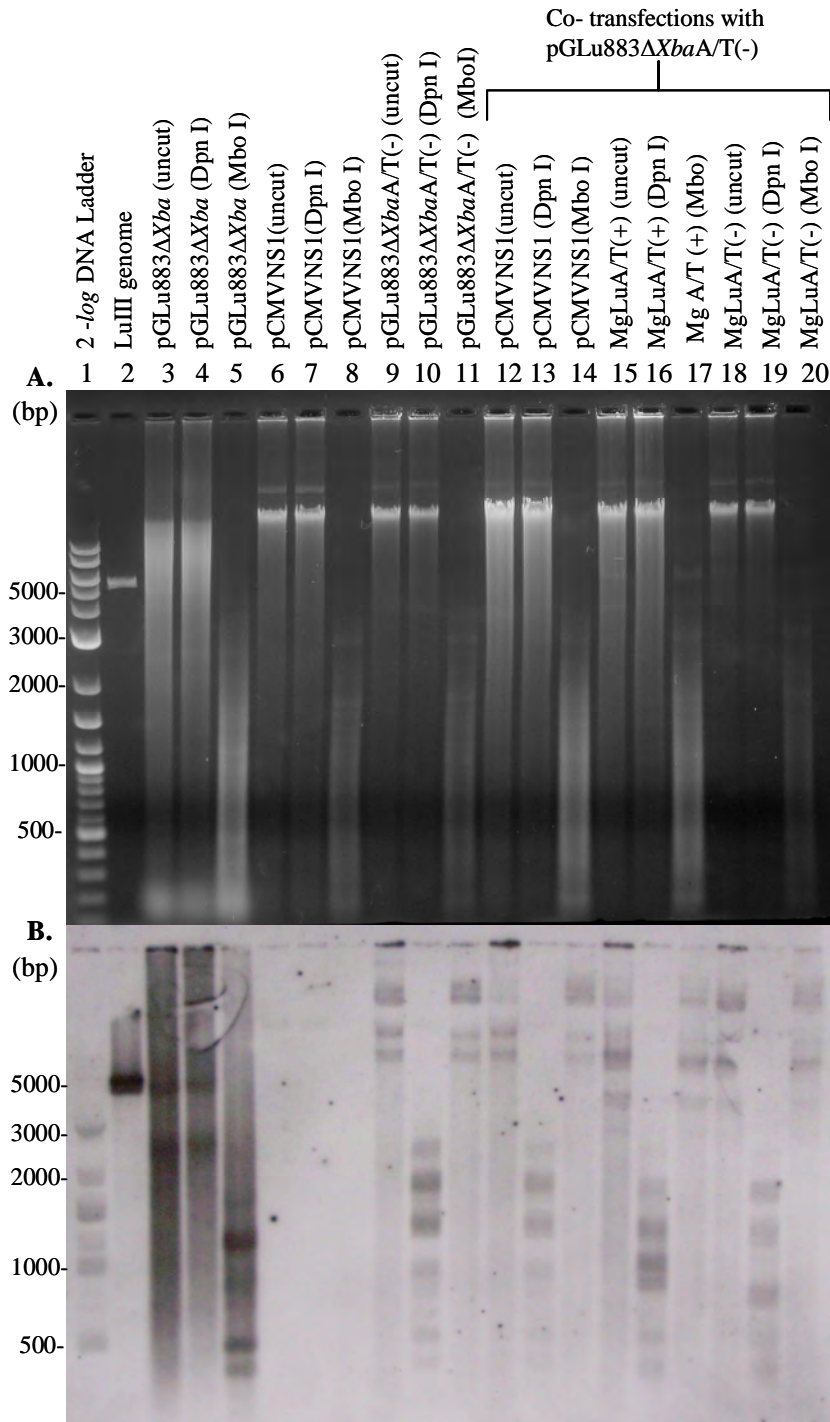


Figure 21. Gel electrophoresis (A) and Southern Blot (B) of DNA isolated from transfected HeLa cells. Samples electrophoresed are indicated above. The 1.2% agarose gel was electrophoresed in 1X TAE buffer at 80 V. The blot was hybridized with the LuIII probe. The radiograph was exposed for 14 hours.

Six assays of pGLu883 Δ XbaA/T- cotransfections with the minigenomes and the pCMVNS1 have been done with similar results on each time. The lack of replication could be explained by one of two possibilities, either because the integrity of one of the viral termini was affected in a molecular rearrangement or because the absence of the AT-rich region can inhibit the replication of the virus. The NS1 protein is responsible for DNA excision of the viral genome from the pUC 19 plasmid and it is also directly involved in its viral replication. Since NS1 moiety was assembled in *trans* orientation, and there is conclusive data suggesting that genomic APV vectors need NS1 in either *cis* or *trans* orientation in order to replicate, their lack of replication could not be attributed only to a defective NS1 sequence. Given that pGLu883 Δ XbaA/T- was not able to replicate when cotransfected with MgLuIII A/T- and MgLuIII A/T+, it is possible that LuIII needs the AT-rich sequence in order to replicate efficiently and that the AT-rich sequence can not be provided in *trans* and instead the *cis* arrangement is preferred.

Rhode deleted 75% of the right-end palindrome of LuIII (from nt 4970 to nt 5088). This deletion did not include the AT-rich sequence (Rhode, 1989). The mutation did not eliminate the replication entirely. A decrease in the excision and replication efficiency was noticeable. He also observed *Dpn* I resistance in a portion of the full-length linear DNA, thus indicating that some DNA synthesis had occurred. The synthesis was presumably done, on one strand, using the intact viral left-end as the origin. Taking all these data into account, a strategy to prove the viability of the viral termini was determined. If the left terminus can replicate and compensate the absence of a 75% of the right terminus the pGLu883 Δ XbaA/T- molecule might have a damaged left-end. Thus, the right terminus of pGLu883 Δ Xba has to be cloned into the AT-site.

pGLu883Δ*Xba* Reverse plasmid:

The AT-rich sequence of pGLu883Δ*Xba* was cloned into pGLu883Δ*Xba*A/T- in order to determine if the integrity of the LuIII terminal sequences, in particular the left-end. To determine if the left end terminus was responsible for the inability of pGLu883Δ*Xba*A/T- to replicate when transfected into HeLa cells and not the AT-rich sequence a clone containing the left terminal sequence of pGLu883Δ*Xba* and the right terminal sequence of pGLu883Δ*Xba*A/T- was constructed.

Bacterial transformation of the pGLu883Δ*Xba* Reverse recombinat molecules:

The transformation efficiency of SURE[®]2 was $\sim 3.5 \times 10^5$ CFU/ μ g DNA. The results are shown in Table 7. A total of 80 colonies grew on these experimental plates. A bacterial lawn was observed on the cell growth control plate and there were no colonies on the ampicillin control plate.

Table 7. Transformation of SURE cells with pGLu883Δ*Xba* Reverse

Transformation Sample	Plate	DNA added	DNA Concentration ^a (ng)	Results
1	Control for cell growth	none	0	bacterial lawn
2	Control for antibiotic	none	0	no colonies
3	Control of Transformation efficiency	pUC 19	~10	~3,500 blue colonies
4	Experimental	pGLu883Δ <i>Xba</i> Reverse	~50	80 white colonies

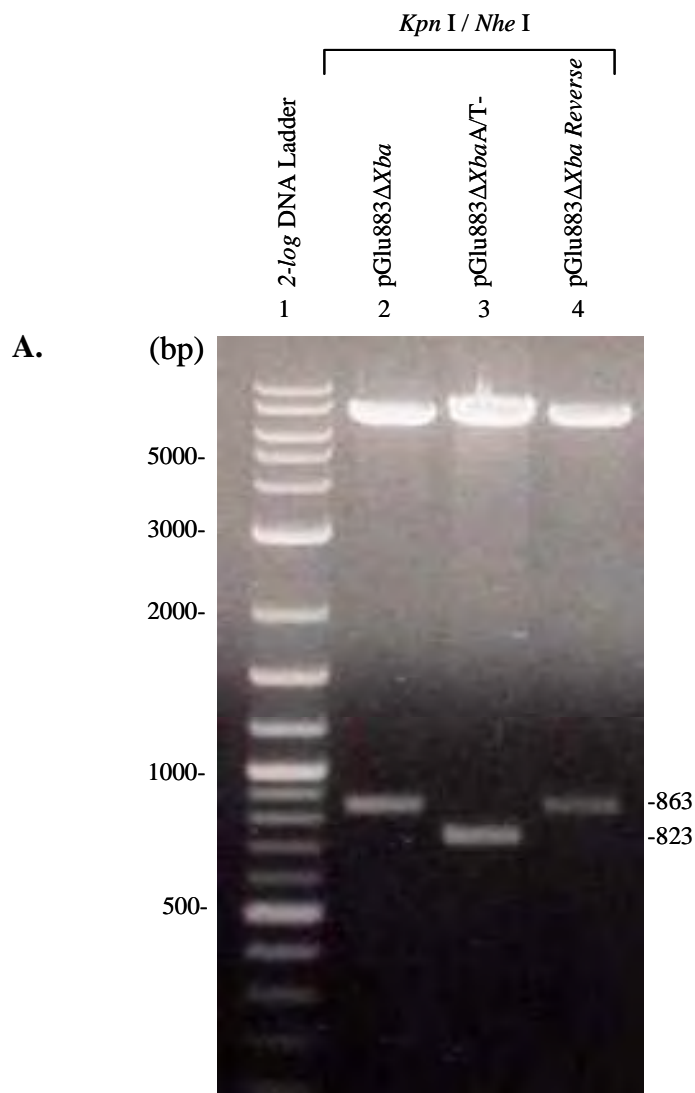
^a Estimated concentration is based on the amount of vector in the ligation reaction per 100 μ l of competent cells.

Restriction enzyme analysis:

Recombinant molecules of pGLu883Δ*Xba Reverse* were digested first with the restriction endonucleases *Kpn* I and *Nhe* I. The DNA fragments from clones with the correct insert is expected to be ~863 bp DNA fragment from pGLu883Δ*Xba* and a 6968 bp DNA fragment from pGLu883Δ*Xba*A/T- (Figure 22, lane 4). Only mini-preparations exhibited the desired restriction pattern, termed as mp 16 (Figure 22, lane 4). *Reverse* was subsequently used for transfection, by electroporation into HeLa cells.

Transfection of HeLa cells with pGLu883Δ*Xba Reverse*:

pGLu883Δ*Xba Reverse* was transfected into HeLa cells to attest for the inability of pGLu883Δ*Xba*A/T- to replicate and to determine if the lack of replication was due to rearrangements in the left terminus. Cells were harvested on day 8 post-transfection (Figure 23). No CPE was visible on the cell control flask and on the day 5, localized CPE areas were first observed on the pGLu883Δ*Xba* flask. On day 6, the first signs of CPE appeared. By day 8, a 100% of CPE was observed on the flask containing pGLu883Δ*Xba Reverse*. These results suggest that the AT was able to restore the capabilities of the recombinant molecule for infection and that the NS1 sequence of pGLu883Δ*Xba*A/T- as well as the left terminus regions of LuIII A/T- have the capacity to cause excision, replication and encapsidation for viral infection.



B.

Plasmid	Cut sites	Approximate Length (bp)
pGlu883Δ <i>Xba</i>	5152-4289	6968, 863
pGlu883Δ <i>Xba</i> A/T-	5152-4289	6968, 823
pGlu883Δ <i>Xba</i> Reverse	5152-4289	6968, 863

Figure 22. Digestions of possible pGlu883Δ*Xba* Reverse with *Kpn* I / *Nhe* I. **A.** Samples from the pGlu883Δ*Xba* Reverse minipreparations were electrophoresed on a 1.2% agarose gel in 1X TBE buffer at 76 V. Digestions of pGlu883Δ*Xba* Reverse (lane 4) were compared to the *Kpn* I / *Nhe* I digestion of pGlu883Δ*Xba* (lane 2) and pGlu883Δ*Xba*A/T- (lane 3). Sizes of the 2-log DNA Ladder (lane 1) are indicated. **B.** Approximate length of the DNA fragments generated for each plasmid when digested with the indicated restriction enzymes.

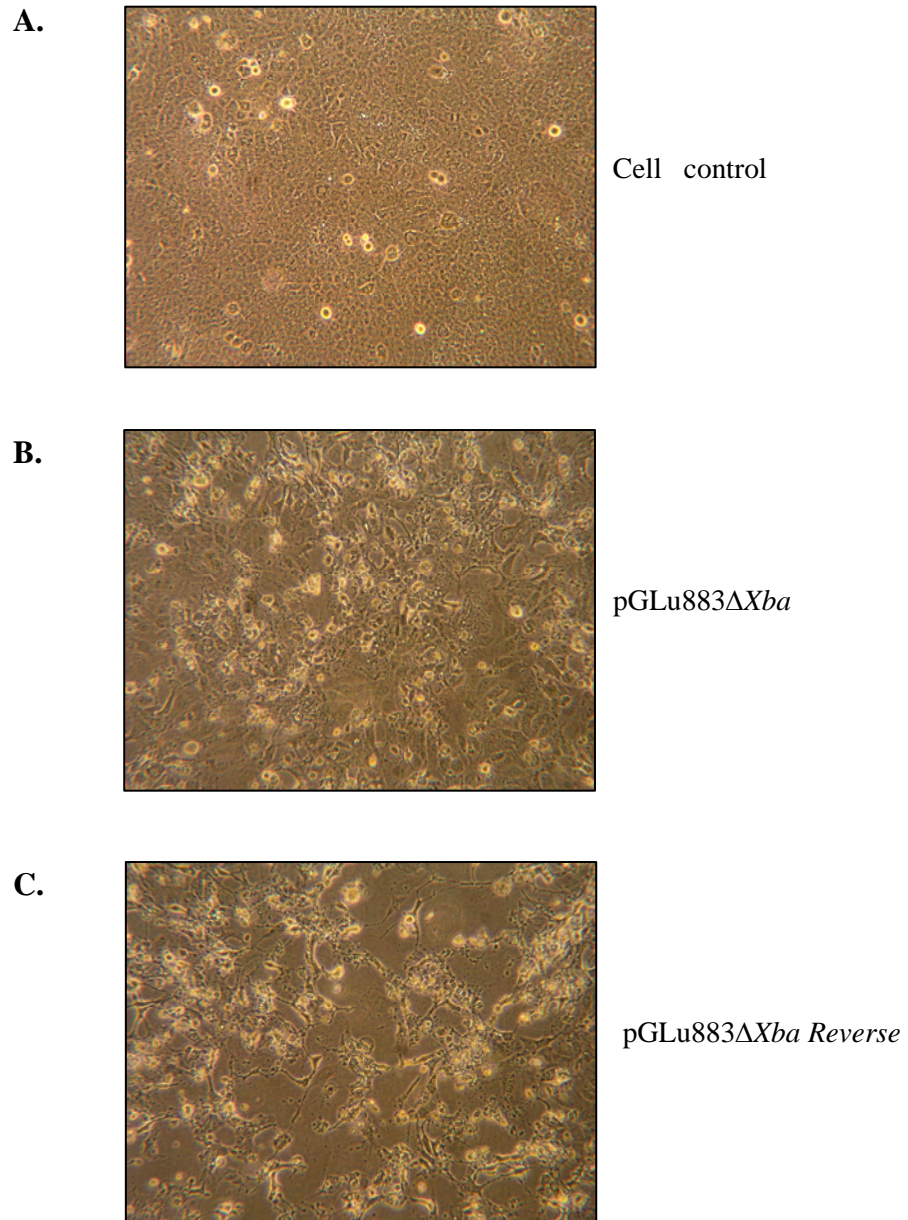


Figure 23. HeLa cells electroporated with pGLu883Δ*Xba Reverse* recombinant clone. Cells were photographed after day 8 post-transfection.

Southern blot analysis of samples from transfections with pGLu883Δ*Xba* Reverse:

Total DNA was extracted from the transfected HeLa cells and a replication analysis was performed by the restriction endonucleases *Dpn* I and *Mbo* I (Figure 24, A). Southern blot analysis (Figure 24, B) of the samples was carried out as follows as described on Ausubel et al., 2005. Lane 1 shows the 2-*log* DNA Ladder. In lane 2, the LuIII 5,135 bp DNA band that correspond to the full genome is shown and was used to compare the migration of the double stranded viral DNA. Lanes 3 to 5 show the pGLu883Δ*Xba* sample; uncut, digested with *Dpn* I and with *Mbo* I, respectively. The uncut and the *Dpn* I digested DNA samples shown in lanes 3 and 4, respectively have similar mobility, two bands of ~5 kb and ~3 kb. Uncut samples of replicated pGLu883Δ*Xba* resulted in two bands with sizes of ~5 kb and ~2.5 kb comparable with the LuIII 5.1 kb genome band and with the single strand DNA (lane 2). The construct pGLu883Δ*Xba* was able to replicate since it was not sensitive to *Dpn* I digestion and sensitive to digestion with *Mbo* I. Lanes 6 to 8 show the pGLu883Δ*Xba* Reverse transfected samples; uncut, digested with *Dpn* I and *Mbo* I, respectively. In the uncut sample, two fairly weak bands were observed above the 5 kb, that likely represent input DNA. Uncut samples of unreplicated pGLu883Δ*Xba* result in two bands. These bands migrate as 12 and 7 kb double strand linear DNA molecule. In lane 7, the bands described before (lane 6) disappear, and a band pattern similar to that expected for viral DNA, digested with *Dpn* I, is visible. In lane 8, the pGLu883Δ*Xba* Reverse plasmid bands were clearly observed, but there is a band pattern also similar to replicated DNA digested with *Mbo* I. It is possible that the Reverse DNA went through less cycles of replication than with pGLu883Δ*Xba*. Thus, resulting in a mixture of replicated and unreplicated DNA. If pGLu883Δ*Xba* Reverse was able to replicate, there is a possibility that the AT-rich sequence thought before to play a role in the encapsidation pattern of LuIII, might

actually be more related to the viral replication or the resolution of the 5' termini. However pGLu883Δ*Xba*A/T- had the 3' or left terminal from pGLu883Δ*Xba* and the 5' or right terminal from the LuIII M_gA/T- and the right termini of pGLu883Δ*Xba Reverse* comes from pGLu883Δ*Xba* and not from the MgLuIII A/T- there is also a possibility that this terminal was damaged. To address this issue a second attempt was made by designing the construct pGLu883Δ*Xba*A/T-. In this case with both DNA termini from pGLu883Δ*Xba*.

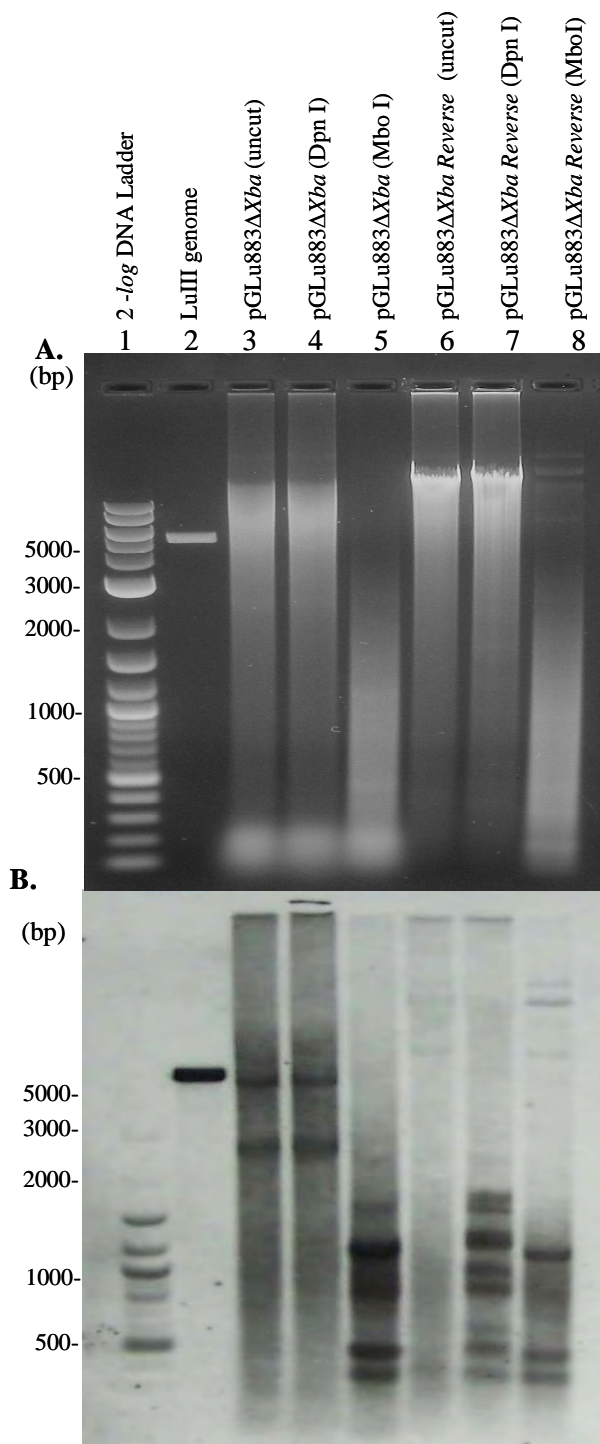


Figure 24. (A) Agarose gel electrophoresis and (B) Southern blot of DNA samples purified from transfected HeLa cells. Samples DNA electrophoresed are indicated above. Samples were run on a 1.2% agarose gel in 1X TAE buffer at 80 V. The blot was hybridized with LuIII probe. The radiograph was exposed for 16 hours.

pGLu883Δ*Xba*A/T- *de novo* plasmid:

A plasmid containing the full genome of LuIII without the AT-rich sequences was constructed by using *Ssp* I as shown in the third cloning strategy of the Materials and Methods Chapter. This plasmid has both the 3'- and 5'-ends from the same parental molecule, pGLu883Δ*Xba*, but lacks the AT-rich sequence.

Bacterial transformation:

The transformation efficiency of SURE[®]2 was $\sim 5.3 \times 10^5$ CFU/ μ g DNA. Results of cell transformation are shown on Table 8. A total of 52 colonies grew on the experimental plates (*de novo*). Whereas blue colonies grew on the transformation control plates with the pUC 19 vector.

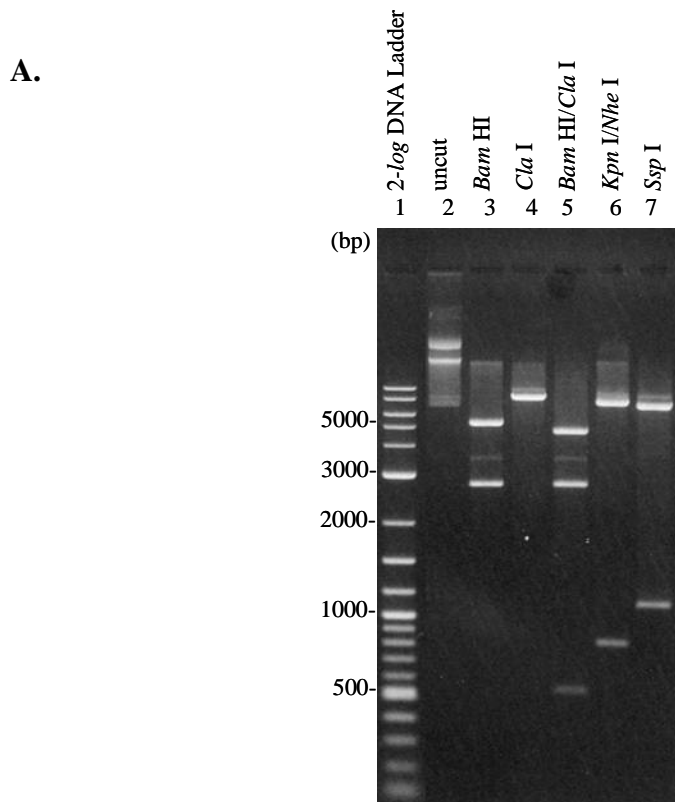
Table 8. Transformation of SURE[®]2 cells with pGLu883Δ*Xba*A/T- *de novo*

Transformation Sample	Plate	DNA added	DNA Concentration ^a (ng)	Results
1	Control for cell growth	none	0	bacterial lawn
2	Control for antibiotic	none	0	no colonies
3	Control of Transformation Efficiency	pUC 19	~10	~5,300 blue colonies
4	Experimental	pGLu883Δ <i>Xba</i> A/T- <i>de novo</i>	~50	52 white colonies

^a Estimated concentration is based on the amount of vector in the ligation reaction per 100 μ l of competent cells.

Restriction enzyme analysis:

De novo recombinant DNA molecules were digested with restriction enzyme described in Figure 25. Recombinants were digested with *Bam* HI (Figure 25, lane 3), which liberates the LuIII genome from pUC19, giving rise a pattern of two bands, one from the viral genome of approximately ~5069 bp and a second from a ~2686 bp DNA fragment of the pUC19 vector. *De novo* has the *Cla* I site of pGLu883Δ*Xba*A/T- (Figure 25, lane 4). The presence of a *Cla* I site proves the absence of the AT-rich region in the molecule; hence a digestion with both *Bam* HI and *Cla* I produced 3 bands of sizes: ~ 4570 bp, ~2686 bp and ~499 bp (Figure 25, lane 5). Digestion of the recombinant molecules with *Nhe* I and *Kpn* I should result in a fragment of ~787 bp and a fragment of ~6968 bp (Figure 25, lane 6). Two recombinant molecules gave all the desired restriction patterns. They were termed as mp1 and mp 5. The *Ssp* I digestion generated the DNA fragments of ~6687 bp and a ~1068 bp, respectively (Figure 25, lane 7). This restriction analysis demonstrated that the *De novo* clone was obtained successfully.



B.

Plasmid	Restriction Enzyme	Cut sites	Approximate Length (bp)
pGlu883Δ <i>Xba</i> A/T- <i>de novo</i>	<i>Bam</i> HI	7749, 5063	5069, 2686
	<i>Cla</i> I	4564	7755
	<i>Bam</i> HI/ <i>Cla</i> I	7749, 5063, 4564	4570, 2686, 499
	<i>Nhe</i> I/ <i>Kpn</i> I	5076, 4289	6968, 787
	<i>Ssp</i> I	5667, 4599	6687, 1068

Figure 25. Digestions of the pGlu883Δ*Xba*A/T- *de novo* recombinant molecule. A. 1.2 % agarose gel in 1X TAE at 76 V. The pGlu883Δ*Xba*A/T- *de novo* recombinant molecule miniprep was digested with *Bam* HI, *Cla* I, *Bam* HI/*Cla* I, *Kpn* I/*Nhe* I and *Ssp* I. Sizes of the 2-log DNA Ladder are shown on lane 1. **B.** Approximate length of the expected fragments generated for each plasmid when digested with the indicated restriction enzymes.

Transfection of HeLa cells with pGLu883 Δ XbaA/T- *de novo*:

To explore the possibility that the new construct of LuIII without the AT-rich sequence is able to replicate, the pGLu883 Δ XbaA/T- *de novo* molecule was transfected into HeLa cells and incubated at 37°C for a period of 8 days. HeLa cells were expected to achieve confluency unless infected by the virus. The cells on the control flask achieved confluency on day 7 post-transfection after which some cells started to detach from the flask. Extracted DNA obtained from the cell control sample was not loaded on the agarose gel electrophoresis because of limited space. The pGLu883 Δ Xba flask showed signs of CPE on day 6 post-transfection (Figure 26). As observed before, no CPE was observed on the pCMVNS1 flask and no signs of CPE were visible on any other experimental samples.

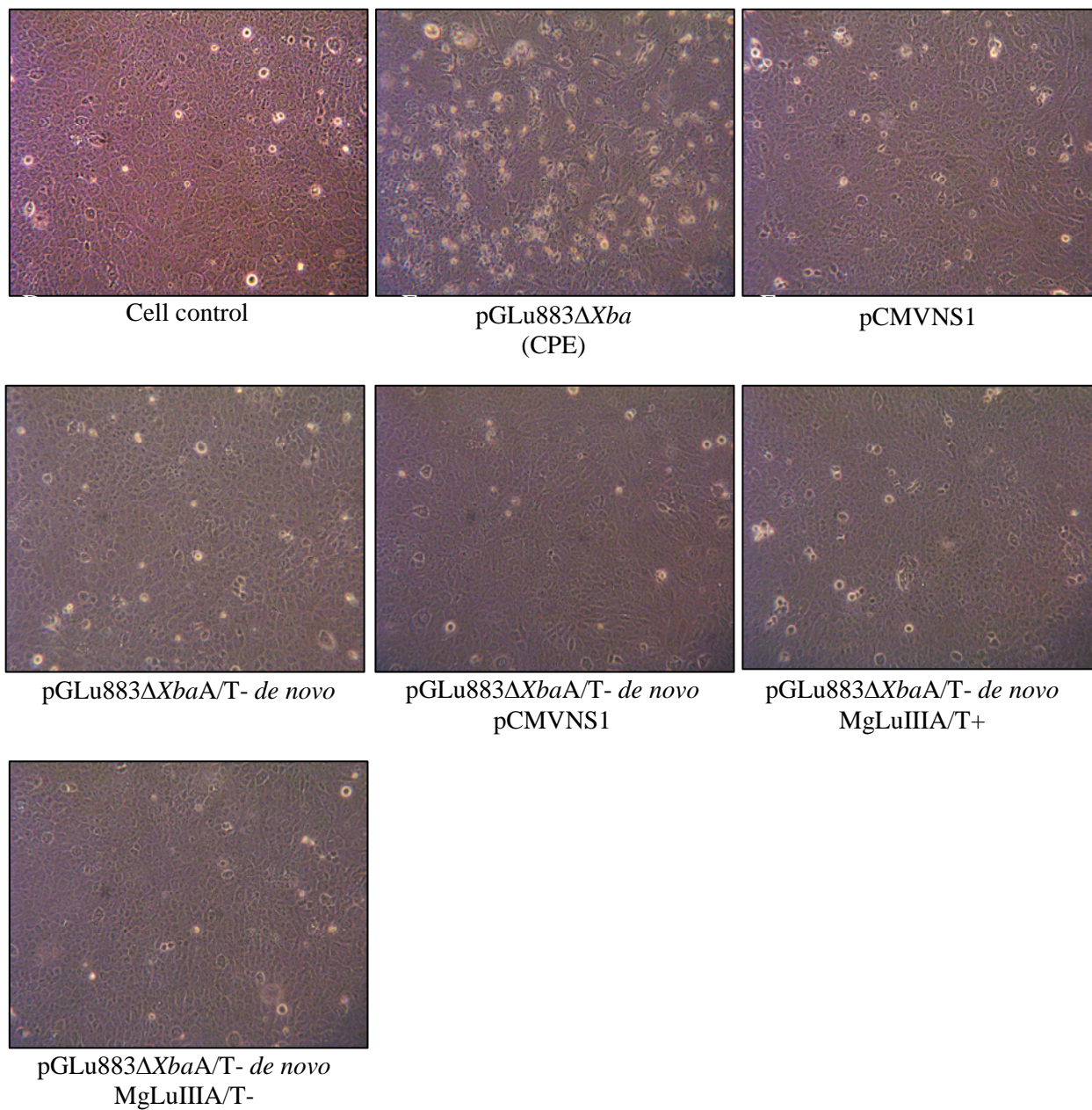


Figure 26. HeLa cells electroporated with pGLu883ΔXbaA/T- *de novo* recombinant clone. Cells were photographed at day 8 post-transfection.

Southern blot analysis of samples from transfections with pGLu883Δ*Xba*A/T- *de novo*:

A replication analysis was performed on all of the transfected cell samples by endonuclease digestion with *Dpn* I and *Mbo* I (Figure 27). Southern blot results obtained from samples analyzed by *Dpn* I/*Mbo* I digestion are shown on Figure 27, A. Samples were loaded as follows: lane 1 shows the 2-*log* DNA Ladder used as a molecular weight marker, lane 2 has the 5,135 bp band that corresponds to the linear double stranded genome of LuIII. Lanes 3 to 20 samples were loaded in the following order: transfected samples of pGLu883Δ*Xba*, pCMVNS1, pGLu883Δ*Xba de novo*, pGLu883Δ*Xba de novo* with pCMVNS1, pGLu883Δ*Xba de novo* with MgLuIII A/T+ and pGLu883Δ*Xba de novo* with MgLuIII A/T-. These samples are shown uncut, followed by the same sample digested with *Dpn* I and *Mbo* I. The pGLu883Δ*Xba* digested with *Dpn* I showed the same pattern as the uncut sample while the sample digested with *Mbo* I showed the restriction pattern as expected from the replicated plasmid DNA. Samples of pCMVNS1 did not appear on the Southern blot because of the high specificity of the LuIII probe used. On the transfected and cotransfected samples of pGLu883Δ*Xba de novo*, restriction band patterns were visible only on the samples digested with *Dpn* I. Digestion with *Dpn* I is indicative of unreplicated plasmid DNA.

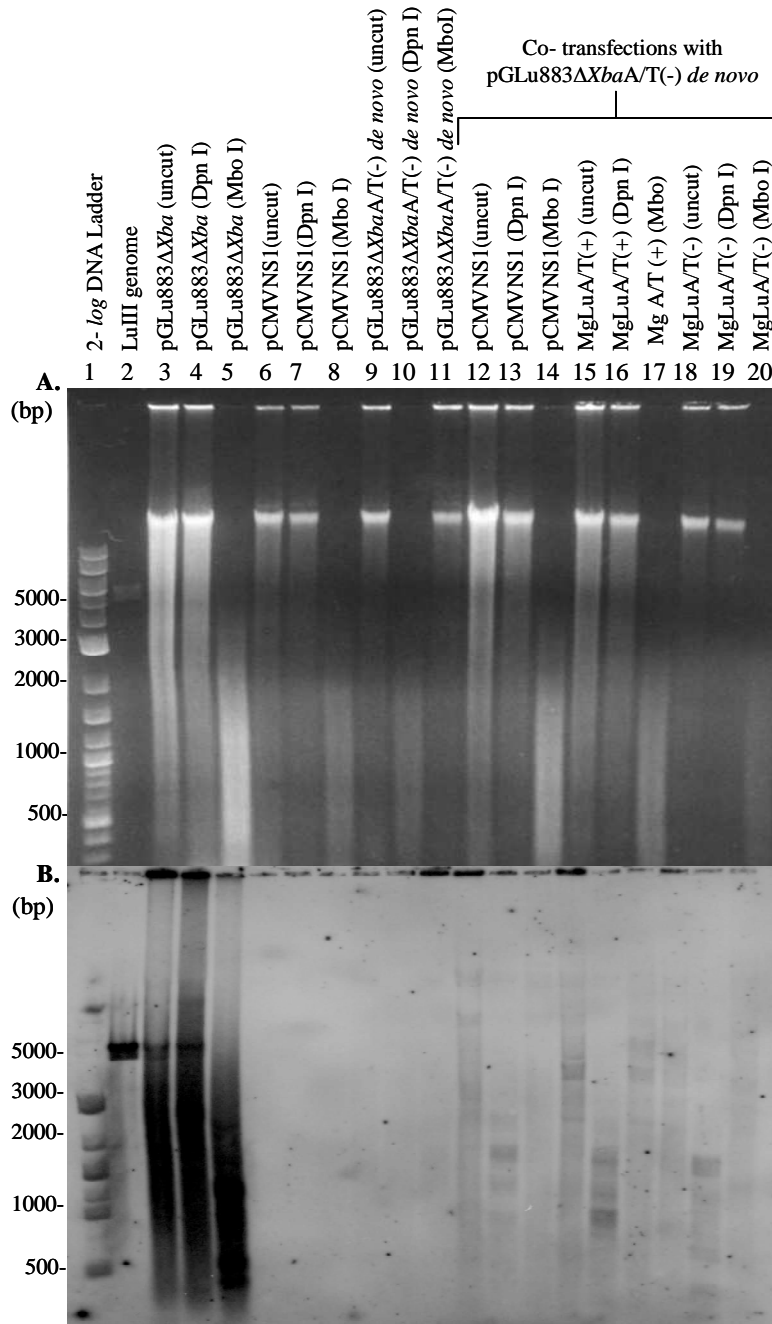


Figure 27. Gel electrophoresis (A) and Southern Blot (B) of DNA isolated from transfected HeLa cells. Samples electrophoresed are indicated above. The 1.2% agarose gel was electrophoresed in 1X TAE buffer at 80 V. The blot was hybridized with the LuIII probe. The radiograph was exposed for 14 hours.

Several *cis*-acting sequences of the 5' end of the MVM virus have been linked to its replication (Tam and Astell, 1993; Tam and Astell, 1994; Brustein and Astell, 1997). Deletions on the 5' terminal palindrome demonstrated that there were *cis*-acting genetic elements in the viral terminus were essential for the excision and replication of the viral DNA. Removal of one copy of a tandemly arranged 65 bp repeat (4720-4849 nt) has found to be inboard of the 5' terminal palindrome and inhibited viral DNA replication. There is a 26 bp AT-rich sequence twenty eight nucleotides downstream of the 65 bp repeat in the MVM genome. Sequence comparison of the 65 bp repeats and the AT-rich sequence to the autonomous replicating sequence of yeast revealed similarities between both sequences (Brustein and Astell, 1997). Studies to investigate an ARS like sequence in the right end terminus of LuIII resulted in data that suggests that the 600 bp from map units 88-100 of the viral genome may act as an origin of replication in lower eukaryotes (Román-Pérez, 2000; Arroyo, 2000; De Jesús-Maldonado, 2004). Studies with MVM minigenomes with two right end terminals (RR) and two left end terminals (LL) revealed that the RR minigenomes were more efficient in replication than the LL minigenomes (Tam and Astell, 1993). A detailed analysis of the right end terminus of MVM has exposed two specific elements inboard the right hairpin between the nucleotides position 4489-4636 (element A) and the nucleotide position 4636-4694 (element B). These two elements were found to be necessary for efficient replication of MVM and were considered as replication sequences (Tam and Astell, 1993). Sequences that reduce or abolish the replication of MVM are known as Internal Replication Sequences (IRS). Due to this study, the *cis*-acting sequences required for replication of the MVM DNA has been considered to reside in nucleotide positions 140 and 660 of the left and right termini, respectively. Later, studies exposed three specific short sequence elements that contribute to the activity of the IRS. All the elements that constitute the

so-called IRS were believed to be a form of multipartite origin of DNA replication similar to that of the ARS (Brustein and Astell, 1997). This region has been shown to bind unidentified cellular proteins which are thought to be involved with the replication of the MVM genome. (Tam and Astell, 1993; Tam and Astell, 1994). Similar sequences in LuIII have not been examined for such activity. Alignment of LuIII with the MVMp genome (Diffoot et al., 1993) revealed that, in LuIII, the AT-rich region exists as an insertion with respect to the MVM genome (Figure 28). Thus, the sequence near the right palindrome of MVM causes a disruption that has been identified as a *cis*-acting replication signal (Astell et al., 1983). Since the plasmids of LuIIIA/T(-) were not able to self-replicate and the AT-rich sequence of LuIII resides in nt 574, inside the 5'-end, this region could be also considered a *cis*-acting element. The ITR were believed to resemble a multipartite origin of replication, further studies should be done to evaluate the regions surrounding this AT-rich sequence. APV genomes have two origins of replication, one on each terminal region, so data from studies with minigenomes containing two left end terminal regions showed replication capabilities (Diffoot-Carlo et al., 2005). It may be possible that LuIIIA/T- is also replicating at an undetectable level.

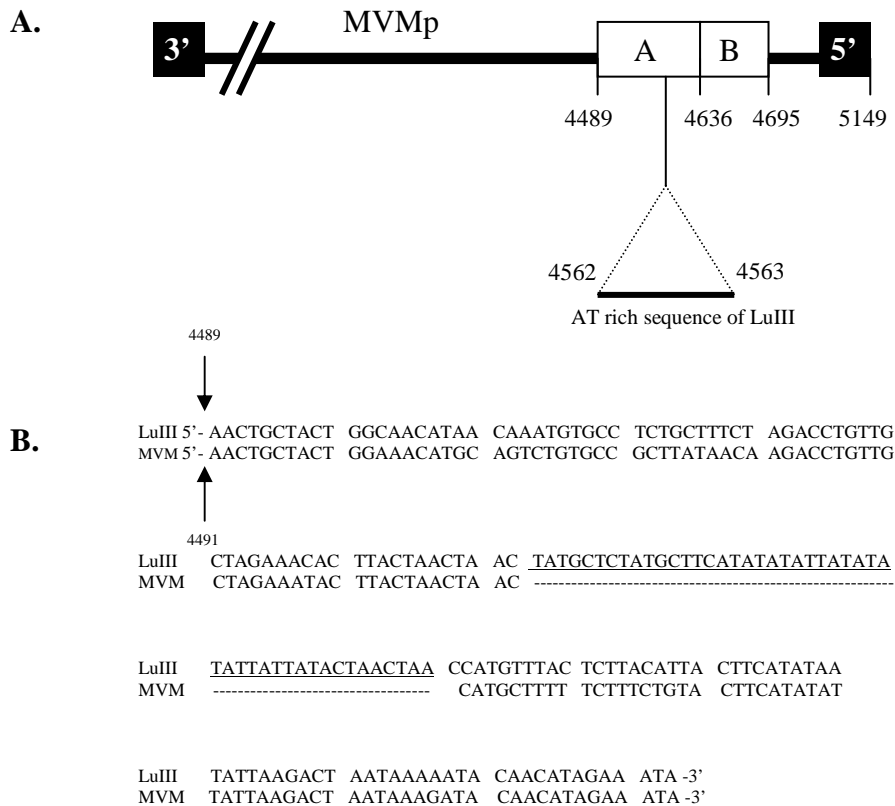


Figure 28. Schematic diagram of the position of the LuIII AT-rich region with respect to the inboard *cis*-acting elements of MVMp. A. The AT-rich sequence of LuIII occurs as an insertion into MVMp (Difffoot et al., 1993). The solid line represents the MVMp genome, black boxes depicts the viral termini, white boxes show *cis*-acting elements A and B. **B.** Nucleotide sequence of MVMp *cis* elements aligned with the LuIII AT-rich sequence are underlined. (Reprinted from Corsini et al., 1995)

CHAPTER V

Conclusions

A clone of pGLu883 Δ *Xba* lacking the 47 bp AT-rich region present at nucleotide position 4558 of parvovirus LuIII was constructed using the LuIII genomic clone pGLu883 Δ *Xba* and the MgLuIIIA/T-. Transfection of HeLa cells with pGLu883*Xba*A/T- recombinants did not result in cytopathic effects suggesting that pGLu883 Δ *Xba*A/T- was not replication competent. Meanwhile transfection of HeLa cells with pGLu883 Δ *Xba Reverse* resulted in replication and infection.

A second clone of pGLu883*Xba*A/T-, termed pGLu883*Xba*A/T- *de novo* was also constructed, in this case with both termini from the original genomic clone. HeLa cells transfected with this construct resulted in no replication. Cotransfection assays of both pGLu883*Xba*A/T- and with a helper construct containing NSI (pCMVNSI) did not change the outcome of the previous experiments. In addition cotransfection of the pGLu883*Xba*A/T- with the minigenomes MgLuIIIA/T- and MgLuIIIA/T+ also resulted in no replication. The data obtained here suggest that the AT-rich sequence may be needed only *in cis*. Both recombinant LuIII genomes lacking the AT-rich sequence were effectively constructed and transfected into HeLa cells, but the Southern blot analysis and probe hybridization assays of isolated DNAs from transfections demonstrated no replication. These results suggest that the AT-rich sequence is essential for the replication of the LuIII genome, but is not directly linked to the encapsidation pattern. Finally, the data also supports previous studies the 600 bp from LuIII m.u. 88 to m.u. 100 could represent an origin of replication at the 5' terminus of LuIII, an origin strictly tied to the replication of the viral genome.

CHAPTER VI

Recommendations

The following recommendations should be considered in order to determine the IRS capabilities of the AT-rich and the AT flanking sequences:

4. Deletions from internal sequences spanning from m.u. 88 to m.u.100 of the LuIII genome will be useful to identify all functional regions required for the IRS and to study the replication and encapsidation capabilities of each of the deleted forms.
5. Transfection of HeLa cells with an expression vector containing the 600 bp of the 5' terminus of LuIII, as its only origin of replication, in order to determine if the 600 bp is a replication origin.
6. Construction of a minigenome with two 5' terminus (m.u. 88 to m.u. 100) in order to compare its replication efficiency to the 3'LuIII 3' minigenome.
7. Protein analysis of cellular extracts obtained from HeLa cells transfected with the pGLu883 Δ XbaA/T- constructs in order to test for the presence of NS1 as a signal for initiation of replication, and to determine if the constructs are replicating deficiently.
8. Insertion of the AT-rich region of LuIII into the genomic clone of MVM in order to study the replication and nature of the encapsidated progeny.

Literature Cited

- Arroyo, N. 2000. Possible autonomously replicating sequence ARS of the unique A/T rich nucleotide sequence of parvovirus LuIII. M.S. Thesis. University of Puerto Rico at Mayagüez, PR.
- Astell, C. R., M. B. Chow and D. C. Ward. 1985. Sequence analysis of the termini of virion and replicative forms of Minute Virus of Mice DNA suggests a modified rolling hairpin model for autonomous parvovirus DNA replication. *J. Virol.* 54:171-177.
- Astell, C. R., M. Thompson, M. Merchlinsky and D. C. Ward. 1983. The complete nucleotide sequence of Minute Virus of Mice, an autonomous parvovirus. *Nucl. Acids Res.* 11:999-1018.
- Atchison, R.W., B.C. Castro and W.M. Hammon. 1965. Adenovirus associated defective virus particles. *Science.* 13;149:754-756.
- Ausubel, F. M., B. Roger, R. E. Kingston, D. D. Moore, J. G. Seidman, J. A. Smith and K. Struhl. 2005. *Current protocols in Molecular Biology.* Current Protocols, Wiley, USA.
- Avalosse, B., F. Dupont, P. Spegelaere, N. Mine and A. Burny. 1996. Method for concentrating and purifying recombinant autonomous parvovirus vectors designed for tumour-cell-targeted gene therapy. *J. Virol. Methods.* 62(2):179-183.
- Baldauf, A. Q., K. Willwand, E. Mumtsidu, J. P. F. Nüesch and J. Rommelaere. 1997. Specific initiation of replication at the right-end telomere of the closed species of Minute Virus of Hice replicative-form DNA. *J. Virol.* 71:971-980.
- Bando, H., H. Choi, Y. Ito and S. Kawase. 1990. Terminal structure of a Densovirus implies a hairpin transfer replication which is similar to the model for AAV. *Virology.* 179(1):57-63.
- Banerjee, P. T., W. H. Olson, D. P. Allison, R. C. Bates, C. E. Snyder and S. Mitra. 1983. Electron Microscopic Comparison of the Sequences of Single-standed Genomes of Mammalian Parvoviruses by Heteroduplex Mapping. *J. Mol. Biol.* 166:257-272.
- Bärbel, K., A. Simpson, and M. G. Rossmann. 2004. The structure of human parvovirus B19. *Proc. Natl. Acad. Sci. USA.* 10; 101(32):11628-11633.
- Bashir, T., J. Rommelaere and C. Cziepluch. 2001. In vivo accumulation of cyclin A and cellular replication factors in autonomous parvovirus Minute Virus of Mice-associated replicon bodies. *J. Virol.* 75:4394-4398.
- Bates, R. C., E. Snyder, P. T. Banerjee and S. Mitra. 1984. Autonomous parvovirus LuIII encapsidates equal amounts of plus and minus DNA strands. *J. Virol.* 49:319-324.

Berns, K. I. 1990. Parvovirus Replication. *Microbiol Mol Biol Rev.* 54(3):316-329.

Berns, K. I. 1996. Parvoviridae: the viruses and their replication. *Fields virology*, 3rd ed. Raven Publishers, Philadelphia, Pa, p. 1017-1036.

Besselsen, D., D. Pintel, G. Purdy, C. Besch-Williford, C. Franklin, R. Hook and L. Riley. 1996. Molecular characterization of newly recognized rodent parvoviruses. *J. Gen. Virol.* 77 (Pt 5):899-911.

Bossin, H., P. Fournier, C. Royer, P. Barry, P. Cerutti, S. Gimenez, P. Couble and M. Bergoin. 2003. Junonia coenia densovirus-based vectors for stable transgene expression in Sf9 cells: influence of the densovirus sequences on genomic integration *J. Virol.* 77(20):11060-11071.

Brister J. and N. Muzyczka. 1999. Rep-mediated nicking of the adeno-associated virus origin requires two biochemical activities, DNA Helicase activity and transesterification. *J. Virol.* 73:9325-9336.

Brockhaus, K., S. Plaza, D. Pintel, J. Rommelaere and N. Salome. 1996. Nonstructural proteins NS2 of minute virus of mice associate in vivo with 14-3-3 protein family members. *J. Virol.* 70:7527-7534.

Brunstein, J. and C. Astell. 1997. Analysis of the internal replication sequence indicates that there are three elements required for efficient replication of Minute Virus of Mice minigenomes. *J. Virol.* 71:9087-9095.

Burnett, E., J. Christensen and P. Tattersall. 2001. A consensus DNA recognition motif for two KDWK transcription factors identifies flexible length, CpG-methylation sensitive cognate binding sites in the majority of human promoters. *J. Mol. Biol.* 314:1029-1039.

Chen, K. C., B. C. Shull, M. Lederman, E. R. Stout and R. C. Bates. 1988. Analysis of the termini of the DNA of Bovine Parvovirus: demonstration of sequence inversion at the left terminus and its implication for the replication model. *J. Virol.* 62:3807-3813.

Christensen, J., S. F. Cotmore and P. Tattersall. 1997a. A novel cellular site-specific DNA-binding protein cooperates with the viral NS1 polypeptide to initiate parvovirus DNA replication. *J. Virol.* 71:1405-1416.

Christensen, J., S. F. Cotmore and P. Tattersall. 1997b. Parvovirus initiation factor PIF: a novel human DNA-binding factor which coordinately recognizes two ACGT motifs. *J. Virol.* 71:5733-5741.

Christensen, J., S. F. Cotmore and P. Tattersall. 2001. Minute Virus of Mice initiator protein NS1 and a host KDWK family of transcription factor must form a precise ternary complex with origin DNA for nicking to occur. *J. Virol.* 75:7009-7017.

Clément, N., B. Avalosse, K. El Bakkouri, T. Velu and A. Brandenburger. 2001. Cloning and sequencing of defective particles derived from the autonomous parvovirus Minute Virus of Mice for the construction of vectors with minimal *cis*-acting sequences. *J. Virol.* 75:1284-1293.

Cornelis, J., Y. Chen, N. Spruyt, N. Duponchel, S. Cotmore, P. Tattersall and J. Rommelaere. 1990. Susceptibility of human cells to killing by the parvoviruses H-1 and minute virus of mice correlates with viral transcription. *J. Virol.* 64:2537-2544.

Cornelis, J., N. Salome, C. Dinsart and J. Rommelaere. 2004. Vectors based on autonomous parvoviruses: novel tools to treat cancer? *J. Gene. Med.* 6 Suppl 1:S193-S202.

Corsini J., J. Carlson, F. Maxwell and I. H. Maxwell. 1995. Symmetric strand packaging of recombinant parvovirus LuIII genomes that retain only the terminal regions. *J. Virol.* 69:2692-2696.

Corsini, J., I. Maxwell, F. Maxwell and J. Carlson. 1996. Expression of parvovirus LuIII NS1 from a Sindbis replicon for production of LuIII-luciferase transducing virus. *Virus Res.* 46(1-2):95-104.

Costello, E., P. Saudan, E. Winocour, L. Pizer and P. Beard. 1997. High mobility group chromosomal protein 1 binds to the adeno-associated virus replication protein (Rep) and promotes Rep-mediated site-specific cleavage of DNA, ATPase activity and transcriptional repression. *EMBO J.* 16:5943-5954.

Cotmore, S. and P. Tattersall. 1986. Organization of the nonstructural genes of the autonomous parvovirus Minute Virus of Mice. *J. Virol.* 58:724-732.

Cotmore, S. and P. Tattersall. 1987. The autonomously replicating parvoviruses of vertebrates. *Adv. Virus Res.* 33:91-173.

Cotmore S. and P. Tattersall. 1988. The NS-1 polypeptide of Minute Virus of Mice is covalently attached to the 5' termini of duplex replicative-form DNA and progeny single strands. *J. Virol.* 62:851-860.

Cotmore S. F., and P. Tattersall. 1992. In vivo resolution of circular plasmids containing concatemer junction fragments from Minute Virus of Mice DNA and their subsequent replication as linear molecules. *J. Virol.* 66: 420-431.

Cotmore, S. and P. Tattersall. 1994. An asymmetric nucleotide in the parvoviral 3' hairpin directs segregation of a single active origin of DNA replication. *EMBO J.* 13:4145-4152.

Cotmore, S. and P. Tattersall. 1995. DNA replication in the autonomous parvoviruses. *Semin. Virol.* 6:271-281.

Cotmore, S. and P. Tattersall. 1996. Parvovirus DNA Replication. DNA Replication in Eukaryotic Cells (ed. M.L. DePamphilis), pp. 799-813. Cold Spring Harbor Lab. Press. Cold Spring Harbor New York.

Cotmore, S. and P. Tattersall. 2005a. Encapsidation of minute virus of mice DNA: Aspects of the translocation mechanism revealed by the structure of partially-packaged genomes. *Virology*. 336:100-112.

Cotmore, S. and P. Tattersall. 2005b. Packaging sense is controlled by the efficiency of the nick site in the right-end replication origin of parvoviruses MVM and LuIII. *J. Virol.* 79:2287-2300.

Cotmore, S. and P. Tattersall. 2006. Parvovirus. DNA Replication and Human Disease. (ed. M.L. DePamphilis), pp. 593-608 Cold Spring Harbor Lab. Press. Cold Spring Harbor New York.

Cotmore, S., J. Christensen and P. Tattersall. 2000. Two widely spaced initiator binding sites create an HMG1-dependent parvovirus rolling-hairpin replication origin. *J. Virol.* 74:1332-1341.

Cotmore, S., J. Nüesch and P. Tattersall. 1993. Asymmetric resolution of a parvovirus palindrome in vitro. *J. Virol.* 67:1579-1589.

Cotmore, S., J. Christensen, J. Nüesch and P. Tattersall. 1995. The NS1 polypeptide of the murine parvovirus Minute Virus of Mice binds to DNA sequences containing the motif (ACCA)₂₋₃. *J. Virol.* 69:1652-1660.

De Jesús-Maldonado, I. 2004. Study of an ARS-like function of map units 88-100 of Parvovirus LuIII. M.S. Thesis. University of Puerto Rico at Mayagüez, PR.

De La Mota-Peynado, A. 2004. Infectious capabilities of the plus (+) and minus (-) strands of Parvovirus LuIII. M.S. Thesis. University of Puerto Rico at Mayagüez, PR.

Delau, L., A. Pujol, S. Faisst and J. Rommeleare. 1999. Activation of promoter P4 of the autonomous parvovirus minute virus of mice at early S phase is required for productive infection. *J. Virol.* 73:3877-3885.

Diffoot, N., K. Chen, R. Bates and M. Lederman. 1993. The complete nucleotide sequence of parvovirus LuIII and localization of a unique sequence possibly responsible for its encapsidation pattern. *Virology*. 192:339-345.

Diffoot, N., B. Shull, K. Chen, E. Stout, M. Lederman and R. Bates. 1989. Identical ends are not required for the equal encapsidation of plus- and minus- strand parvovirus LuIII DNA. *J. Virol.* 63:3180-3184.

- Difffoot-Carlo N., L. Vélez-Pérez and I. De Jesús-Maldonado. 2005. Possible active origin of replication in the double stranded extended form of the left terminus of LuIII end its implication on the replication model of the parvovirus. *Viol. J.* 31;2:47.
- Ding, L., S. Lu and N. Munshi. 1997. In vitro packaging of an infectious recombinant adeno-associated virus 2. *J Gene Therapy.* 4:1167-1172.
- Doerig, C. 1986. Nucleoprotein complexes of minute virus of mice have a distinct structure different from that of cromatin. *J. Virol.* 58:817-824.
- Dorsch, S., G. Liebisch, B. Kaufmann, P. von Landenberg, J. H. Hoffmann, W. Drobnik and S. Modrow. 2002. The VP1 Unique Region of Parvovirus B19 and Its Constituent Phospholipase A2-Like Activity. *J. Virol.* 76:2014-2918.
- Dumas, B., M. Jourdan, A. Pascaud and M. Bergoin. 1992. Complete nucleotide sequence of the cloned infectious genome of *Junonia coenia* densovirus reveals an organization unique among parvoviruses. *Virology.* 191:202-222.
- Eiji, M., A. Nakashima, H. Asao, H. Sato and K. Sugamura. 2003. Human Parvovirus B19 Nonstructural Protein (NS1) Induces Cell Cycle Arrest at G₁ Phase. *J. Virol.* 77:2915-2921.
- Faisst, S. and J. Rommelaere (eds). 2000. Parvoiruses. From Molecular Biology to Pathology and Therapeutic Uses. *Contrib. Microbiol. Basel, Karger.* Vol 4:163-202.
- Flotte, T. 2001. Size does matter: overcoming the adeno-associated virus packaging limit. *Respir Res.* 1:16-18.
- García-Tapia, A., M. Lozano-Dominguez and C. Fernández-Gutiérrez del Álamo. 2005. Infección por *Erythrovirus* B19. *Enferm. Infecc. Microbiol. Clin. Supl.* 1:24-29.
- Gareus, R., A. Gigler, A. Hemauer, M. Leruez-Ville, F. Morinet, H. Wolf and S. Modrow. 1998. Characterization of cis-acting and NS1 protein-responsive elements in the p6 promoter of parvovirus B19. *J. Virol.* 72:609-616.
- Gautschi, M., G. Siegl and G. Kronauer. 1976. Multiplication of parvovirus LuIII in a synchronized culture system. IV. Association of the viral structural polypeptides with the host cell chromatin. *J. Virol.* 20:29-38.
- Giraud, C., G. Devauchelle and M. Bergoin. 1992. The Densovirus of *Junonia coenia* (JcDENV) as an insect cell expression vector. *Virology.* 186:207-218.
- Goudy, K., S. Song, C. Wasserfall, Y. Zhang, M. Kapturczak, A. Muir, M. Powers, M. Scott-Jorgensen, M. Campbell-Thompson, J. Crawford, T. Ellis, T. Flotte and M. Atkinson. 2001. Adeno-associated virus vector-mediated IL-10 gene delivery prevents type 1 diabetes in NOD mice. *Proc Natl Acad Sci.* 20;98:13913-13918.

- Hanson, N. and S. Rhode III. 1991. Parvovirus NS1 Stimulates P4 Expression by Interaction with the Terminal Repeats and through DNA Amplification. *J. Virol.* 65:4325-4333.
- Heegaard, E. and K. Brown. 2002. Human parvovirus B19. *Clin. Microbiol. Rev.* 15: 485-505.
- Heegaard, E. and A. Hornsleth. 1995. Parvovirus: the expanding spectrum of disease. *Acta Paediatr.* 84:109-117.
- Hickman, A., D. Ronning, Z. Pérez, R. Kotin and F. Dyda. 2004. The nuclease domain of adeno associated virus Rep coordinates replication initiation using two distinct DNA recognition interfaces. *Mol Cell.* 13:403-414.
- Im, D. and N. Muzyczka. 1990. The AAV origin binding protein Rep68 is an ATP-dependent site-specific endonuclease with DNA Helicase activity. *Cell.* 61:447-457.
- James, J., A. Aggarwal., R. Linden and C.R. Escalante. 2004. Structure of adeno-associated virus type 2 Rep40-ADP complex: Insight into nucleotide recognition and catalysis by superfamily 3 helicases. *Proc. Natl. Acad Sci.* 101:12455-12460.
- Kerr, J. 2000. Pathogenesis of human parvovirus B19 in rheumatic disease. *Ann. Rheum. Dis.* 59:672-683.
- Kimsey, P., H. Engers, B. Hirt and C. Jongeneel. 1986. Pathogenicity of fibroblast- and lymphocyte-specific variants of minute virus of mice. *J. Virol.* 59:8-13.
- King, J., R. Dubielzig, D. Grimm and J.A. Kleinschmidt. 2001. DNA helicase-mediated packaging of adeno-associated virus type 2 genomes into preformed capsids. *EMBO J.* 15;20:3282-3291.
- Kontou, M., L. Govindasamy, H. Nam, N. Bryant, A.L. Llamas, C. Foces-Foces, E. Hernando, M. Rubio, R. McKenna, J. Almendral and M. Agbandje-McKenna. 2005. Structural determinants of tissue tropism and in vivo pathogenicity for the parvovirus Minute Virus of Mice. *J. Virol.* 79:10931-10943.
- Kuntz-Simon, G., T. Bashir, J. Rommelaere and K. Willwand. 1999. Neoplastic transformation-associated stimulation of the in vitro resolution of concatemer junction fragments from Minute Virus of Mice DNA. *J. Virol.* 73:2552-2558.
- Lefebvre, R., S. Riva and K. Berns. 1984. Conformation Takes Precedence over Sequence in Adeno-Associated Virus DNA Replication. *Mol. Cel. Biol.* 4:1416-1419.
- Li, C., D. Bowles, T. van Dyke and R. Samulski. 2005. Adeno-associated virus vectors: potential applications for cancer gene therapy. *Cancer Gene Ther.* 12:913-925.
- Linden M., P. Ward, C. Giraud, E. Winocour and K. I. Berns. 1996. Site-specific integration by adeno-associated virus. *Proc. Natl. Acad. Sci.* 93:11288-11294.

- Liu, Q., C. Yong and C. Astell. 1994. In vitro resolution of the dimmer bridge of the Minute Virus of Mice (MVM) genome supports the modified rolling hairpin model for MVM replication. *Virology*. 201:251-262.
- Llamas-Saiz, A., M. Agbandje-McKenna, W. Wikoff, J. Bratton, P. Tattersall and M. Rossmann. 1997. Structure Determination of Minute Virus of Mice. *Acta Cryst.* D53:93-102.
- Lombardo, E., J. Ramírez, J. García and J. Almendral. 2002. Complementary Roles of Multiple Nuclear Targeting Signals in the Capsid Proteins of the Parvovirus Minute Virus of Mice during Assembly and Onset of Infection. *J. Virol.* 76:7049-7059.
- López-Guerrero, J., B. Rayet, M. Tuynder, J. Rommelaere and C. Dinsart. 1997. Constitutive activation of U937 promonocytic cell clones selected for their resistance to parvovirus H-1 infection. *Blood*. 1;89:1642-1653.
- Lukashov V. and J. Gouudsmiit. 2001. Evolutionary Relationships among Parvoviruses: Virus-Host Coevolution among Autonomous Primate Parvoviruses and Links between Adeno-Associated and Avian Parvoviruses. *J. Virol.* 75:2729-2740.
- Lusby, E., R. Bohenzky and K. Berns. 1980. Nucleotide sequence of the inverted terminal repetition in adeno-associated virus DNA. *J. Virol.* 34:402-409.
- Lusby, E., R. Bohenzky and K. Berns. 1981. Inverted terminal repetition in adeno-associated virus DNA: independence of the orientation at either end of the genome. *J. Virol.* 37:1083-1086.
- Maxwell, I. and F. Maxwell. 2004. Parvovirus LuIII transducing vectors packaged by LuIII versus FPV capsid proteins: the VP1 N-terminal region is not a major determinant of human cell permissiveness. *J. Gen. Virol.* 85(Pt 5):1251-1257.
- Martyn, J., B. Davidson and M. Studdert. 1990. Nucleotide sequence of feline panleukopenia virus: comparison with canine parvovirus identifies host-specific differences. *J Gen Virol.* 71 (Pt 11):2747-53.
- Maxwell, I. and F. Maxwell. 1994. A modified plaque assay and infected cell hybridization assay for wild-type and recombinant LuIII autonomous parvovirus. *Biotechniques*. 16:876-881.
- Maxwell, I. and F. Maxwell. 1999. Control of parvovirus DNA replication by a tetracycline-regulated repressor. *Gene Ther.* 6:309-313.
- Maxwell, I., and F. Maxwell, S. Rhode, J. Corsini and J. Carlson. 1993. Recombinant LuIII autonomous parvovirus as a transient transducing vector for human cells. *Hum. Gene Ther.* 4:441-450.

- Maxwell, I., A. Spitzer, C. Long and F. Maxwell. 1996. Autonomous parvovirus transduction of a gene under control of tissue-specific or inducible promoters. *Gene Ther.* 3:28-36.
- Maxwell, I., A. Spitzer, F. Maxwell and D. Pintel. 1995. The capsid determinant of fibrotropism for the MVMp strain of minute virus of mice functions via VP2 and not VP1. *J. Virol.* 69:5829-32.
- Maxwell I., K. Terrell and F. Maxwell. 2002. Autonomous parvovirus vectors. *Methods* 28:168-181.
- McLaughlin, S., P. Collins, P. Hermonant and Muzyczka. 1988. Adeno-Associated Virus general transduction analysis of parvoviral structures. *J. Virol.* 62:1963-1973.
- McKenna, R., N. Olson, P. Chipman, T. Baker, T. Booth, J. Christensen, B. Aasted, J. Fox, M. Bloom, J. Wolfenbanger and M. Agbandje-McKenna. 1999. Three-Dimensional Structure of Aleutian Mink Disease Parvovirus: Implications for Disease Pathogenicity. *Virology.* 73:6882-6891.
- Moffatt, S., N. Yaegashi, K. Tada, N. Tanaka and K. Sugamura. 1998. Human Parvovirus B19 Nonstructural (NS1) Protein Induces Apoptosis in Erythroid Lineage Cells. *J. Virol.* 72:3018-3028.
- Morita, E., A. Nakashima, H. Asao, H. Sato and K. Sugamura. 2003. Human parvovirus B19 nonstructural protein (NS1) induces cell cycle arrest at G(1) phase. *J. Virol.* 77(5):2915-2921.
- Muller, D. and G. Siegl. 1983. Maturation of Parvovirus LuIII in a subcellular system. I. Optimal conditions for *in vitro* synthesis and encapsidation of viral DNA. *J. Gen. Virol.* 64:1043-1054.
- Musatov, S., J. Roberts, D. Pfaff and M. Kaplitt. 2002. A cis-acting element that directs circular adeno-associated virus replication and packaging. *J. Virol.* 76:12792-802.
- Pallier, C., A. Greco, J. Le Junter, A. Saib, I. Vassias and F. Morinet. 1997. The 3' untranslated region of the B19 parvovirus capsid protein mRNAs inhibits its own mRNA translation in nonpermissive cells. *J. Virol.* 71:9482-9489.
- Parrish, C., C. Aquadro and L. Carmichael. 1988. Canine host range and a specific epitope map along with variant sequences in the capsid protein gene of canine parvovirus and related feline, mink, and raccoon parvoviruses. *Virology.* 166:293-307.
- Prasad, K. and J. Trempe. 1995. The adeno-associated virus Rep78 protein is covalently linked to viral DNA in a preformed virion. *Virology,* 214:360-370.

Pujol, A., L. Deleu, J. Nüesch, C. Cziepluch, J. Jauniaux and J. Rommelaere. 1997. Inhibition of Parvovirus Minute virus of Mice Replication by a Peptide Involved in the Oligomerization of Nonstructural Protein NS1. *J. Virol.* 71:7393-7403.

Qiu, J., F. Cheng and D. Pintel. 2006. Expression profiles of bovine adeno-associated virus and avian adeno-associated virus display significant similarity to that of adeno-associated virus type 5. *J. Virol.* 80:5482-5493.

Raab, U., B. Bauer, A. Gigler, K. Beckenlehner, H. Wolf and S. Modrow. 2001. Cellular transcription factors that interact with p6 promoter elements of parvovirus B19. *J. Gen. Virol.* 82(Pt 6):1473-1480.

Respondek, M., J. Bratosiewicz, T. Pertynski and P. Liberski. 1997. Parvovirus particles in a fetal-heart with myocarditis: ultrastructural and immunohistochemical study. *Arch. Immunol. Ther. Exp. (Warsz).* 45(5-6):465-470.

Rhode, S., 1989. Both Excision and Replication of Cloned Autonomous Parvovirus DNA Require the NS1 (rep) Protein. *J. Virol.* 63:4249-4256.

Román-Pérez, E. 2000. Replication of bacterial plasmid containing LuIII A/T rich flanking sequences in Newborn Human Embryonic Kidney cells. M.S. Thesis. University of Puerto Rico at Mayagüez, PR.

Russell, S., A. Brandenburger, C. Flemming, M. Collins and J. Rommelaere. 1992. Transformation-dependant expression of interleukin genes delivered by a recombinant parvovirus. *J. Virol.* 66:2821-2828.

Servant, A., S. Laperche, F. Lallemand, V. Marinho, G. De Saint-Maur, J. F. Meritet, and A. Garbarg-Chenon. 2002. Genetic Diversity within Human Erythroviruses: Identification of Three Genotypes. *J. of Virol.* 76(18): 9124-9134.

Simpson, R., L. McGinty, L. Simon, C.A. Smith, C.W. Godzeski and R.J. Boyd. 1984. Association of parvoviruses with rheumatoid arthritis of humans. *Science.* 30;223(4643):1425-1428.

Siegl, G. and M. Gautschi. 1976. Multiplication of parvovirus LuIII in a synchronized culture system. III. Replication of vira; DNA. *J. Virol.* 17:841-53.

Snyder, R., D. Im and N. Muzyczka. 1990a. Evidence for covalent attachment of the adeno-associated virus (AAV) rep protein to the end of the AAV genome. *J. Virol.* 64:6204-6213.

Snyder, R., D. Im and N. Muzyczka. 1990b. In vitro resolution of covalently joined AAV chromosome ends. *Cell.* 60:105-113.

- Snyder, R., D. Im, T. Ni, X. Xiao, R. Samulski and N. Muzyczka. 1993. Features of the adeno-associated virus origin involved in substrate recognition by the viral Rep protein. *J. Virol.* 73:9325-9336.
- Spear, I., K. Fife, W. Hauswirth, C. Jones and K. Berns. 1977. Evidence for two nucleotide sequence orientations within the terminal repetition of adeno-associated virus DNA. *J. Virol.* 24:627-34.
- Spegelaere P, B. van Hille, N. Spruyt, S. Faisst, J. Cornelis and J. Rommelaere. 1991. Initiation of transcription from the minute virus of mice P4 promoter is stimulated in rat cells expressing a c-Ha-ras oncogene. *J. Virol.* 65:4919-28.
- Stierle, G., K. Brown, S. Rainsford, C. Smith, D. Hamerman, H. Stierle and D. Dumonde. 1987. Parvovirus associated antigen in the synovial membrane of patients with rheumatoid arthritis. *Ann. Rheum. Dis.* 46:219-223.
- Soike, K., M. Latroupolis and G. Siegl. 1976. Infection of Newborn and Fetal hamsters Induced by Inoculation of LuIII Parvovirus. *Arch. Virol.* 51:235-241.
- Tam, P. and C. Astell. 1993. Replication of Minute Virus of Mice minigenomes: novel replication elements required for MVM DNA replication. *Virology.* 193:812-824.
- Tam, P. and C. Astell. 1994. Multiple cellular factors bind to *cis*-regulatory elements found inboard of the 5' palindrome of Minute Virus of Mice. *J. Virol.* 68:2840-2848.
- Timpe, J., K. Verrill and J. Trempe. 2006. Effects of adeno-associated virus on adenovirus replication and gene expression during coinfection. *J. Virol.* 80:7807-15.
- Tullis, G. and T. Shenk. 2000. Efficient Replication of Adeno-Associated Virus Type 2 Vectors: a *cis*-acting element outside of the terminal repeats and minimal size. *J. Virol.* 74:11511-11521.
- Van Munster, M., A. Dullemans, M. Verbeek, J. van den Heuvel, C. Reinbold, V. Brault, A. Clériveret and F. van der Wilk. 2003. A new virus infecting *Myzus persicae* has a genome organization similar to the species of the genus *Densovirus*. *J. Gen. Virol.* 84(Pt 1):165-172.
- Vélez-Pérez, L. 2004. Replication of the 3' LuIII 3' subgenomic clone in human cells. M.S. Thesis. University of Puerto Rico at Mayagüez, PR.
- Wang, X., M. Yoder, S. Zhou and A. Srivastava. 1995. Parvovirus B19 promoter at map unit 6 confers autonomous replication competence and erythroid specificity to adeno-associated virus 2 in primary human hematopoietic progenitor cells. *Proc. Natl. Acad. Sci.* 92:12416-12420.

Ward, P., P. Elias and M. Linden. 2003. Rescue of the Adeno-Associated Virus Genome from a plasmid Vector: Evidence for Rescue by Replication. *J. Virol.* 77(21):11480-11490.

Xie, Q., and M. Chapman. 1996. Canine Parvovirus Capsid Structure, Analysed at 2.9 Å resolution. *J. Mol. Biol.* 264:497-520.

Yoon-Robarts, M., A. Blouin, S. Bleker, J. Kleinschmidt, A. Aggarwal, C. Escalante and R. Linden. 2004. Residues within the B' motif are critical for DNA binding by the superfamily 3 helicase Rep 40 of adeno-associated virus type 2. *J. Biol. Chem.* 26;279:50472-50481.

Young, P., K. Jensen, L. Burger, D. Pintel and C. Lorson. 2002. Minute Virus of Mice NS1 interacts with the SMN protein and they colocalize in novel nuclear bodies induced by parvovirus infection. *J. Virol.* 76:3892-3904.

Zhi, N., I. Mills, J. Lu, S. Wong, C. Filippone, and K. Brown. 2006. Molecular and functional analyses of a human parvovirus B19 infectious clone demonstrates essential roles for NS1, VP1, and the 11-kilodalton protein in virus replication and infectivity. *J. Virol.* 80:5941-5950.